TOPOGRAPHIC REACTIONS OF CELLS IN TISSUE REPAIR

KAREN MACDONALD B.Sc. (Hons.)

Centre for Cell Engineering

Division of Infection and Immunity

Institute of Biomedical and Life Sciences

University of Glasgow

A thesis submitted to the Faculty of Science of the University of Glasgow for the degree of Doctor of Philosophy.

September 1997

ProQuest LLC.
789 East Eisenhower Parkway
P.O. Box 1346
Ann Arbor, MI 48106 – 1346

ACKNOWLEDGEMENTS

First and foremost I would like to thank my supervisor Professor Adam Curtis for his guidance and encouragement throughout the completion of this thesis. Thanks must also go to himself and his wife, Ann, for the generous hospitality they have shown over the years. A special mention also to Dr Tony Lawrence and Dr Geoffrey Moores who have both shown continued support and interest since my undergraduate years.

Thanks go to everyone at Ethicon Ltd (Edinburgh) who always conspired to make my time there most interesting and enjoyable. I am especially grateful to David Bewsey for providing invaluable assistance with SEM and photography; to Roseann Young for sharing her histological expertise; to Marjory Willins for her kind help with the *in vivo* work; and to Dr Grant Robertson for helpful discussion of results.

I must also thank Dr Gordon Reid for much appreciated help and assistance with molecular studies (not to mention use of the computer; the videos; and all the coffee); Bill Monaghan for fabrication of quartz and PDS structures essential to the project; Andy Hart for help with photographic processing; Scott Arkison for his molecular and computing knowledge; and Graham Tobasnick for being "the wasp's elbows". I must also thank the aforementioned "Boys" for being such good company over the years and thank every member of The West Lab, past and present, for making my time there so enjoyable. Special thanks must go to "The Girlies" (Dad, DeasL, Irene, LP, and Sheona), as without holidays there would be no work!

Finally, I am indebted to my parents for their continued support and encouragement throughout my academic training.

This work was supported by an EPSRC CASE award in association with Ethicon Ltd, Bankhead Avenue, Edinburgh.

TABLE OF CONTENTS

LIST OF FIGURES AND TABLES

CHAPTER 1

CHAPTER 2

CHAPTER 3

CHAPTER 4

CHAPTER 5

ABBREVIATIONS

ATP	Adenosine triphosphate
BHK	Baby Hamster Kidney cells
cDNA	Complemetary deoxyribonucleic acid
DNA	Deoxyribonucleic acid
dNTP	2'-deoxyribonucleotides
DRG	Dorsal root ganglion cells
EGF	Epidermal growth factor
F-actin	Filamentous actin
FAK	Focal adhesion kinase
GTP	Guanosine triphosphate
IGF	Insulin-like growth factor
IL-1	Interleukin-1
IL-2	Interleukin-2
IL-4	Interleukin-4
LPA	Lysophosphatidic acid
MDCK	Madin-Darby Canine Kidney cells
mRNA	Messenger ribonucleic acid
PCR	Polymerase chain reaction
PDGF	Platelet-derived growth factor
PDS	Polydioxanone suture material
PI	Phosphatidylinositol
PIP	Phosphatidylinositol phosphate
PMMA	Polymethylmethacrylate
SDS-PAGE	Sodium dodecylsulphate polyacrylamide gel electrophoresis
SEM	Scanning electron microscopy
SH2	Src-homology domain 2
SH3	Src-homology domain 3

TGF-β	Transforming growth factor-β
TNF	Tumour necrosis factor

SUMMARY

In this study, cells have been grown on micro- and nano-fabricated silica grooved structures in order to investigate further the mechanism of contact guidance, and with a view to producing a possible implant to guide tissue regrowth in wound healing. Previous work had shown that when cells are grown on microgrooved structures they align parallel with the grooves and the actin cytoskeleton of the cells aligns in a similar way. Results from this study have shown ordered staining of phosphorylated tyrosine along groove/ridge boundaries (on micro- and nano-grooved structures), suggesting a possible role for tyrosine phosphorylation in the mechanism that guides cell alignment on grooved substrates. It would appear that P388D1 macrophage-like cells show greater sensitivity to topographical cues than other cell types investigated, as these cells were shown to react to grooves of a depth as shallow as 44nm.

Grooved structures were also fabricated in a biodegradable polyester, polydioxanone suture material (PDS), thought to be a suitable material for use as an implanted device. *In vitro*, cells reacted to these grooves in the same way as silica grooved structures. When the biodegradable structures were implanted intramuscularly in rats no adverse tissue reaction was observed, and the polydioxanone absorption profile remained normal. From histological and Scanning Electron Microscopy (SEM) studies, it was not possible to determine whether cells are oriented by the polydioxanone grooves *in vivo*.

Messenger RNA fingerprinting experiments have also shown that cells grown on grooved substrates show differential gene expression compared with cells grown on flat substrates. Bands expressed in samples from cells grown on grooved substrates, but not in samples from cells grown on flat substrates, were excised from gels then cloned and sequenced.

CHAPTER 1

INTRODUCTION

Many important cell behavioural processes, including cell adhesion, cell shape, cell migration, contact guidance, and tissue organisation, are affected to some degree by the topography of the surface with which the cells come in contact. It is very likely that because cells look different on surfaces of differing topography that they also function differently. Despite this, although reaction of various cell types to surface topography has been well documented (see reviews by Chehroudi and Brunette, 1995, Curtis and Clark, 1990 and Singhvi *et al*, 1994), the mechanism of topographical contact guidance is not resolved and there is little information on the effects on cell function at the molecular level.

This cellular sensitivity to topographical cues has important implications in biomaterials research. It is desirable that topography of an implanted device should not interfere with normal cell behaviour but, historically, the surface topography of biomaterials was considered to be of much less importance than other factors, such as strength, chemistry and durability. However, the surface topography of a particular implant could result in preferential attachment of certain cell types and exclusion of others, which would, in turn, affect tissue organisation and overall stability of the implant. Thus, if more information was available concerning the effects of topography on cell functions, it is posssible that implants of the future could be engineered to produce desired cell responses.

CONTACT GUIDANCE

"Contact guidance" refers to the tendency of cells to be guided in their direction of locomotion by the topography (shape) of the substrate on which they are growing. Topographic guidance was first observed by Harrison (1910 and 1914) in early cell culture experiments using plasma clots and spider web-fibres. In experiments using tissues of the frog embryo (*Rana palustris*), Harrison observed movement and alignment of the cultured cells, in direct relation to the fibres of the web. In later years, Weiss and Garber (1952) also reported cell shape changes in correlation with the fibrin network of clotted plasma. Weiss and coworkers carried out further studies using a wide variety of substrates (Weiss and Garber, 1952; Weiss, 1959) and named the phenomena "contact guidance", in reference to the guidance of the extension of nerve cells grown on fish scales (Weiss and Taylor, 1956). As a number of different cues are present, the phenomenon of contact guidance is very difficult to demonstrate *in vivo*, although there is some evidence from studies in: the developing fish fin (Wood & Thorogood, 1984); regeneration of the optic nerve in toads (Horder and Martin, 1978) and the glial sling, described by Poston *et al* (1988), involved in the development of the mammalian brain.

A number of theories have been proposed to explain contact guidance. For example, Weiss (1945) suggested that a colloidal exudate preferentially adsorbed along the long axis of a fibre and thus helped orient the cells in this direction. Curtis and Varde (1964) showed that such an interpretation was unlikely and suggested that the cells reacted to the topography of fibres and grooves. This topographical theory was supported by Rovensky *et al* (1971) who studied cell migration and orientation on grooved substrata and concluded that cell guidance due to topographical features was a result of differences in the attachment of cells to surfaces with varying geometrical configurations. Dunn and Heath (1976)

used fibres of different diameters to propose that cells demonstrated contact guidance because they tend to avoid discontinuities in their movement. Using prism-shaped substrata, they showed that substratum morphology and shape impose restrictions on the formation of linear bundles of microfilaments that are important in cell adhesion and locomotion. They suggested that this mechanical restriction on the locomotory apparatus of the cell was the mechanism responsible for fibroblast alignment on patterned substrata.

Ohara and Buck (1979), using grooved substrata with subcellular features, showed that cells were sufficiently rigid to bridge over surface irregularities. They proposed that focal contacts can only form on crests of grooved substrata, thus the orientation of the focal contacts themselves is constrained, and such a restriction influences the direction of the cell cytoskeleton, and ultimately the cell itself. This theory is supported by Meyle *et al* (1994) who reported alignment of gingival fibroblasts on microstructured silicone, and showed that the focal adhesion sites of the fibroblasts were also oriented along the substratum.

PHOTOLITHOGRAPHY

Although very early experiments began to provide an insight into cell reaction to surface morphology, quantitative studies were inhibited mainly due to a lack of uniform structures with well-defined and reproducible surfaces. This problem was overcome with the adoption of photolithographic techniques, used in the electronics industry, to pattern subtrates (Camporese *et al*, 1981; Meyle *et al*, 1991). Using this technique, features in the micrometre range can be precisely etched onto a variety of substrates, including: quartz (Dunn and Brown, 1986; Wood, 1988); plastic (Clark *et al*, 1987 and 1990); glass (Singhvi *et al*, 1992);

and titanium-coated silicon (Brunette *et al*, 1983; Brunette, Exp. Cell Res. volumes 164 and 167, 1986; Brunette, 1988; Chehroudi *et al*, 1990 and 1992).

Substratum patterning using photolithography and plasma etching may result in chemical heterogeneity between the etched and unetched regions, as plasma etching is known to alter surface properties. For instance, Clark *et al* (1987) found, via scanning electron microscopy (SEM) analysis, a difference in the surface roughness between the etched and unetched portions of the perspex plastic used in their studies, the degree of roughening being dependent on etch depth. Their solution was to expose the entire surface of the structure to a blanket (oxygen plasma) etch at the end of the patterning process. Wood (1988) encountered a similar problem using quartz structures, but argued that any effects the etched/unetched regions of the structure exerted on cell behaviour would be negligible compared with the effect of surface topography.

CELL PROPERTIES AFFECTED BY SURFACE TOPOGRAPHY

CELL ADHESION

Attachment and spreading of cells on any surface involves the dynamic reorganization of three filamentous structures: microtubules, microfilaments and intermediate filaments. The involvement of the actin cytoskeleton in cell attachment is of particular interest as cell-substratum adhesion complexes, or "focal contacts" (as described by Abercrombie and Dunn, 1975), were shown to be the cytoplasmic membrane terminal points of actin microfilament bundles (Heath and Dunn, 1978). The cytoskeletal proteins, vinculin (Wilkins and Lin, 1982), paxillin (Turner *et al*, 1990), talin (Muguruma *et al*, 1990), tensin (Bockholt and Burridge, 1993), α-actinin (Otey *et al*, 1990), and focal adhesion

kinase (FAK) (Burridge *et al*, 1992) are found associated with actin microfilament bundles at the site of focal adhesion complexes.

When a cell encounters extracellular matrix, clustering of cell surface integrins occurs at areas of cell-substratum contact. This leads to accumulation of the aforementioned proteins at the cytoplasmic face of cell-substratum contacts, and formation of focal adhesion complexes. The discovery that many of the components of focal adhesion complexes have signalling functions led to the theory that, as well as maintaining cell structural integrity, these structures could play an active role in signalling between the external surroundings and the intracellular environment (Burridge *et al*, 1988). As integrins lack intrinsic catalytic activity, the discovery of a protein tyrosine kinase, focal adhesion kinase, associated with focal adhesions (Schaller *et al*, 1992) resulted in this kinase being the favoured candidate for a signalling molecule acting between integrins and intracellular second messengers; and also phosphorylating the other protein components of focal adhesion complexes. Therefore it would follow that changes in cell-substrate contact could result in the cell receiving varying intracellular signals.

It has been shown that various cell types show preferential attachment on surfaces with different topography. For example, osteoblast-like (Bowers *et al*, 1992) and macrophage-like cells prefer roughened surfaces, whereas human gingival fibroblasts prefer smooth surfaces (Könönen *et al*, 1992). This preference for specific surface topography shown by certain populations of cells may result in cell selection. This could have implications in the use of implanted biomaterials, for instance if certain parts of the prosthesis were exclusively occupied by one cell type to the, perhaps, detrimental exclusion of others.

CELL SHAPE

There is evidence that surface topographies of many implanted devices can alter cell shape (Brunette *et al*, 1988; Chehroudi *et al*, 1995). It is well known that cell shape can regulate cell growth (Folkman and Moscona, 1978), and alter cellular gene expression (Ben-Ze'ev, 1987; Ben-Ze'ev, 1991; Werb *et al*, 1986; Hong and Brunette, 1987; Chou *et al*, 1995) and differentiation (Watt *et al*, 1988). Despite this, little is known about the effects of surface topography on properties associated with cell shape changes, such as gene expression. The signals received by a cell that cause that cell to change shape are not known and therefore neither is the mechanism of cellular contact guidance.

CELL MIGRATION

Cell migration plays a central role in a variety of biological phenomena. Processes that depend on cell migration include: organ formation; embryogenesis (Nakatsuji *et al*, 1982) ; migration of leukocytes in the inflammatory response; germ cell migration; tumour cell migration into the circulatory system during metastasis (Parish *et al*, 1987).

In an *in vitro* study, Curtis *et al* (1995) investigated the effects of various grooved substrata on the speed of cell movement. They found that the speed of movement of endothelial and epitenon cells was significantly increased when cells were grown on microgrooved silica, compared with flat (planar) surfaces. Neuronal extension was also increased almost four-fold on the grooved substrates. These observations led Curtis *et al* (1995) to suggest that such cell behaviour should have a major effect on the speed of tissue repair. Cell migration is crucial to tissue engineering, playing an important role in colonization of biomaterials and mechanical interlocking of tissue to implant; efficient wound healing also relies on migration of fibroblasts and vascular endothelial cells.

TISSUE ORGANISATION

Attachment and orientation of cells on a particular surface topography will affect the subsequent attachment and growth of further cells that are layed down, thereby affecting the overall organisation of the tissue being formed (Gumbiner, 1996). Contact guidance is believed to be the major cue in many developmental processes, as cells in the developing embryo must somehow be guided to the appropriate position for normal tissue formation to occur. In contrast, aberrant cell guidance, during development, can result in pathological processes such as congenital abnormalities and can also be responsible for cell invasion during tumourigenesis (Parish *et al*, 1987). Specific guidance of cells is also essential for satisfactory repair and regeneration of wounded tissue, for example in tendon and nerve injuries.

OTHER DIRECTIONAL CUES

Cell behaviour *in vivo* will be influenced not only by the topography of the surrounding substrate, but by other environmental factors such as adhesive, chemotactic, or galvanotropic cues. Evidence from *in vitro* experiments (Clark *et al*, 1987) has shown that BHK cells can detect adhesive cues in the presence of topographical cues. When the upper surface of perspex (PMMA [polymethylmethacrylate]) steps was made less adhesive for cells than the wall and floor of the steps, then cells were more likely to cross steps in the direction of lower to higher adhesiveness than in the opposite direction, on these substrates. Britland *et al* (1996) superimposed adhesive tracks over shallow grooves (1μm deep) and found that, at this groove depth, neurites (rat dorsal root ganglion [DRG] cells) aligned preferentially to the adhesive cue. But, as groove depth was increased the neurites aligned increasingly to the grooves.

Chemotactic cues have also been shown to play an important role in cell guidance. Chemotaxis is a response to chemical signals in which movement is affected by the gradient of a diffusable substance. For example, chemotaxis is observed when the single cells of the slime mould, *Dictyostelium discoideum*, respond to chemical gradients of cyclic AMP (adenosine monophosphate) as they congregate into a multicellular body (Bray, 1992). The chemotactic nature of cytokines is also important in their role in the immune response, where certain cytokines (for example, type 1 interferon; tumour necrosis factor [TNF] and interleukin-1 [IL-1]) have a pro-inflammatory effect and others (for example, IL-2; IL-4 and transforming growth factor-β [TGF-β]) regulate activation, growth and differentiation of B- and T-lymphocytes (Abbas *et al*, 1991).

Neutrophils are cells which show strong chemotactic responses and are believed to use chemotaxis to migrate from blood vessels through connective tissue, towards sites of infection or tissue injury. Wilkinson and Lackie (1983) studied neutrophil guidance on aligned fibrin gels, where a chemotactic cue had been placed in competition with the topographic cue. They found that the chemotactic response was more efficient when the cells were moving in the axis of alignment of the fibrous gels than if the cells had to cross the aligned fibres.

The galvanotactic response of cultured neuronal growth cones, where neurite growth is directed towards the cathode in a DC (direct current) electric field, has been shown to be modified by topographic features (McCaig, 1986). This provides further evidence for the interaction between various cell guidance cues. It is likely that both physical (topographic and mechanical) and chemical (adhesive) cues are involved in contact guidance *in vivo*, to varying degrees, depending on the cells and tissue involved.

DIFFERENT SUBSTRATES

ROUGH/POROUS

In Vitro Studies

Rich and Harris (1981) found that macrophages prefered to attach to rough tissue culture plastic rather than smooth, whereas fibroblasts preferred the smooth surface. Roughness has also been shown to affect the adhesion of platelets to hydrophobic and hydrophilic surfaces (Zingg *et al*, 1982). Studies by Clark *et al* (1987) found that exposure of perspex plastic to oxygen plasma initially roughens the surface of the plastic and increases its adhesiveness for BHK (Baby Hamster Kidney) cells. But continued exposure, though increasing roughness, did not further increase surface adhesiveness. This oxygen plasma etching would alter the surface chemistry of the perspex, therefore the observed effects may not have been due to topography alone.

"Roughness" implies a non-uniform surface topography that is less well-defined than other, easily reproducible, surface topographies, such as grooves. These studies demonstrate the difficulty in defining roughness, as it is difficult to determine whether the cells are responding to the general roughness of a certain substrate, or a more specific topographic (or chemical) cue.

In Vivo Studies

Many implants used in clinical applications (for example, dental, orthopaedic, and cardiovascular prosthesis (Chehroudi *et al*, 1990; Clark *et al*, 1974; Thomas and Cook, 1985; Thomas *et al*, 1987) have rough or porous surfaces, which can differ even among implants with identical applications. Some implants have been specifically designed with porous surfaces, as studies have suggested that porous surfaces can enhance mechanical-interlocking of tissue and implant, thus stabilizing the device (Haddad *et al*, 1987). This can be especially useful in

bone-contacting implants, as motion at the implant-tissue interface can be reduced, resulting in quicker osseointegration of the prosthesis (Pilliar *et al*, 1986; Aspenberg *et al*, 1992).

SPIRALS

Using a spiral structure of width 10μm and depth 3μm, etched into quartz, Dow *et al* (1987) reported that the structure acted as a trap for BHK cells. Cells near the centre of the spiral did not spread well, whereas cells further from the centre of the spiral, in regions of lower curvature, spread more completely. Following the work of Stoker *et al* (1968) on anchorage dependence of cell growth, Maroudas (1972) grew BHK cells on glass beads of varying diameter and found a threshold for cell growth existed at 50μm. Beads of larger diameter tended to produce multilayers of cells and smaller diameters did not support cell growth. This discovery was supported by Dunn (1982) who also reported an affect of topographical curvature on cell spreading. He showed that cells attached, but were unable to spread, on spheres with small radii (less than 50μm). This may be because the cells are unable to make successful protrusions, a necessary requirement for cell spreading, in any direction.

GROOVES

In Vitro Studies

Various types of grooved substrata have been used to study cell attachment, migration, and guidance. These structures include both v-shaped (Chehroudi *et al*, 1990; Ohara and Buck, 1979; Dunn, 1982; Brunette, Exp. Cell Res., volumes 164 and 167, 1986; Brunette, 1988) and vertical (Clark *et al*, 1990; Wood, 1988; Meyle *et al*, 1991) parallel grooves, with dimensions ranging from: 130nm - 162μm wide; 100nm - 92μm deep; 2μm - 220μm repeat spacing (pitch). In general, it has been found that cells align to the long axis of microfabricated parallel grooves.

Using v-shaped grooves, Brunette *et al* (Exp. Cell Res., volumes 164 and 167, 1986) found no effect on degree of cell orientation when varying repeat distance and groove depth, but subsequently Brunette and coworkers showed that cell orientation was dependent on groove depth (Chehroudi *et al*, 1990; Chehroudi *et al*, 1992; Hong and Brunette, 1987). These contradictory results may have occurred due to the fact that many of the initial experiments were carried out using grooved structures that had dimensions larger than the size of a typical cell. Dunn and Brown (1986) showed improved alignment of chick heart fibroblasts on structures of narrower ridge (space between grooves) width, when the cells were grown on grooved substrata with varying groove width, ridge width, and groove depth. They concluded that, over the range 1.6μm - 9.0μm groove width and 1.4μm - 23μm ridge width, spacing between grooves is more important in alignment than groove width.

A subsequent study carried out by Clark *et al* (1990) claimed that groove depth was of greater importance in determining cell alignment than pitch or width. Using vertical parallel grooved substrata of varying dimensions, and three different cell types (BHK, chick embryo neurons, and MDCK [Madin Darby Canine Kidney]), they showed that groove depth had a significant effect on cell alignment whereas repeat distance had little effect. In further studies (Clark *et al*, 1991) they have shown that ultrafine grooved substrata (260nm wide; 100nm - 400nm deep), that mimic the topography of the extracellular matrix *in vivo*, have the same effect on cell guidance. It was also found that the guidance displayed by cells on both nano- and micro-grooved structures was cell-type dependent and was inhibited by cell-cell interactions.

Wood (1988) used a cell type known to be contact guided *in vivo*, teleost fin mesenchyme cells, to demonstrate that on multiple grooved substrata of various widths highest cell alignment was observed on substrata with the largest groove

width, in this case 3μm. On these structures cell migration within individual grooves was commonly observed, whereas when the width of the ridges (areas separating grooves) exceeded that of the grooves, or the groove width was reduced below 2 μm, the fin mesenchyme cells rarely conformed entirely to the grooves and were likely to bridge across grooves. Wood concluded from these results that there may be a minimum threshold width of groove, somewhere between 2μm and 3μm, to which migrating fin mesenchyme cells are able to conform, such that the entire cell margin is confined within an individual groove.

In Vivo Studies

The properties of contact guidance exhibited *in vitro* by grooved substrates have been exploited to enhance the performance of dental implants. It was shown by Chehroudi *et al* (1990 and 1992) that percutaneous dental implants with parallel grooved surfaces resulted in an inhibition of epithelial downgrowth, a problem that can lead to implant loss.

ROLE OF PROTEIN PHOSPHORYLATION IN CELL ADHESION

Covalent modification of proteins by tyrosine phosphorylation is strongly implicated in the formation of adhesive complexes. Upon cellular adhesion to a substratum or extension of a filopodium, a group of cytoskeletal-associated proteins (as described previously) are phosphorylated on one or more tyrosine residues. Focal adhesion kinase (FAK), paxillin, and tensin are among the most prominent of these phosphoproteins that comprise adhesive complexes (Lo *et al*, 1994; Schaller *et al*, 1992; Turner, 1994).

Although there is no convincing evidence yet available to demonstrate a definite role for either FAK, tensin, or paxillin in formation of adhesive structures, these molecules are prime candidates. The reasoning for this lies in the fact that they are among the earliest adhesive proteins to undergo phosphorylation, and inhibitors of tyrosine phosphorylation inhibit their phosphorylation and diminish cell migration and spreading (Burridge *et al*, 1992). A mechanism through which these molecules contribute to the formation of adhesive complexes remains to be clarified, but tyrosine phosphorylation of each of the proteins, paxillin, tensin, and FAK, creates recognition sites for proteins containing src-homology 2 (SH2) domains. These sites, in conjunction with their other binding sites, are likely to play key roles in the formation of adhesive complexes. For example, FAK can bind src-related tyrosine kinases, including fyn, csk, and src, via its SH2-binding domain; it also has binding sites for structural proteins such as paxillin, talin, and integrins (Schaller and Parsons, 1994; Chen and Guan, 1994; Chen *et al*, 1995). In addition to its binding properties, FAK exhibits tyrosine kinase activity itself and is therefore able to phosphorylate cytoskeletal-associated substrates such as src and paxillin. This, in turn, could initiate further recruitment of structural and signalling components (Schaller and Parsons, 1995). Paxillin also has many SH2-binding domains, an SH3-binding domain, and binds structural components such as vinculin as well as signalling molecules, including src, csk, FAK, and crk (Schaller and Parsons, 1995; Turner, 1994). Tensin binds to src and paxillin through its SH2 domain and also to actin and other SH2 - containing proteins via other domains. Thus, through these multiple binding domain proteins, the structural components of the cell are linked to signalling pathways which may have a key role in regulation of cell shape changes.

Although the exact mechanism of adhesion complex formation is not known, certain molecules that regulate the generation of adhesive complexes have been identified. There is evidence that members of the rho subfamily of the ras family

of GTP-binding proteins, namely cdc42, rac, and rho, play a major role in regulating the formation of adhesions . These regulatory proteins comprise a cascade that initiates the formation of filopodia, lamellipodia, focal adhesions, and stress fibres (Hall, 1994). Formation of filopodia and lamellipodia is regulated by cdc42 and rac, respectively. Focal adhesion formation is regulated by rho (Ridley and Hall, 1994). The mechanisms through which cdc42, rac, and rho exert their effects are not known, but as the processes they control each involve distinct organisations of F-actin, they may have a role in regulation of actin-binding proteins. Possible intermediary messengers involved in this signalling cascade are: tyrosine kinases, including focal adhesion kinase (FAK), which is thought to initiate formation of adhesions; lipid kinases, including phosphatidylinositol phosphate (PIP) 5- and phosphatidylinositol (PI) 3-kinases. PIP 5-kinase makes PIP_2, which is implicated in the assembly of actin filaments, and PI3-kinase is implicated in chemotactic responses and modulation of integrin affinity; also phospholipase Cγ, which is required for platelet-derived growth factor (PDGF)-, insulin-like growth factor-1 (IGF-1)-, and epidermal growth factor (EGF)-induced migration, probably via hydrolysis of PIP_2 and mobilisation of actin-binding proteins.

Evidence that signals can be generated when cells make adhesions to substrates, and that the actin-based cell motor responds to these signals, has meant that the control of cell motility can no longer be thought of as being under the exclusive control of mechanical effects of adhesive pathways regulated by chemotactic signals from diffusable molecules. Instead, cells could use their sense of "touch" to respond to topographical cues and thereby produce signals to generate the appropriate cellular response (Gingell, 1993).

EXPLOITATION OF CONTACT GUIDANCE FOR TISSUE REPAIR

TENDON HEALING

Tendons are structures which transmit the forces of muscle contraction to bones, thereby producing movement at joints. In order to carry out this specialised function tendons must be strong, flexible and have the ability to glide between the walls of synovia. These properties are reflected in the structure of tendons: strength and flexibility are provided by a core of longitudinally arranged collagen bundles. These collagen fibres along with small numbers of fibroblasts make up the tendon proper. Ability to glide is provided by a, one or two cell thick, coating layer of synovial cells, known as epitenon cells. These cells are surrounded by less extracellular matrix than the tendon fibroblasts and their collagen fibrils are oriented randomly rather than aligned with the rest of the tendon (Reiderer-Henderson *et al,* 1983). In sites where large gliding movements take place, for example in the fingers, the tendon is enclosed in a tightly fitting fibrous synovial sheath and lubrication is provided by a thin layer of synovial fluid.

It was originally thought that, following tendon injury, formation of fibrous adhesions between the site of tendon injury and the surrounding synovial sheath was an essential part of tendon repair (Potenza, 1963). But, it has since been discovered that tendons have an intrinsic capacity for repair that begins with proliferation of epitenon cells. These cells migrate into the gap between divided tendon ends and synthesize collagen which restores strength and continuity (Wojciak and Crossan, 1993). Surgical repair is undertaken to facilitate this process by holding the tendon ends together with a core suture and a circumferential suture to approximate epitenon.

The main, and relatively common, complication following tendon repair is formation of fibrous adhesions between tendon and synovial sheath due to uncontrolled migration of epitenon and synovial cells into the synovial space (Figure 1). These adhesions cause considerable disability by preventing tendon gliding movements, and often result in stiffness and deformity in the affected joints.

Attempts to reduce adhesion formation have been largely unsuccessful. The least successful approach has been treatment with anti-inflammatory agents or drugs which block collagen synthesis, and the most successful has been the introduction of passive mobilisation programmes in the first six weeks following tendon surgical repair. Controlled passive movements reduce the severity of adhesion formation but require great patient cooperation and awkward plasters or mechanical devices strapped to the patients hand for at least four weeks. Also, mobilisation therapy still produces a number of unsatisfactory results and repairs after crush injury, or those involving concomitant bone or nerve injury, cannot benefit from mobilisation and are therefore still subject to severe adhesion formation (Rothkopf *et al*, 1991).

Therefore, it would be beneficial to be able to guide and orientate the growth of epitenon cells between the ends of a divided tendon, in order to reduce the haphazard migration of epitenon and synovial cells and thereby minimise adhesion formation. It would also be of benefit if inflammatory cells and their cytokine products could be excluded from the site of tendon repair as these are major factors in adhesion formation. Development of a biodegradable plastic sheath with microgrooves on one surface, that could be wrapped around tendon repairs at the time of surgery, would serve the dual purpose of guided epitenon cell growth and also exclusion of inflammatory infiltrate at the site of tendon repair (see Curtis and Wilkinson patent's; Wojciak *et al*, 1995).

Figure 1. Schematic drawing showing the anatomy of a healthy intrasynovial flexor tendon (upper diagram), and an immobilised tendon that is healing by adhesion and endotenon cellular ingrowth (lower diagram). (After Gelberman *et al*, 1983).

Flexor tendon healing and restoration of the gliding surface

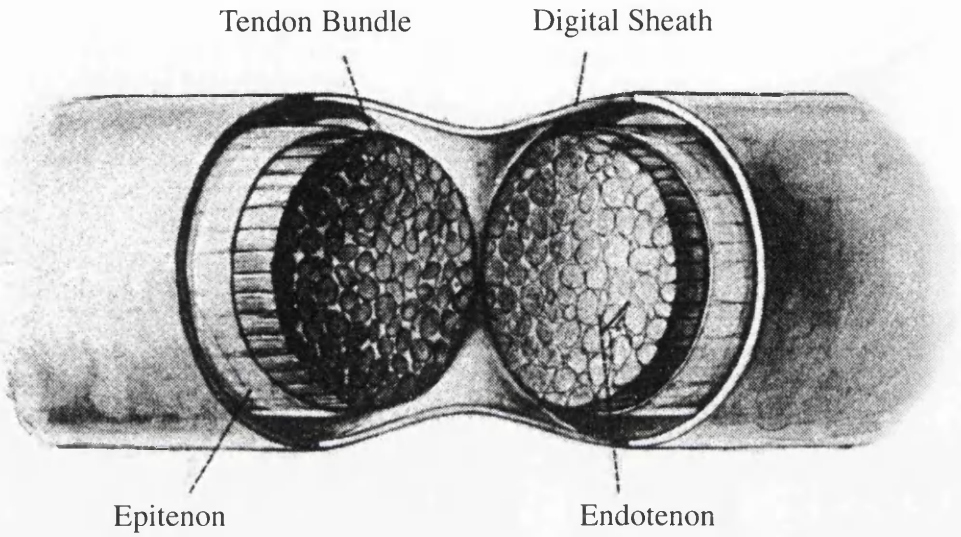

Anatomy of an intrasynovial flexor tendon

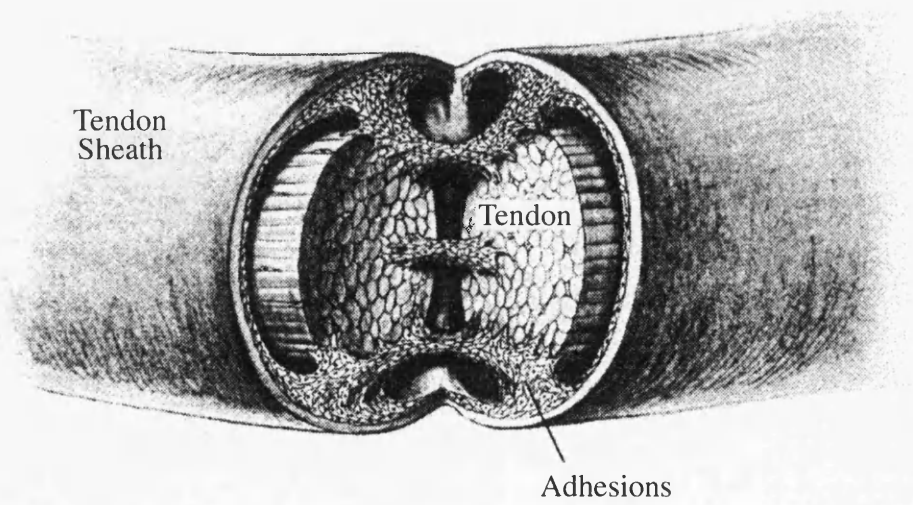

Adhesion formation in a healing tendon

OTHER TISSUES

Obviously the use of a grooved implant as a cell guidance mechanism *in vivo* would not be exclusively beneficial to healing of tendons. Many other tissues would benefit from the design of such an implant, for instance the guidance of endothelial cells in angiogenesis, or of regenerating nerve axons. Brunette *et al* (1983) have already designed grooved titanium implants in an effort to encourage attachment of the gum epithelium.

SUTURE MATERIALS

HISTORY

Historically, catgut was the surgeon's favoured suture material due to the absence of any alternative absorbable suture. "Catgut" suture is fabricated from intestinal collagen (usually ovine or bovine) and can be used as "chromic" (treated with chromium to form chemical crosslinks in the collagen, thereby prolonging its biodegradation) or "plain". The suture material is now radiation sterilised, but previously ethylene oxide and heat sterilisation have been used (Dr Grant Robertson, Ethicon Ltd.). However, as catgut is degraded through attack by cellular enzymes, the typical inflammatory response around the suture and its unpredictable time of absorption led to the search for a suitable synthetic replacement material (Lerwick, 1983). This material would, ideally, possess the positive traits of collagen, namely strength and ease of absorption, combined with a predictable absorption time and minimal tissue reaction.

Advances in polymer science led to various synthetic fibres, for example polyamides such as nylons, and polyesters such as Dacron and Terylene, being used for sutures with varying degrees of success. In the nineteen fifties efforts were directed towards synthesizing polymers specifically suited to surgical

applications. The first product possessing reasonable biological and physical properties, a braided polyester suture made of poly-L-lactide, was created, in the nineteen sixties, by Du Pont Research Laboratories. Although strong and inert, this suture material was not ideal as it absorbed much more slowly than catgut and collagen, the other absorbable sutures available at the time (Artandi, 1980).

POLYDIOXANONE SUTURE MATERIAL (PDS)

Postlethwait described the first commercially available synthetic absorbable suture, also a braided polyester, polyglycolic acid, in 1970. This was followed in 1974 by another polyester suture, polyglactin 910, a copolymer of lactide and glycolide (Conn *et al*, 1974). Polyglactin 910, Vicryl suture, and polyglycolic acid, Dexon suture, offer improved and predictable tensile strength retention and also low tissue reaction, as they are absorbed in the body by hydrolysis rather than enzymatic degradation.

Although these sutures were an improvement on natural catgut sutures, the inherent rigidity of the polymers meant that monofilament sutures produced from polyglycolic acid and polyglactin 910 were too stiff for general surgical use and could only be used in the very finest sizes. The handling characteristics were improved by braiding fine filaments of the polymers. However, this was not an ideal solution as various studies (Owens and Rubbra, 1946; Chu and Williams, 1984) have shown that the topography of braided sutures can encourage selective adherence of pathogenic bacteria at the site of the wound. This led researchers on the trail of a more flexible, and preferably monofilament, synthetic absorbable suture material.

A novel monofilament synthetic absorbable suture fulfilling the necessary flexibility, strength, and biocompatibility requirements was developed at the Research and Development Division of Ethicon Inc., in Somerville, New Jersey,

U.S.A. (Ray *et al*, 1981). The suture is called polydioxanone (PDS) and is derived from a unique polymer that can be processed into a flexible monofilament suture. The empirical formula of the polymer is $(C_4H_6O_3)n$ (Figure 2). Synthesis of the polyester suture, poly (p-dioxanone), involves polymerizing the monomer, para-dioxanone, in the presence of a suitable catalyst (stannous octoate). The resulting product is polydioxanone, a colourless, crystalline polymer which, either dyed or natural, is processed into small granules, dried, and melt extruded into monofilaments of any desired suture size. A dyed version of the suture is achieved by adding drug and cosmetic violet No.2 dye. The monofilaments are then oriented and heat treated in order to achieve a smooth monofilament with optimum biologic and physical properties.

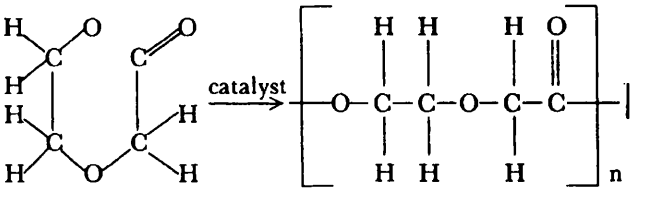

para-dioxanone **poly-p-dioxanone**

Figure 2. Structure of the polyester, poly-p-dioxanone, synthesised from para-dioxanone monomer (After Lerwick, 1983).

The general mechanism by which *in vivo* degradation of polydioxanone occurs is by non-enzymatic hydrolysis of the ester bonds (the ultimate product of hydrolytic breakdown, after metabolism in the body, being sodium-B-hydroxy ethoxyacetate). This results in a mild tissue reaction during absorption of the suture material, as no cellular activity is required. Pre-clinical studies (Ray *et al*, 1981) using ^{14}C-labelled polydioxanone suture found that absorption of the

suture from rat muscle was complete by approximately 180 days. Furthermore, ^{14}C-label did not accumulate in any organ or tissue following suture absorption, indicating that the degradation products of the suture are rapidly excreted by the body. Polydioxanone also possesses a much higher degree of flexibility when compared with other polyester sutures, monofilament polyglactin 910 suture and polyglycolic acid suture. This flexibility is achieved due to the ether oxygen group present in the backbone structure of the polydioxanone.

Studies carried out by Ray *et al* showed that the strength of monofilament polydioxanone suture prior to implantation exceeds that of non-absorbable monofilament sutures. Also, its strength is maintained *in vivo* much longer than that of braided synthetic absorbable sutures. Data obtained from implantation studies in rats show the following absorption profile for polydioxanone monofilament suture: 14 days post-implantation the suture retains 70% of its breaking strength; 28 days post-implantation the suture retains 50% of its breaking strength; 56 days post-implantation the suture retains 14% of its breaking strength. The absorption, or loss of mass, of the polydioxanone is minimal until around the 90th post-implantation day and is essentially complete within 180 days (Ethicon Limited, Edinburgh, UK). This compares favourably with the absorption of braided synthetic absorbable sutures which retain only 1-5% of their strength 28 days post-implantation (Ray *et al*, 1981).

During pre-clinical trials, the tissue reaction elicited by polydioxanone was judged to be slight to minimal for all sizes of polydioxanone and all timeperiods tested (Ray *et al*, 1981). Cellular responses were localised to the implant site (in rat gluteal muscle) and were primarily mononuclear in character. A small number of macrophages and proliferating fibroblasts were present 5 days post-implantation, but neutrophils, foreign body giant cells, eosinophils and lymphocytes were rarely seen. At 91 days and later, only macrophages and

fibroblasts were consistently present at implant sites until the suture was completely absorbed. Post-absorption, tissue reaction was either absent or characterised by the presence of a few enlarged macrophages or fibroblasts localised between otherwise normal muscle cells. Occasionally, after absorption of the suture, a small number of fat cells were noted to occupy the implant site.

Clinical studies carried out by Lerwick (1983) supported the results of the pre-clinical trials conducted by Ray *et al* (1981). Lerwick's clinical trials involved a comparison of either dyed or undyed polydioxanone monofilament absorbable suture with surgical gut suture in nine "performance characteristics": visibility; pliability; strength; ease of passage; ease of tying; fraying; knot security; overall handling; final evaluation. The overall characteristics of dyed and undyed polydioxanone monofilament absorbable sutures were found to rate as "significantly better" than surgical gut sutures in every operative procedure performed.

AIMS

The purpose of this research was to investigate the possible use of polydioxanone suture material as a suitable substrate for fabrication of a microgrooved implant that could be used to facilitate wound repair. *In vitro* and *in vivo* experiments would be carried out to investigate cellular reactions to the polydioxanone structures. Although cellular alignment on grooved microstructures had been observed previously, it was also hoped to further elucidate the molecular mechanisms involved when cells respond to topographical stimuli, as cellular reactions to topography at the molecular level have not been widely investigated.

CHAPTER 2

MATERIALS AND METHODS

CELLS AND CELL CULTURE MATERIALS

Baby Hamster Kidney Cells (BHK)

BHK 21 clone 13 (Stoker and MacPherson, 1964), obtained from stocks routinely grown in the Centre for Cell Engineering (University of Glasgow) were cultured in Glasgow modified Eagle's Minimal Essential Medium (GMEM) (Gibco Life Technologies Ltd., Paisley, UK), containing 10% calf serum (Gibco) and 10% tryptose phosphate broth (Sigma Chemical Co., Poole, England) (ECT medium). This was supplemented with 5ml of 7.5% bicarbonate (BDH, Merck Ltd., Lutterworth, England) and GPSA. GPSA is a mixture containing glutamine (3mM) (Sigma), penicillin (48U/ml), streptomycin (48U/ml) and the antimycotic fungizone amphotericin B (0.3μg) (All from Gibco). Cells were used when the culture had attained or almost attained confluency.

Madin-Darby Canine Kidney Cells (MDCK)

MDCK cells (Gausch *et al*, 1966), an epithelial cell line, obtained from stocks routinely grown in the department were cultured and maintained in Dulbecco's Modified Eagle's Medium (Gibco), containing 10% calf serum; 10% tryptose phosphate broth; and supplemented with 5ml of 7.5% bicarbonate and GPSA.

P388D1 Macrophages

This mouse macrophage-like cell line (Koren *et al*, 1975) (a gift to the lab from Prof. P. Bongrand, Marseille) was cultured from cell stocks. Cells were grown in RPMI (Roswell Park Memorial Institute) 1640 medium (Gibco), supplemented

with 10% fetal calf serum, 20mM Hepes buffer (N-2-hydroxyethylpiperazine-N'-2-ethanesulfonic acid, pH 7.4) (Sigma), 10ml of 7.5% bicarbonate, and GPSA.

Epitenon Cells

Epitenon cells were isolated according to the method described by Wojciak and Crossan (1993). The cells were cultured in GMEM medium as described for BHK21 cells and used for up to 30 passages.

Human Osteosarcoma Cells (MG-63)

This cell line (obtained from stocks at Ethicon Ltd., Edinburgh) was cultured and maintained in Minimal Essential Medium (MEM) (Gibco), supplemented with 10% fetal calf serum, GPSA, and 1% non-essential amino acids.

MISCELLANEOUS MATERIALS USED

Hanks HEPES Buffer

Sodium chloride	8g
Potassium chloride	0.4g
Calcium chloride ($2H_2O$)	0.19g
Magnesium chloride ($6H_20$)	0.2g
D-Glucose	1g
HEPES	2.38g
Phenol Red	0.5%

Made up to 1 litre with deionised water and pH adjusted to 7.5 with 5M NaOH.

HEPES Saline

A calcium- and magnesium-free HEPES buffered balanced salt solution, suitable for washing cell monolayers prior to trypsinisation:

Sodium chloride	8g
Potassium chloride	0.4g
D-Glucose	1g
HEPES	2.38g
Phenol Red	0.5% (2ml)

Made up to to 1 litre with deionised water and pH adjusted to 7.5 with 5M NaOH.

HEPES Buffered Water

A non-isotonic buffer solution for dilution of cell culture media x10 concentrates:

HEPES (Sigma)	5.25g

Made up to 1 litre with deionised water and pH adjusted to 7.5 with 5M NaOH.

'Versene'

A HEPES buffered balanced salt solution containing EDTA (Ethylenediaminetetra acetic acid), for use in conjunction with trypsin for the dissociation of cell monolayers:

Sodium chloride	8g
Potassium chloride	0.4g
d-Glucose	1g
HEPES	2.38g
EDTA	0.2g
Phenol Red	0.5% (2ml)

Made up to 1 litre with deionised water and pH adjusted to 7.5 with 5M NaOH.

(HEPES and Phenol Red were from Sigma; all other materials were from BDH-Merck Ltd., Lutterworth, Leics., England).

Trypsin-Versene

(Trypsin stock - 2.5% w/v in physiological saline)

0.25 % v/v trypsin (Gibco) in Versene, pH=7.5 (1:40 dilution)

Tryptose Phosphate Broth

In 1 litre of deionised water, 29.5g of tryptose phosphate powder (Sigma) were suspended. This was mixed thoroughly, boiled and dispensed in 100ml aliquots.

Sodium Bicarbonate

A 7.5% solution of Sodium Hydrogen Carbonate (BDH-Merck) in high quality water: In 1 litre of deionised water, 75g of sodium bicarbonate were dissolved. When fully dissolved, the solution was sterilised by Millipore ultra-filtration (0.2μm pore size) and dispensed in 20ml aliquots.

Phosphate Buffered Saline (PBS)

Sodium chloride	8g
Potassium chloride	0.2g
Na_2HPO_4 (di-sodium hydrogen orthophosphate)	1.15g
KH_2PO_4 (potassium di-hydrogen orthophosphate)	0.2g

Made up to to 1 litre in deionised water and pH adjusted to 7.2 with 5M NaOH. (All reagents were from BDH-Merck).

Buffered Formaldehyde

To 900ml of Phosphate Buffered Saline, 100ml of formaldehyde (40%) (BDH-Merck) were added.

SUBSTRATUM PATTERNING

FABRICATION OF GROOVED STRUCTURES IN FUSED SILICA

Fused silica (quartz) samples (Multi-lab) were cut into 25mm^2, 1mm thick samples. The silica was cleaned by soaking in a solution of 3:1 sulphuric acid: hydrogen peroxide for 5-10 minutes at 80°C followed by a rinse in R.O. (reverse osmosis) water, then blow dried with filtered air. The silica was coated with AZ 1400-31 photoresist (Shipley) by spinning on at 4000 rpm for 30 seconds followed by a soft bake at 90°C for 30 minutes. This gave a resist thickness of 1.8μm. The resist was then patterned by exposing to ultraviolet light, through a chrome mask patterned with the required grating pattern, using a mask aligner (HTG) for 10 seconds. The exposed resist was developed by immersing the sample in a solution of 1:1 Shipley developer: R.O. water for 65-75 seconds folowed by a rinse in R.O. water, then blown dry.

The exposed silica was dry etched using a Reactive Ion Etch Unit (Plasma Technology). The following parameters applied:

Gas - Trifluoromethane

R.F. Power - 100 watts

D.C. Bias - -400 volts

Etch Rate - 2μm/hour

After etching the residual resist was removed, and all samples were blanket etched for 1 minute (see Figure 3).

FABRICATION OF GROOVED STRUCTURES IN POLYDIOXANONE SUTURE MATERIAL (PDS)

PDS granules were melted between two glass slides at 120°C. The PDS was allowed to cool, then cut into four and re-melted between two scratch-free

Figure 3. Diagram representing the quartz (fused silica) microfabrication process.

FABRICATION OF QUARTZ TEMPLATE FOR PDS PATTERNING

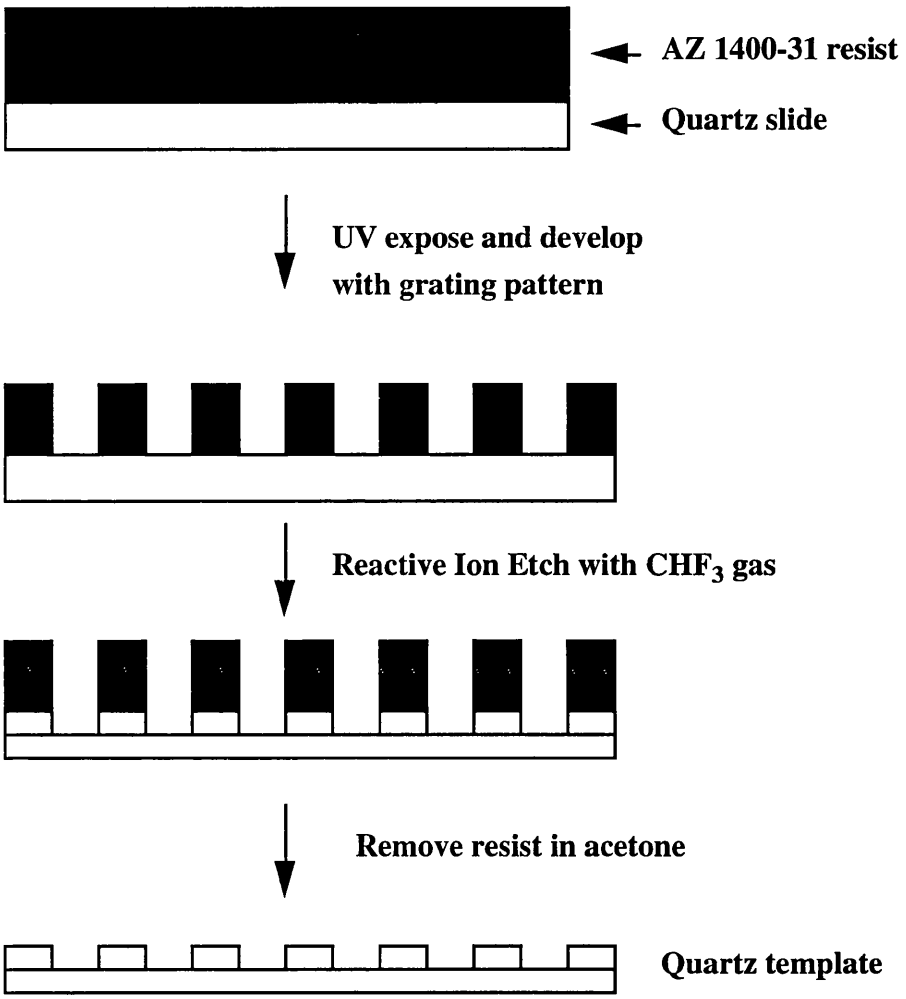

Figure 4. Diagram representing the method of fabrication of microgrooved PDS structures, using a quartz template.

PREPARATION OF PATTERNED PDS

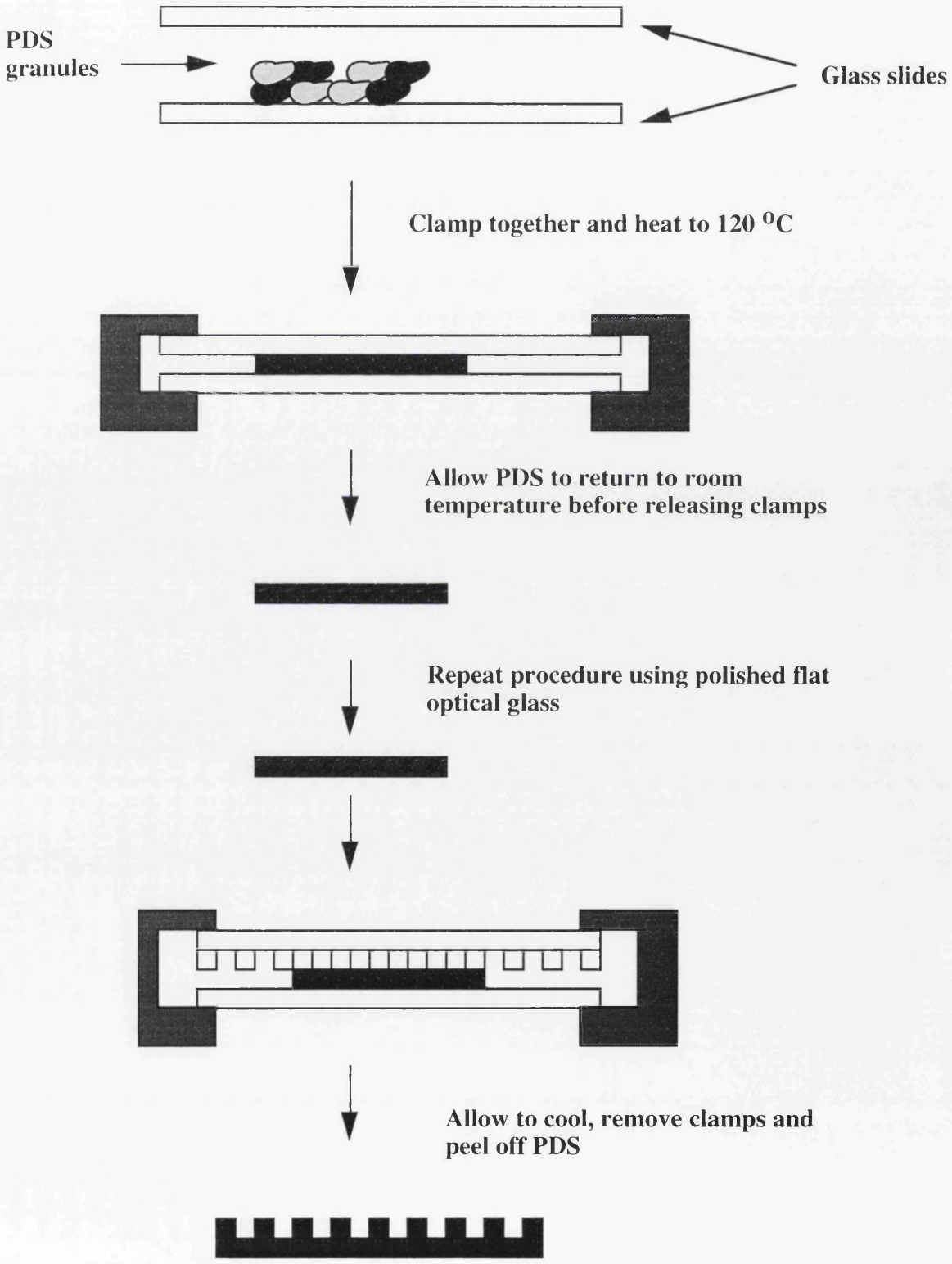

optically flat glass plates (in order to prevent unwanted cell guidance), held together by spring-loaded clamps. This gave a flat PDS substrate.

After cooling again, the pressure was released and one of the glass plates was removed and replaced with a patterned quartz template (fabricated as described above). The clamps were then loaded; reheated to 120°C; and allowed to cool. Once cool, the patterned PDS structure was peeled from the quartz template (see Figure 4).

"CELL LAWN EXPERIMENT"

Microgrooved quartz structures were washed in Caro's acid (concentrated sulphuric acid/hydrogen peroxide, 3:1, at 66°C); sterilized in 70% ethanol; then left in ECT (Eagles Calf serum Tryptose phosphate broth) medium (for at least 5 minutes). The structures were then placed in a tissue culture plastic petri dish and 5ml cell suspension (at concentration of approximately $5x10^5$ cells/ml) added. Cells were grown until confluent on grooves.

Fluorescein diacetate (5mg/ml) was diluted 1:50 in ECT medium, at room temperature. Immediately, one volume of fluorescein diacetate suspension was added to nine volumes cell suspension (cells at concentration of $4x10^4$ cells/ml) and the mixture allowed to stand at room temperature for 15 minutes. The cells/fluorescein diacetate were centrifuged (speed 2000 r.p.m., for 6 minutes) and cells resuspended in 5ml ECT medium. The ECT medium was then removed from the structures and the fluorescent cell suspension added. This was left for approximately 10 minutes, to allow cells to settle.

Random fields on each structure were examined under a fluorescence microscope (Vickers) and the number of fluorescent cells per field that had attached on the grooved/non-grooved surfaces counted. (Non-grooved surface being flat area of quartz surrounding grooves).

CELL ADHESION TO PDS STRUCTURES *IN VITRO*

PDS structures (approximately 0.5cm^2), with both grooved (6μm deep; 12.5μm wide) and flat areas on their surface, were placed into 60 x 35mm tissue culture dishes (Nunc). Epitenon cells and P388D1 macrophages were plated onto the structures, at a concentration of 2 x 10^4 cells/ml and the dishes were placed in a CO_2 incubator (Heraeus). Fixation of cells was carried out (according to the method for fixation of cell cultures for scanning electron microscopy [SEM]) at 1 hour, 4 hour, and 24 hour time intervals. The cells/structures were then examined and photographed using the SEM.

From SEM images, the numbers of rounded and spread cells on the grooved and flat surfaces were counted, using a Vidas Image Analysis programme.

IMPLANTATION OF PDS MICROGROOVED PLATES

Grooved PDS plates (cut to 10mm x 5mm) were implanted intramuscularly in rats (male, Sprague Dawley) for 7, 21, 35, 49, 70 and 91 days. Grooves (approximately 6μm deep and 12.5μm wide) were oriented along the long axis of the implants, which were placed in pouches in the lumbar muscle, one piece on either side of the midline. Grooves were thus oriented antero-posteriorly, parallel with the muscle fibres.

After the requisite periods in tissue, one of the implants and surrounding muscle tissue was removed, fixed in formalin and processed to thin sections by wax histology (two blocks per implant). Ethicon Trichrome stain (Haematoxylin, Saffron, Phloxine) was used (see "Histology" methods below). Sections were examined under the light microscope for analysis of effects on the implant and also the local tissue reaction.

The remaining implant, and surrounding tissue, was cut into two halves, one of which was processed as above (one block) and the other prepared for scanning electron microscope (SEM) examination, after glutaraldehyde fixation and critical-point drying.

HISTOLOGY

Tissue was fixed in neutral buffered formalin for forty eight hours; dehydrated; and embedded in tissue wax. Five micron sections were cut using a Leitz rotary microtome; mounted on 76x22mm glass slides (Fisher/Raymond A. Lamb); then dried on a hot plate for at least one hour.

STAINING

Tissue sections were dewaxed in Citroclear (HD Supplies) for 5 minutes, then transferred to clean Citroclear for a further 5 minutes. Sections were then placed into industrial methylated spirit (Tennants [BP Chemicals]) for 5 minutes, transferred to fresh industrial methylated spirit for a further 5 minutes, then rinsed in tap water for 5 minutes. Lillie's haematoxylin (made up in-house) was used to stain the sections for 5 minutes, then sections were rinsed again in tap water. Sections were dipped in 1% acid alcohol (made up in-house) until weak pink in colour, then placed into running tap water for approximately 5 minutes until a

colour change from blue to pink was observed. The sections were stained in 1% aqueous phloxine (Raymond A. Lamb) for 6-7 minutes; rinsed in tap water; dehydrated in industrial methylated spirit for 1 minute, then transferred to fresh industrial methylated spirit for a further 1 minute. Sections were then placed into ethanol (Hayman Ltd., 70 Eastway End Park, Withen, Essex) for 1 minute, before staining in alcoholic saffron (Raymond A. Lamb) for 7 minutes. Sections were transferred to ethanol for half a minute to rinse off excess stain; rinsed in fresh ethanol for half a minute; then rinsed in fresh ethanol for a further thirty seconds. The sections were cleared in Citroclear for 2 minutes, transferred to fresh Citroclear for 5 minutes and, finally, mounted in depex (Raymond A. Lamb).

As a result of this staining procedure collagen stains yellow/orange; nuclei stain blue/black and other tissue elements are stained shades of pink.

SCANNING ELECTRON MICROSCOPY

REAGENTS

a) Earle's Balanced Salts Solution (EBSS, Gibco).

b) 0.2M Sodium cacodylate Buffer.

c) 2% Glutaraldehyde in 0.1M Sodium cacodylate Buffer:
250ml of 0.2M Sodium cacodylate (sodium methyl arsenate) + 20ml of 50% Glutaraldehyde + 10ml of 0.2M Calcium chloride solution. The pH was corrected to 7.35 with approximately 15ml of 0.2M HCl and water added to 500ml.

d) 1% Osmium tetroxide solution in 0.1M Sodium cacodylate Buffer.

e) Acetone (Specified Laboratory Reagent [SLR]).

f) Acetone (Dried Distilled Grade).

g) Distilled Water.

h) Liquid Carbon Dioxide (Air Products).

Unless stated otherwise all products were from Fisher Scientific.

FIXATION OF TISSUE EN BLOCK

All fixation procedures were carried out at room temperature.

The tissue was washed with balanced salt solution (EBSS), in order to remove any extraneous material from the tissue surface, then placed into buffered formalin for at least 72 hours. Secondary fixation was then carried out in 2% glutaraldehyde in 0.1M cacodylate buffer. The tissue was washed in 0.1M cacodylate buffer, then post-fixed in 1% Osmium tetroxide buffered with 0.1M Sodium cacodylate (for preservation of lipids, intracellular detail by specialised techniques, or for ensuring total preservation of components of cell cultures). The tissue was then washed in distilled water to remove any remaining osmium. Tissue was then ready for dehydration.

FIXATION OF CELL CULTURES

Culture medium was discarded and cells and their substrate rinsed in EBSS. Half the volume of EBSS was removed and replaced with the same volume of 2% glutaraldehyde in 0.1M cacodylate buffer, for 2 minutes. All medium/fixative was removed and replaced with fresh cacodylate-buffered glutaraldehyde for 10 minutes. Samples were removed from the culture dish and placed into a glass petri

dish containing 0.1M cacodylate buffer, for at least one hour. The buffer was removed and samples were post-fixed in 1% Osmium tetroxide for 10 minutes. Samples were rinsed (three times) in distilled water, then dehydration was carried out.

DEHYDRATION

Dehydration of samples was carried out, in glass vessels, using graded acetone of 20%, 50%, 70%, 80%, 90%, 95%, 100% (v/v) 'SLR' grade (diluted in distilled water) and 100% 'Dried Distilled' grade strengths, successively.

Tissue samples were left in each dilution of 'SLR' grade acetone for approximately 30 minutes, and 60 minutes in the final 'Dried Distilled' grade acetone. Cell culture samples were left in each acetone dilution (including 'Dried Distilled') for 5 minutes. Samples were then critical point dried.

CRITICAL POINT DRYING

Samples were critical point dried, using liquid carbon dioxide, in a Polaron E3000 critical point drier, then mounted onto aluminium specimen stubs, using carbon adhesive discs (Agar Scientific).

Samples were then coated with approximately 5nm of gold and examined under the Scanning Electron Microscope (SEM) (Cambridge Instruments [now LEO Electron Microscopy Ltd.] Stereoscan 250, Mark 3).

FLUORESCENCE MICROSCOPY

INDIRECT IMMUNOFLUORESCENCE

Cells (at a concentration of 1 x 10^4/ml) were plated onto structures, in 60 x 15mm tissue culture dishes (Falcon), for varying lengths of time. After removing growth medium, cells were washed in (warmed) phosphate buffered saline (PBS) and fixed in 4% formaldehyde for 10 minutes. Cells were rinsed well in PBS, then permeabilised in 0.5% Triton X-100 (Sigma) in PBS (13 minutes for fibroblasts; 10 minutes for macrophages). After rinsing in PBS, non-specific binding sites were blocked with PBS/0.5% BSA (Sigma), then cells were incubated with PY20 mouse monoclonal anti-phosphotyrosine antibody (ICN), diluted 1:200, for 2 hours at room temperature. Cells were then rinsed in PBS, blocked again with PBS/0.5% BSA, and labelled with sheep anti-mouse Texas Red second antibody (Amersham), diluted 1:100, for 1 hour 30 minutes at room temperature. After a final wash in PBS, cells were rinsed once in distilled water, then structures were mounted under a 22 x 40mm coverslip (BDH) using a drop of PBS:glycerol (1:1).

The cells were examined using a Nikon Optiphot-2 microscope or Nikon confocal scanning microscope, and photographed with a Nikon FX-35DX camera or Nikon F801 camera, respectively.

Leupeptin Fast Adhesion

For fast adhesion of (non-macrophage) cells, trypsin was inhibited using 25µg/ml leupeptin (Sigma), as follows:

Following routine trypsinisation and cell detachment, cells were washed twice in 25µg/ml leupeptin (in HEPES saline) then resuspended in serum-free medium.

F-ACTIN STAINING

Cells were rinsed in warm (37°C) Hanks HEPES, then a pre-warmed solution of 0.25% glutaraldehyde/0.5% Triton X-100 in PBS was added for 1 minute. This was poured off and cells were fixed in 1% glutaraldehyde (in PBS) for 15 minutes; then permeabilised in 0.5% Triton X-100 (in PBS) for 15 minutes. Cells were rinsed three times in PBS and, after draining, incubated in 1μg/ml TRITC (tetramethylrhodamine isothiocyanate)-phalloidin (Sigma) solution (in PBS) for 1 hour. Cells were then washed twice in PBS and examined under a Leitz fluorescent microscope.

EFFECT OF TYRPHOSTINS ON BHK CELL ADHESION

BHK (Baby Hamster Kidney) cells were routinely trypsinised, then resuspended in 5ml of various Tyrphostins (Calbiochem, Nottingham, UK), ranging in concentration from 10-50μM. The cells were seeded on 22x22 mm glass coverslips (BDH), in 35x10 mm tissue culture dishes (Greiner) then left in a moist, CO_2-containing atmosphere overnight.

The following day the cells were: rinsed twice in (warmed) PBS; fixed in 4% formaldehyde (in PBS) for 10 minutes; washed 3 times in PBS; stained with Coomassie blue for 5 minutes; rinsed in distilled water. The coverslips were left to air dry then, finally, mounted on glass slides (BDH) using Histomount.

The slides were examined using a Leitz microscope, and the number of spread cells were counted for random fields.

SDS PAGE (SODIUM DODECYLSULPHATE POLYACRYLAMIDE GEL ELECTROPHORESIS)

REAGENTS

Isoelectric Focussing (IEF) sample mix

CHES (2-[N-Cyclohexylamino] Ethane-Sulfonic acid)	0.05mM	100mg
SDS	2%	200mg
Glycerol	10%	1ml

CHES (Sigma) was dissolved in 8.5ml of water and pH adjusted to 9.5. The SDS (ICN) and the glycerol (BDH) were added, then the solution made up to 10ml with distilled water. The IEF sample mix was aliquoted in 500µl volumes and stored at -20°C.

Before use 10µl 2-mercaptoethanol (BioRad) and 10µl 100mM PMSF (Phenylmethanesulfonyl Fluoride; Sigma) were added to each aliquot of 500µl.

N.B. Prior to boiling a small amount of 1% bromophenol blue (Sigma) was added (e.g. 5µl to a 100µl sample).

30% Acrylamide solution was "Easigel" from Scotlab Ltd. (Coatbridge, Strathclyde, Scotland).

Running buffer

In 50ml water, 18.15g of Tris (Tris-[Hydroxymethyl]amino-methane; ICN) were dissolved, then 0.4g of SDS (ICN) added; the pH was adjusted to 8.9 with 5M HCl and the volume made up to 100ml with distilled water.

Stacking buffer

To 90ml distilled water, 5.9g Tris, then 0.4g SDS were added; the pH was adjusted to 6.7 and the volume made up to 100ml with distilled water.

Upper tank buffer (5X concentration)

In 5 litres of distilled water, 31.8g Tris, 20.1g Glycine (Bio-rad) and 5g SDS were dissolved.

Lower tank buffer (5X concentration)

To 900ml distilled water, 60.5g Tris and 5g SDS were added; the pH was adjusted to 8.1 and the volume brought up to 5 litres with distilled water.

Stain

Coomassie blue for gels (1g Brilliant blue G [Sigma] dissolved in 1L of 500ml methanol/500ml water and 70ml acetic acid).

Ponceau stain (Sigma) for nitrocellulose blots.

Destain

To 880ml distilled water, 50ml methanol and 70ml acetic acid were added.

Transfer buffer

In 400ml of distilled water, 1.51g 25mM Tris base and 5.68g 150mM Glycine were dissolved. The pH was adjusted to 8.3 (using Tris [alkaline] or Glycine [acidic]); then the volume made up to 450ml, and 50ml of methanol added.

Tris-HCl buffer

20mM TRIZMA Hydrochloride (Sigma) in distilled water; pH adjusted to 7.4.

PREPARATION AND RUNNING OF GELS

Glass plates were cleaned with Decon and rinsed thoroughly with tap water. Plates, gasket and spacers were wiped with 100% ethanol, then assembled and held in place with clips. Water was added to the apparatus to check for any leaks, then removed and the running gel was added (7.5% or 10%, see below).

To pour slab gels:

Gel strength	**5%**	**7.5%**	**10%**
30% Acrylamide	2	6	8
Stacker/Run buffer	3	6	6
Distilled water	7	12	10
TEMED	0.005	0.01	0.01
10% A.persulphate*	0.1	0.15	0.1
Total volume(ml)	12	24	24

* Made up fresh each day.

TEMED (N, N, N', N'-Tetra-methyl-ethylenediamine) and Ammonium persulphate were from Biorad.

(Normally a 7.5% gel was used with a 5% stacker).

N.B. Only half volumes were used with the mini gel system.

The running gel was overlaid gently with distilled water and allowed to set in hot room (1 hour). When the gel had set, the water was removed; comb inserted; and stacking gel poured (see above). The stacking gel was allowed to set at room temperature (approximately 15 minutes). The comb was then carefully removed and the wells washed once with distilled water. After removing the gasket, the gel plates were placed into a tank containing lower tank buffer and held in place using

clips. Any bubbles were removed from the base of the gel plates (by gently tipping the apparatus to one side). The upper tank buffer was added and, finally, molecular weight markers and samples were loaded on the gel.

Gels were run at 25mA for 2-3 hours, or alternatively 20mA for one hour if using mini gel system.

WESTERN BLOTTING

Gel plates were removed from the tank and one corner gently prised open. A scalpel blade was used to free gel from spacers and the gel was lifted into a plastic tray containing transfer buffer. The gel was measured and two pieces of filter paper (Biometra) and one piece of nitrocellulose membrane (Hybond C-Super, from Amersham) were cut to the same size. The first piece of filter paper was soaked in transfer buffer and placed onto the blotter, followed by the gel, the membrane, then the second piece of filter paper (all of which had been soaked in transfer buffer). The lid was placed onto the blotter; tap water was run (slowly) through the system and an ice pack placed onto the lid, in order to keep the temperature down. The blotter was run at 300mA for 25 minutes, making sure the power did not exceed 20 watts.

When blotting was complete, one corner of the membrane was cut in order to indicate the uppermost surface. Membranes were stained with Ponceau S stain to check protein transfer. The membrane was placed into a hybridisation bag containing blocking solution (4% bovine serum albumin [BSA, from Sigma] in Tris-HCl), for 20 minutes, to block non specific binding of antibody. The blocking agent was removed and ^{125}I PY20 monoclonal antibody, raised in mouse (ICN), added. The antibody was used at a concentration of 1:250 (diluted in

blocking solution) and the membrane incubated, at 37°C, for two hours. The membrane was then washed twice with PBS, over one hour, and an autoradiograph was set up.

MESSENGER RNA FINGERPRINTING

REAGENTS

Diethyl Pyrocarbonate (DEPC)-treated water

To deionised water, 0.1% DEPC was added. The solution was then autoclaved.

TBE buffer (5X concentration)

In 900ml distilled water, 54g of Tris base (ICN) and 27.5g of Boric acid (Sigma) were dissolved. Then, 20ml of 0.5M EDTA pH 8.0 (Sigma) were added.

High glycerol loading dye

Bromophenol blue (0.25%, Sigma), combined with 40% glycerol (BDH) and 1% Orange G (Sigma).

ISOLATION OF TOTAL RNA

When cells had been cultured on structures (as described previously) for the appropriate timepoints, the structures/cells were removed to the lids of the tissue culture dishes and rinsed twice in PBS. The PBS was drained off, then 1ml sterile PBS was added directly to each structure and the cells were gently scraped from the surface, using a cell scraper (Sigma). The cell solution from each sample was pipetted into a sterile 1.5ml microcentrifuge tube (Scotlab) and spun at 3000 r.p.m. for 3 minutes in a centrifuge (MSE). Whilst cells were spinning, 0.9ml RNAzol (Biogenesis Ltd.) were added to each structure. The PBS was discarded from the

microcentrifuge tubes and the RNAzol was pipetted from the structures and added to the cell pellet in the appropriate tube. To each tube, 100µl of chloroform (Sigma) were added (in order to precipitate out protein and DNA) and the tubes were vortexed (solution should turn white), then left on ice for 5 minutes. The samples were centrifuged at 13000 r.p.m. for 9-10 minutes in a microcentrifuge (at 4°C), then the supernatant was removed to a new tube and an equal volume of (ice cold) isopropanol added. The solution was vortexed, then samples were left in a -20°C freezer, for 40 minutes.

The samples were then centrifuged at 13000 r.p.m. for 10 minutes in a microcentrifuge (at 4°C). The supernatant was carefully removed to a new tube; 0.8ml ethanol were added to each tube and samples were placed in -20°C freezer, for 5 minutes. Samples were centrifuged at 13000 r.p.m. for 8 minutes in a microcentrifuge (at 4°C), then the supernatants were discarded and tubes were left (lids open) in a flow hood, for approximately 10 minutes, to allow the RNA pellets to dry. The pellets were then resuspended in 20µl of DEPC-treated water.

From each sample, 10µl were used for a spectrophotometer reading, to find the RNA concentration; 5µl were used to run on an agarose gel, to check the purity of the RNA; and the remainder of the sample was used for RNA fingerprinting, as described below. (N.B: Samples were normally run in duplicate, so that one sample could be used to check RNA concentration and purity, and there was still plenty of sample left for use in fingerprinting reactions).

FIRST STRAND cDNA SYNTHESIS

Fingerprinting was carried out using the Delta™ RNA Fingerprinting Kit (CLONTECH Laboratories, Inc.), as follows:

For each RNA sample, a sterile 0.5ml microcentrifuge tube was labelled with a number followed by "A". (This was to distinguish each sample from the "B" dilution prepared later - see below).

The following were combined in the appropriately labelled tubes:

2µg	Total RNA sample
1µl	cDNA synthesis primer (1µM)

Sterile water was added to a final volume of 5µl, then the contents were mixed and the tubes were given a pulse-spin in a microcentrifuge. The tubes were incubated at 70°C for 3 minutes; cooled on ice for 2 minutes; then given another pulse-spin.

Enough cDNA master mix for each cDNA synthesis reaction plus one additional tube was prepared as follows (amounts given are per reaction):

2µl	5x first-strand buffer
2µl	dNTP mix (5mM)
1µl	MMLV reverse transcriptase (200 units/µl)

To each reaction tube, 5µl of the cDNA master mix were added; the contents were mixed by gently pipetting; and the tubes were given a pulse-spin. The tubes were incubated at 42°C for 1 hour in an air incubator, then the reactions were terminated by incubating at 75°C for 10 minutes. The tubes were placed on ice for 2 minutes, then given a pulse-spin.

From each reaction, 2µl were transferred to a fresh, sterile 0.5ml microcentrifuge tube and 78µl of DEPC-treated water were added. This was the "B" dilution (i.e. 1:40 dilution of original sample) of each cDNA sample. To the tube containing the remaining 8µl of each ss cDNA, 72µl of DEPC-treated water were added. This was the "A" dilution (i.e. 1:10 dilution of original sample) of each cDNA sample.

All cDNA dilutions were stored at -20°C until ready for use.

PCR FINGERPRINTING REACTIONS

For each different experimental fingerprint, the following reagents were combined in a 0.5ml microcentrifuge tube:

1µl	Template (A or B dilution of cDNA)
1µl	P primer
1µl	T primer

The PCR master mix was made up as follows for each reaction. (Enough PCR master mix was prepared for all of the PCR reactions plus one additional tube).

10x PCR reaction buffer	2.0µl
Sterile water	14.2µl
dNTP mix (5mM each; final concentration 50µM)	0.2µl
[a-^{32}P] dATP (1000-3000 Ci/mmole; 3.3µM; final concentration 50nM)	0.2µl
Taq polymerase mix (50x) [14.3µl of *Taq/Pwo* DNA polymerase with 5.7µl of TaqStart Antibody]	0.4µl
Final volume	**17.0µl**

The master mix was vortexed and given a pulse spin in a microcentrifuge.

To each reaction tube, 17µl of PCR master mix were added, to give a final volume of 20µl. A drop of mineral oil was added on top of each PCR mixture and the tubes were tightly capped. PCR reactions were carried out in a Hybaid thermal reactor, using the following programme.

One cycle of:

94°C for 5 minutes

40°C for 5 minutes

68°C for 5 minutes

followed by two cycles of:

94°C for 2 minutes

40°C for 5 minutes

68°C for 5 minutes

followed by 22-25 cycles of:

94°C for 1 minute

60°C for 1 minute

68°C for 2 minutes

followed by 68°C for 7 minutes.

The fingerprinting reactions were stored at -20°C until they were run on a denaturing 5% polyacrylamide/8M urea gel in 0.5x TBE buffer.

ELECTROPHORESIS AND AUTORADIOGRAPHY

A 0.2mm thick, denaturing 5% polyacrylamide/8M urea gel in 0.5x TBE buffer was poured, then the gel was pre-run until the temperature reached 50°C.

For each reaction, 5µl of the PCR reaction mixture were combined with 5µl of loading buffer in a clean 0.5ml microcentrifuge tube. The samples were denatured by incubating (in a Hybaid Thermal Reactor) at 94°C for 2 minutes, then immediately placed onto ice. The wells of the gel were rinsed with buffer, then 4µl of each sample were loaded. The gel was run at 85 watts (constant power) until the xylene cyanol dye had migrated through the entire gel.

The electrophoresis apparatus was dismantled and the top notched plate removed. A piece of Whatmann chromatography paper (46 x 57 cm) was smoothed over the gel, then paper and gel were carefully peeled away from the bottom gel plate. Plastic Saran wrap was placed over the gel and the gel was dried, under vacuum, in a Biorad gel drier at 80°C for 2 hours. X-OMat X-ray film was exposed to the gel at room temperature and autoradiographs were developed as described below.

Development of autoradiographs

X-ray films were placed in developing solution (LX24 [Kodak]; 1:5 dilution in distilled water) for 5 minutes, then films were washed in 2% acetic acid, for 1 minute. Films were then placed in Amfix (Champion Photochemistry); 1:4 dilution in distilled water, with 2.5% Hardener (Champion Photochemistry); for at least 2 minutes. Finally, films were rinsed in tap water, then hung up to dry.

PURIFICATION OF DNA FRAGMENTS FROM DRIED POLYACRYLAMIDE GELS

The autoradiograph was aligned on top of the dried gel (on Whatman paper) and taped in place. Differentially expressed bands were marked, using a needle to poke holes through the film and the gel beneath, then bands were cut from the gel using a scalpel blade and each fragment of dried gel placed in a 0.5ml microcentrifuge tube.

(N.B: Clean needles and blades were used for each band in order to avoid cross contamination of samples).

To each sample, 50µl of DEPC-treated water were added. The tubes were overlayed with one drop of mineral oil then heated, in a Hybaid thermal reactor, at 99°C, for 5 minutes. The Whatman paper was carefully removed from each tube, and the eluted bands stored at -20°C.

REAMPLIFICATION OF DIFFERENTIALLY EXPRESSED BANDS

Each differentially expressed band was reamplified using the primers used in the original fingerprint. For each band, the following reagents were combined in a 0.5ml microcentrifuge tube:

Eluted DNA (template)	3.50µl
10x PCR buffer	2.50µl
1.25mM dNTP	4.00µl
P primer (20µM)	1.25µl
T primer (20µM)	1.25µl
MgCl	1.50µl
W-1	1.25µl
Taq DNA polymerase	0.25µl
DEPC-treated H_2O	9.50µl
Final volume	**25.00µl**

Each reaction was overlayed with a drop of mineral oil; the caps of the tubes were tightly closed; then PCR reactions were carried out in a Hybaid thermal reactor, using the following parameters.

20 cycles of:

94°C for 1 minute

60°C for 1 minute

68°C for 2 minutes.

Analysis of 10µl of each product (combined with 4µl of high glycerol loading dye) was carried out on a 1% agarose/ethidium bromide gel. (The reamplified product should be the same size as the original band). The remaining sample material was stored at -20°C.

The PCR products were purified from primers and unincorporated nucleotides using Spin-X columns (Costar); then cloned into a TA-type cloning vector and sequenced.

CLONING

Cloning of DNA was carried out, as described below, using the pMOS*Blue* T-vector kit (Amersham Life Science).

REAGENTS

Luria broth (L broth)

In 900ml distilled water, 10g Bacto tryptone (Difco), 5g Bacto yeast extract (Difco), and 10g NaCl (Sigma) were dissolved, sequentially. Then, 0.2ml 5M NaOH was added (to give a pH of 7.0) and the volume made up to 1 litre. The broth was sterilised by autoclaving, allowed to cool below 50°C, then (filter sterilised) ampicillin (50µg/ml) and tetracycline (15µg/ml) (both Sigma) were added.

Luria broth agar antibiotic plates (LB agar antibiotic plates)

In 1 litre of L broth (minus antibiotics), 10g agar (Difco) were dissolved. The LB agar was sterilised by autoclaving, allowed to cool below 50°C, then (filter sterilised) ampicillin (50µg/ml) and tetracycline (15µg/ml) were added.

IPTG (isopropyl B-D-thiogalactopyranoside)

A 100mM solution of IPTG (Sigma) in distilled water (23.8mg/ml) was prepared just prior to use, then filter sterilised.

X-gal (5-bromo-4-chloro-3-indolyl-B-galactoside)

A 50mg/ml X-gal (Gibco) solution in dimethylformamide (Sigma) was prepared just prior to use.

INSERT PREPARATION

Inserts (PCR products) were gel purified prior to ligation into the vector.

For optimal cloning efficiencies the vector to insert ratio should be in the range 1:5 to 1:10. To calculate the amount of insert required when using the standard 50ng of vector, the size of the insert (bp) was multiplied by 1.3×10^{-1}. This calculation gives the correct amount of insert to be used in the ligation reaction.

LIGATION INTO pMOS*Blue* T-VECTOR

For each PCR product to be cloned, the following ligation reaction was set up:

10x ligase buffer	1µl
100mM DTT (Dithiothreitol)	0.5µl
10mM ATP	0.5µl
50ng/µl vector	1.0µl
PCR product (insert)	Appropriate amount (up to 2µl)
T4 DNA ligase	0.5µl

The reaction mixture was made up to 10µl with nuclease free water.

The ligation reaction was stirred gently with a pipette tip, then incubated at 16°C for at least two hours (or overnight).

TRANSFORMATION

The MOS*Blue* competent cells were thawed and 20µl added to a pre-chilled microfuge tube (one tube for each transformation). To the cells, 1µl of ligation mix was added and the mixture stirred gently. The tubes were then left on ice for

30 minutes. The cells were heat shocked for exactly 40 seconds in a 42°C water bath, then placed on ice for 2 minutes. To each tube, 80µl of room temperature SOC medium were added, then the tubes were put on to shake (at 200-250 rpm) at 37°C for 1 hour.

L agar plates (82mm), containing 50µg/ml ampicillin and 15µg/ml tetracycline, were each spread with 35µl of 50mg/ml X-gal and 20µl 100mM IPTG. The plates were left to soak for at least 30 minutes prior to plating. Onto the L agar plates, 50µl of each transformation were spread and the inverted plates were incubated overnight at 37°C.

SCREENING OF RECOMBINANTS

The pMOS*Blue* vector allows for blue-white screening, with recombinant colonies appearing white when plated on X-gal and IPTG indicator plates.

White colonies were screened in one of two ways:

a) Miniprep Screening

Plasmid DNA (50µl) was isolated using a Promega Wizard™ miniprep kit. Restriction digests were carried out, on 5µl of each plasmid DNA sample, using EcoR1 and Xba1 restriction enzymes, to determine the presence and size of the inserts. Digests were then run on a standard 1% agarose gel containing ethidium bromide, alongside a molecular weight marker.

b) Rapid Direct Colony Screening

White colonies were picked from plates using a sterile (sequencing) pipette tip. The bacteria were transferred to a microfuge tube containing 5µl DEPC-treated water, then the tubes were placed in a Hybaid thermal reactor at 99°C for 5 minutes (to lyse the cells and denature DNAses). The tubes were placed on ice for 2 minutes, then given a pulse-spin in a microcentrifuge. PCR reactions were then

carried out on each sample and the reaction products were run on a standard 1% agarose gel containing ethidium bromide.

STORAGE OF CLONES

Clones that contained inserts were grown in L broth (at 37°C, with constant shaking) overnight. To a cryovial containing 0.5ml autoclaved (and cooled) glycerol, 1ml of each clone was transferred, then the cryovials were placed into a -20°C freezer for one hour and stored at -70°C.

SEQUENCING

PREPARATION OF SEQUENCING GEL

To a 200ml glass beaker containing 63g urea (Fisons), 25ml acrylamide ("Easigel", from Scotlab) and 30ml of x5 TBE buffer were added. The gel solution was made up to 150ml with deionised water and mixed on a magnetic stirrer until dissolved. From the gel solution, 10ml were removed and 75µl of Temed (N, N, N', N'-Tetramethylethylenediamine, from Biorad) and 75µl of 1ml 10% Ammonium Persulphate (Biorad) added. The solution was mixed and used to make a two centimetre gel plug along the bottom end of the gel plates, using a 2ml syringe. To the remainder of the gel mixture, 75µl of Temed were added, followed by the remaining Ammonium Persulphate. The solution was mixed and loaded between the gel plates with a 50ml syringe. Once the gel was poured, the combs were placed in position, upside down along the top edge of the gel, to form a straight edge.

Approximately one hour after pouring the gel, a piece of blue roll soaked in 0.5x TBE buffer was placed at either end of the gel plates and covered with cling film. The gel was left overnight at room temperature to set.

To a large glass beaker, 1500ml of 0.5x TBE buffer were added and heated at full power in a microwave oven, for 8 minutes. A further 450ml of cold 0.5x TBE buffer was added to the base of the gel rig. The combs were removed from the set gel; the heated buffer was poured between the gel plates; and the gel was pre-run at 95 watts until the temperature reached 50°C. At this point the combs were placed into the gel, right way up, and 4µl of each sample were loaded onto the gel.

The gel was run, maintaining a temperature of 50°C, until the Bromophenol Blue dye front had almost reached the bottom of the gel. The plates were then removed from the rig and the back plate was carefully removed. A sheet of Whatman chromatography paper was smoothed onto the gel then gently removed, along with the attached gel. Gels were dried, for 2 hours at 80°C, on a gel drier (Biorad) and an autoradiograph was taken of the dried gel.

N.B: Before use gel plates were cleaned with Decon, rinsed well with tap water and then with ethanol. The back plate **only** was treated with Repelcote (BDH) for thirty seconds, followed by gentle polishing.

SEQUENCING REACTIONS

Preparation of Plasmid DNA

To "clean up" the (remaining 45µl of) plasmid DNA, it was ethanol precipitated; then incubated at -20°C for 30 minutes, in a 0.5ml microfuge tube. The tubes were centrifuged, for 8 minutes at 13000 r.c.f., and ethanol (supernatant) discarded. The pellets (DNA) were dried and resuspended in 20µl DEPC-treated water. To a quartz cuvette containing, 1ml DEPC-treated water, 10µl of the solution were transferred. The absorption profile was then measured on a spectrophotometer (Shimadzu UV-160A), in order to work out the DNA concentration, and an appropriate amount of DNA was used for the annealing mixture (see below).

Procedure

Sequencing was carried out using the T7 Sequenase™ Version 2.0 DNA Sequencing Kit (Amersham Life Science), as described below.

The double-stranded DNA template was denatured, using an **alkaline-denaturation** method:

0.1 volume of 2M NaOH and 0.1 volume of 2mM EDTA were added to the DNA sample, then the mixture was incubated for 30 minutes at 37°C. The mixture was neutralized by adding 0.1 volume of 3M sodium acetate (pH 4.5-5.5) and the DNA precipitated with 2-4 volumes of 100% ethanol (-70°C, 15 minutes). The DNA was spun down (13000 rcf [relative centrifugal force], 5 minutes); the supernatant was removed; 2-4 volumes of 70% ethanol were added to the tube containing the DNA, then the tube was incubated for 10 minutes at -20°C. The DNA was then spun down again (13000 rcf, 5 minutes), the supernatant discarded, and the DNA dried for 10 minutes in a vacuum oven. The (denatured) DNA pellet was then resuspended in 7µl of DEPC-treated water, ready for use in the annealing reaction (see below).

Annealing mixture was prepared as follows:

DNA	up to 7µl containing 3-5µg (for plasmid)
H_2O	µl to adjust total volume
Reaction buffer	2µl
Primer	1µl of a PCR primer diluted 1:5 (in DEPC-treated H_2O)
TOTAL	10µl

The mixture was heated for 2 minutes at 65°C, then slowly cooled to <35°C over 15-30 minutes. The solution was given a pulse spin, then chilled on ice.

Whilst the annealing mix was cooling, 2.5µl of ddG, ddA, ddT, and ddC termination mixtures were added to the appropriate number of microfuge tubes (4

for each sample) and pre-warmed at 37°C. Also, the labelling mix was diluted 5-fold.

Labelling reaction:

[N.B: Sequenase DNA polymerase was diluted 1:8 in ice cold enzyme dilution buffer, immediately before use.]

Ice cold annealed DNA mixture	(10µl)
DTT, 0.1M	1µl
Diluted labelling mix	2µl
[^{35}S dATP]	0.5µl
Diluted Sequenase polymerase	2µl
TOTAL	15.5µl

The labelling reaction was mixed and incubated at room temperature for 2-5 minutes.

Termination reactions:

To each termination tube, 3.5µl of labelling reaction were transferred and the incubation of the termination reactions continued at 37°C for 5 minutes. The reactions were terminated by adding 4µl of Stop Solution to each tube. Immediately before loading a sequencing gel, the samples were heated to 75°C for 2 minutes in order to get single-stranded DNA, the tubes were plunged into ice, then each well of the gel was loaded with 4µl of sample, as described above.

CHAPTER 3

IN VITRO STUDIES ON CELL ATTACHMENT TO GROOVED/NON-GROOVED SURFACES

PRELIMINARY EXPERIMENTS

"CELL LAWN EXPERIMENT"

Introduction

It has previously been observed (Adam Curtis, personal communication; Chehroudi *et al*, 1989) that an initial cell layer will preferentially attach to a grooved compared with smooth substrate. The aim of this experiment was to determine whether a previously attached confluent cell layer (or "cell lawn", as described by Walther *et al*, 1973) would allow preferential attachment of a second layer of cells on a grooved compared with smooth surface topography. There were three alternative theories as to what the results of the experiment would reveal:

1. Cells attached to grooves use up all their available cytoskeleton in this attachment and this would, therefore, inhibit attachment of a second cell layer.
2. Attachment to a grooved substrate leaves cell cytoskeletons free to attach to other cell layers. Therefore, an initial cell layer grown on grooves would encourage attachment of a further layer of cells.
3. There is no preferential attachment of a second cell layer to an initial cell layer grown on a grooved compared with flat surface.

Results

Means for number of cells attached to grooved surface range from 4.40 to 11.90 and for attachment to flat surface range from 4.70 to 10.65. An unpaired t-test of

significance of difference in means gave t-values from -1.50 to 0.58, and P-values were always greater than 0.14 (where d.f.=38).

Discussion

The results would appear to support the third theory - that a second layer of cells shows no preference of attachment to an already attached cell layer, where the first cell layer has been allowed to colonise either a microgrooved or a planar substrate. This, therefore, suggests that any rise in cell adhesion in the first layer of cells (when grown on a grooved substrate) is confined to the substratum side of the cell.

The results are of importance when considering the colonisation of implants by cells. In order to be biocompatible the surface topography of the implanted device must allow attachment of an initial cell layer, but also must not interfere with the correct tissue formation surrounding the implant. A prosthetic device would serve no useful purpose if it allowed cell colonisation of the implant, but the particular surface topography prevented further cell layers attaching, thus having a detrimental effect on the correct formation of tissue surrounding the implant.

CELL ADHESION TO POLYDIOXANONE STRUCTURES *IN VITRO*

Introduction

Comparisons were made between the numbers of "rounded" (cells showing no evidence of forming protrusions) and "spread" (cells showing evidence of elongation in at least one direction) cells that were found attached to grooved and non-grooved areas of the polydioxanone (PDS) structures. Cells used were: P388D1 macrophage-like cells and epitenon cells. Each structure consisted of a grooved and flat area, the grooves being 12.5μm in width and 6μm in depth. The same number of cells were seeded on each of the structures; cells were fixed at one hour, four hour, and twenty four hour time intervals; then scanning electron

micrographs were taken of the cells/structures. The numbers of attached cells (per square millimetre) were estimated using a Vidas image analysis programme.

Results

The number of rounded epitenon cells attached to grooved and non-grooved PDS is shown in figure 5. The between-group main effect for surface (top row, table 1) is significant (at the 1% level), meaning that averaged over the three timepoints there was a significant difference in the number of rounded epitenon cells attached to the grooved compared with the non-grooved PDS surface. The time after seeding of cells also had a significant effect (third row; table 1); the number of rounded cells being significantly reduced at twenty four hours (where no rounded cells were observed) compared with one hour. The significant number of rounded cells-by-surface interaction indicates that the number of cells attached over time differs significantly depending on the cell surface. Figure 6 shows results for the number of spread epitenon cells attached to grooved and non-grooved PDS over time. The between group main effect for surface is again significant (Table 2), demonstrating a significant difference in the number of spread epitenon cells attached to the grooved compared with the non-grooved surface, averaged over the three timepoints. For spread epitenon cells the time after seeding of cells is not significant in determining cell attachment, nor does the number of cells attached over time differ significantly depending on the surface.

In the case of rounded P388D1 cells the between-group main effect for surface is not significant (Table 3), as a similar number of rounded P388D1 cells appear to be attached to grooved and non-grooved PDS at all timepoints (Figure 7). The time after seeding and number of rounded cells-by-surface interaction also show no significant difference. This is in contrast with the results obtained for spread P388D1 cells (Figure 8). These cells show a significant between-group main effect for surface (Table 4), demonstrating that averaged over the three timepoints

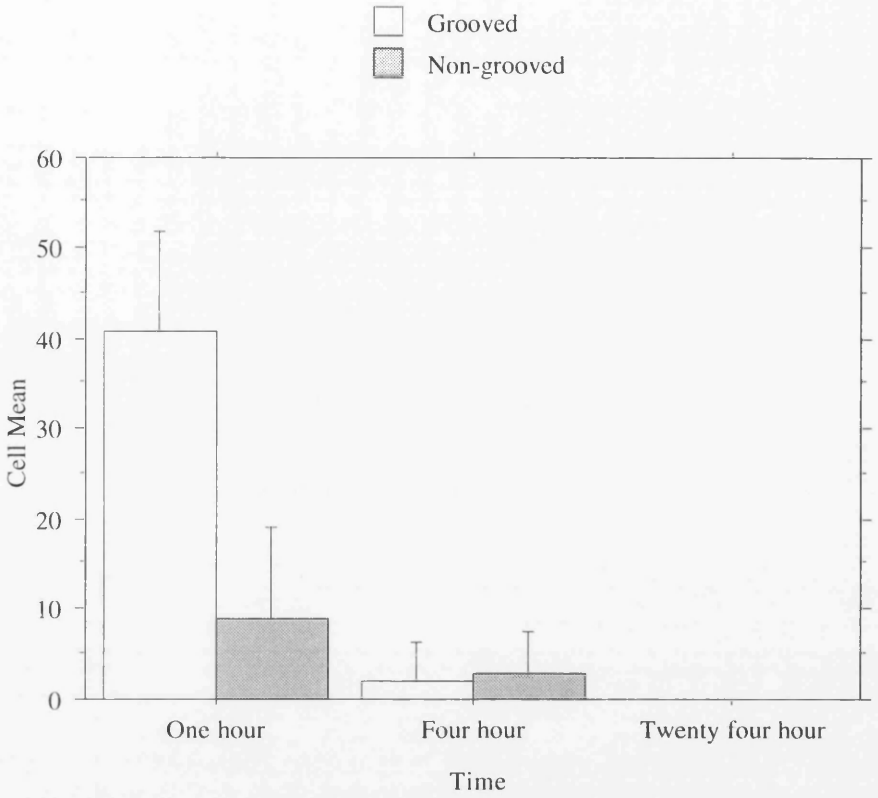

Figure 5. Number of rounded epitenon cells (per mm^2) attached to grooved and non-grooved areas of PDS structures over time, *in vitro*. Error bars indicate +/-1 Standard Deviation. Results are means of 5 counts for each sample.

	DF	Sum of Squares	Mean Square	F-Value	P-Value
Surface	1	791.663	791.663	20.683	.0019
Subject (Group)	8	306.205	38.276		
Category for No. Rounded Epi.10 cells	2	3736.519	1868.260	39.293	<.0001
Category for No. Rounded Epi.10 cells*Surface	2	1745.720	872.860	18.358	<.0001
Category for No. Rounded Epi.10 cells*Subject	16	760.744	47.547		

Table 1. Anova Table for Time, showing results for the number of rounded epitenon cells (per mm^2) attached to grooved and non-grooved PDS over time, *in vitro*.

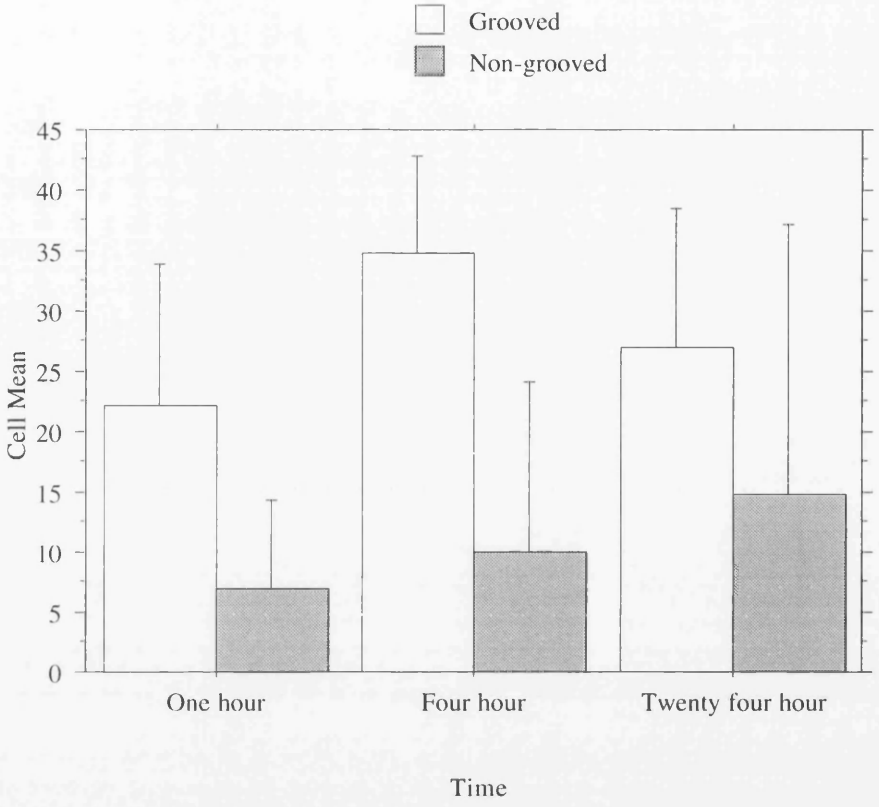

Figure 6. Number of spread epitenon cells (per mm^2) attached to grooved and non-grooved areas of PDS structures over time, *in vitro*. Error bars indicate +/-1 Standard Deviation. Results are means of 5 counts for each sample.

	DF	Sum of Squares	Mean Square	F-Value	P-Value
Surface	1	2281.152	2281.152	16.110	.0039
Subject (Group)	8	1132.801	141.600		
Category for No. Spread Epi.10 cells	2	348.566	174.283	.869	.4382
Category for No. Spread Epi.10 cells*Surface	2	217.202	108.601	.542	.5921
Category for No. Spread Epi.10 cells*Subject	16	3208.059	200.504		

Table 2. Anova Table for Time, showing results for the number of spread epitenon cells (per mm^2) attached to grooved and non-grooved PDS over time, *in vitro*.

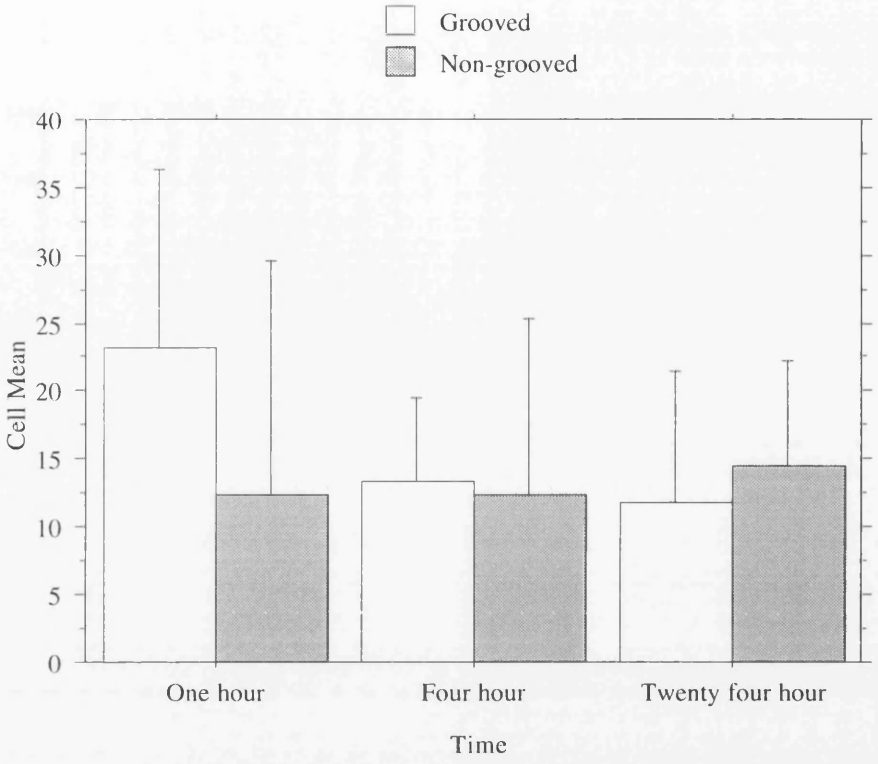

Figure 7. Number of rounded P388D1 cells (per mm^2) attached to grooved and non-grooved areas of PDS structures over time, *in vitro*. Error bars indicate +/-1 Standard Deviation. Results are means of 5 counts for each sample.

	DF	Sum of Squares	Mean Square	F-Value	P-Value
Surface	1	67.500	67.500	.724	.4197
Subject (Group)	8	746.328	93.291		
Category for No. Rounded P388D1 cells	2	148.193	74.096	.464	.6371
Category for No. Rounded P388D1 cells*Surface	2	243.726	121.863	.763	.4826
Category for No. Rounded P388D1 cells*Subject	16	2555.988	159.749		

Table 3. Anova Table for Time, showing results for the number of rounded P388D1 cells (per mm^2) attached to grooved and non-grooved PDS over time, *in vitro*.

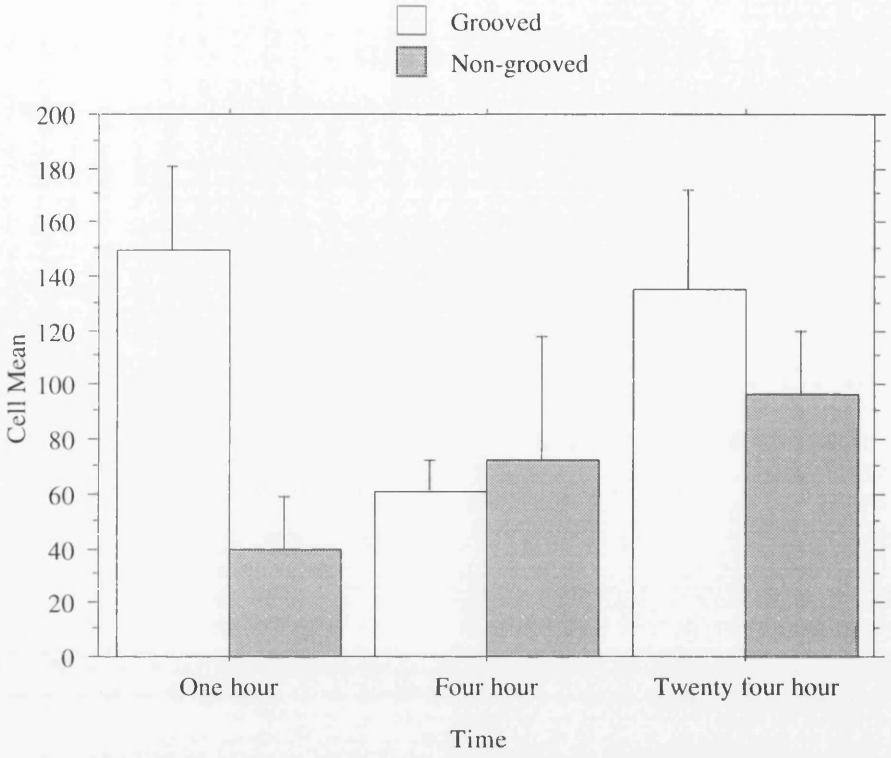

Figure 8. Number of spread P388D1 cells (per mm^2) attached to grooved and non-grooved areas of PDS structures over time, *in vitro*. Error bars indicate +/-1 Standard Deviation. Results are means of 5 counts for each sample.

	DF	Sum of Squares	Mean Square	F-Value	P-Value
Surface	1	15640.833	15640.833	16.462	.0036
Subject (Group)	8	7601.075	950.134		
Category for No. Spread P338D1 cells	2	12342.752	6171.376	6.950	.0067
Category for No. Spread P388D1 cells*Surface	2	18650.419	9325.209	10.502	.0012
Category for No. Spread P388D1 cells*Subject	16	14206.889	887.931		

Table 4. Anova Table for Time, showing results for the number of spread P388D1 cells (per mm^2) attached to grooved and non-grooved PDS over time, *in vitro*.

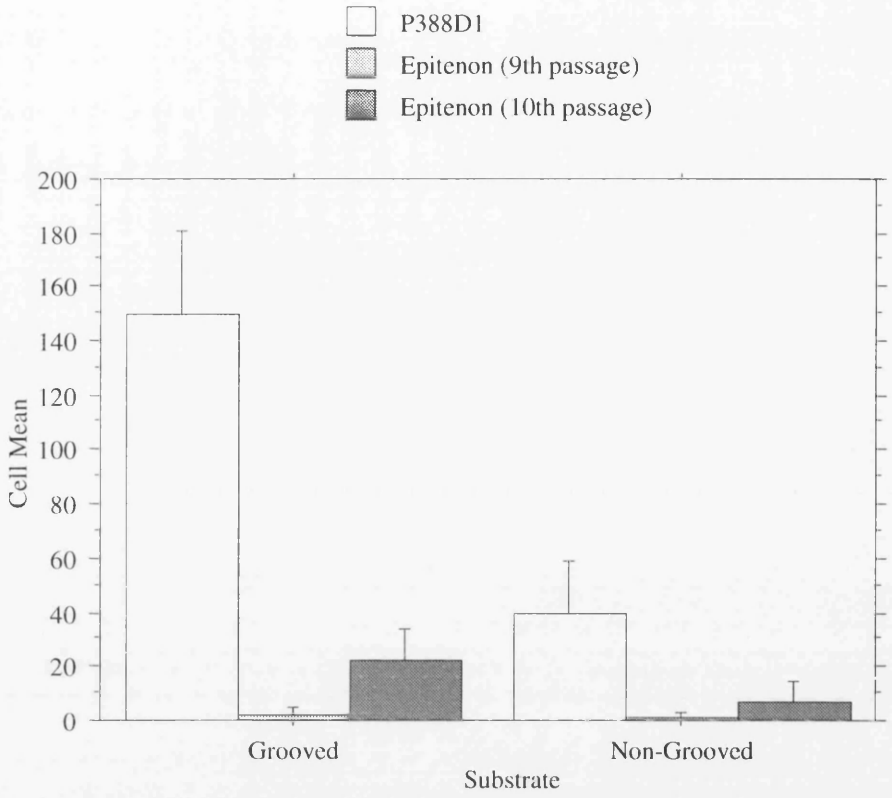

Figure 9. Number of spread cells (per mm^2) attached to PDS after one hour, *in vitro*. Error bars indicate +/-1 Standard Deviation. Results are means of 5 counts for each sample.

	DF	Sum of Squares	Mean Square	F-Value	P-Value
Cell Type	2	51401.760	25700.880	130.096	<.0001
Subject (Group)	12	2370.639	197.553		
Category for Substrate	1	13298.970	13298.970	44.875	<.0001
Category for Substrate*Cell Type	2	17545.152	8772.576	29.601	<.0001
Category for Substrate*Subject	12	3556.294	296.358		

Table 5. Anova Table for Substrate, showing results for the number of spread cells (per mm^2) attached to PDS after one hour, *in vitro*.

there is a significant difference in the number of spread P388D1 cells attached to the grooved compared with the non-grooved substrate. A significant difference is also observed for the number of spread P388D1 cells attached over time, and the number of spread cells attached over time differs significantly depending on the surface.

Both spread epitenon cells and spread P388D1 cells show preferential attachment to the grooved compared with the non-grooved PDS substrate (Figures 6 and 8). Rounded epitenon cells also appear to prefer the grooved substrate (Figure 5), whereas the numbers of rounded P388D1 cells attached to both the grooved and non-grooved surfaces don't appear to vary greatly over time (Figure 7).

A comparison between figures 5 and 6 suggests that epitenon cells react to grooved surfaces by becoming spread in increasing numbers over time, as might be expected. In contrast, figures 7 and 8 suggest that P388D1 cells react and spread rapidly on grooved surfaces (note the large number of spread cells attached to the grooved substrate at the one hour timepoint in figure 8), otherwise they remain rounded (see the relatively constant number of rounded cells attached to the grooved substrate over time in figure 7). For both epitenon and P388D1 cells the numbers of spread cells attached to the non-grooved substrate show a gradual increase over time. The numbers of rounded epitenon cells attached to the non-grooved substrate gradually decrease over time, in contrast with the number of rounded P388D1 cells which remain relatively constant over time.

Discussion

In vitro the cell types tested (epitenon cells and P388D1 macrophage-like cells) show a significant preferential attachment to a microgrooved compared with a non-grooved PDS surface. Epitenon cells adhere and spread quickly on the grooves, so there is no significant difference in attachment of spread epitenon cells

over time (Table 2). But, for the number of rounded epitenon cells attached there is a significant decrease in attachment over time (Table 1). P388D1 cells also show a significant preference for the grooved substrate, where the majority spread almost immediately (Figure 8; Table 4). But, in the population of P388D1 cells that remain rounded there is no significant difference in numbers of cells attached to the grooved/non-grooved substrates, or in cell attachment over time (Table 3). It is possible that these rounded P388D1 cells are dead or restrained from spreading in some way.

Figure 9 is included to demonstrate that as well as differences between the grooved and non-grooved PDS surfaces, there are also significant differences in cell attachment between the cell types tested. It can be seen that there are a significantly higher number of spread P388D1 cells attached to both the grooved and non-grooved surfaces when compared with epitenon cells, after one hour (Table 5). There would also appear to be a significant difference in cell attachment between the ninth and tenth passage epitenon cells. This difference would not be expected between the same cell type differing by only one passage, and as the same number of cells were initially seeded on each PDS structure it is not known why this should have occurred. Although difficult to explain, this difference observed between the two epitenon cell populations does not detract from the overall impression that greater numbers of P388D1 cells appear to attach to both grooved and non-grooved PDS, compared to epitenon cells, and that both P388D1 and epitenon cells show preferential attachment to the grooved compared with the non-grooved PDS surface.

Assuming these results would be mimicked *in vivo*, then this has implications for implanted biomaterials. If a prosthesis containing a grooved surface is implanted, then, according to the results obtained from this *in vitro* study, it may be expected that this area of the implant would be colonised by cells ahead of any flat areas.

This could pose a problem if it resulted in certain parts of the implant being integrated into the surrounding tissue before others. Conversely, this phenomenon could also be utilised to encourage cell growth: if the grooved area of an implant becomes rapidly colonised by cells then it would be expected to enhance cell growth and tissue repair in that area.

The fact that P388D1 macrophage-like cells appear to show a significant increase in attachment to both grooved and non-grooved surfaces compared with epitenon cells should also be noted. If this was the case *in vivo* it could result in preferential colonisation of an implanted device by one cell type at the exclusion of another, thereby causing a possible detrimental effect on new tissue formation surrounding the implant. Or, in the case of biodegradable implant materials, resulting in a possible alteration in the degradation rate of the implant itself.

ROLE OF TYROSINE PHOSPHORYLATION IN CONTACT GUIDANCE

INTRODUCTION

Indirect Immunofluorescence

Many aspects of cell behaviour, *in vitro*, have been reported to be affected by the topography of the substrate on which the cells are grown. The behavioural processes affected include: cell adhesion (Bowers *et al*, 1992; Könönen *et al*, 1992), orientation (Harrison, 1914; Weiss and Garber, 1952; Brunette *et al*, 1983; Brunette, 1986; Clark *et al*, 1990 and 1991) , shape (Brunette *et al*, 1988; Chehroudi *et al*, 1995) and differentiation (Watt *et al*, 1988), and the effects have been observed in many different cell types.

These *in vitro* studies can be related to the growth of cells *in vivo*, where the cells generally have to respond to some substratum topography. This is especially true in certain circumstances where specific topographical guidance cues are thought to be of major importance, for example in morphogenesis and tissue regeneration. It is also important to further elucidate the response of cells to topographical features in order to fully understand how body tissue is likely to react to biological implants. Despite this, few studies have attempted to explain the underlying molecular mechanism that allows a cell to respond to topographical stimuli.

It has been previously shown, by many groups, that cells will align to topographical features *in vitro*, and that the cell cytoskeleton, along with many cytoskeletal-associated proteins is similarly aligned (Rovensky and Samoilov, 1994; Meyle *et al*, 1994; Webb *et al*, 1995; Wojciak-Stothard *et al*, 1996). It is well known that tyrosine phosphorylation of proteins has an important role in many biological signalling processes, and many proteins involved in formation of focal adhesion complexes are phosphorylated on tyrosine. Therefore, it was decided to grow cells on different topographical substrates, *in vitro*, and carry out antibody staining for phosphorylated tyrosine residues, as it was thought that this phosphorylation may play a part in the molecular signalling process involved in the response of cells to substratum topography.

Tyrphostins as Inhibitors of Tyrosine Phosphorylation

Following the results obtained from the indirect immunofluorescence studies, there appeared to be a role for tyrosine phosphorylation in cell alignment on microgrooved structures. Therefore, experiments were carried out using inhibitors of protein tyrosine phosphorylation, "Tyrphostins", in order to find out what effect, if any, they would have on cellular contact guidance. Tyrphostins are competitive inhibitors of tyrosine kinases that have been designed to mimic the structure of a phosphorylated tyrosine residue in a peptide chain. They do not

affect the activity of serine kinases, threonine kinases, protein kinase A, or protein kinase C (Levitzki, 1990).

Western Blots

Western blots were carried out in an attempt to verify the differential tyrosine phosphorylation observed in cells grown on grooved compared with flat substrates, and also to find a molecular weight as an initial step in identifying any of the proteins involved.

RESULTS

Indirect Immunofluorescence

Phosphotyrosine staining in P388D1 macrophage-like cells cultured on grooved fused silica (quartz) subsrata was specifically localised along groove/ridge boundaries. This was true for cells plated on structures ranging in depth from 44nm - 6μm, and from 5μm - 12.5μm in width. The specific staining pattern was observed from 15 minutes after plating the cells and continued for as long as the cells were cultured. Figure 10 shows P388D1 cells, after 20 minutes attachment, on a flat quartz surface, stained with PY20 (anti-phosphotyrosine) mouse monoclonal antibody and Texas Red sheep anti-mouse secondary antibody. Bright dots of staining can be observed dispersed randomly throughout the cell. In contrast, when the cells were cultured on microgrooved quartz substrata for the same length of time a specific staining pattern was observed, localised along the groove/ridge boundaries (Figure 11). Interestingly, all parts of the cell did not always show the same intensity of staining, but staining was consistently observed along cell processes that extended along the grooves (Figure 12). The specific dots of staining were also observed in P388D1 cells grown on microgrooves fabricated in PDS (polydioxanone suture material), despite the PDS itself being slightly autofluorescent (Figure 13). Figures 14 and 15 show that the pattern of F-actin

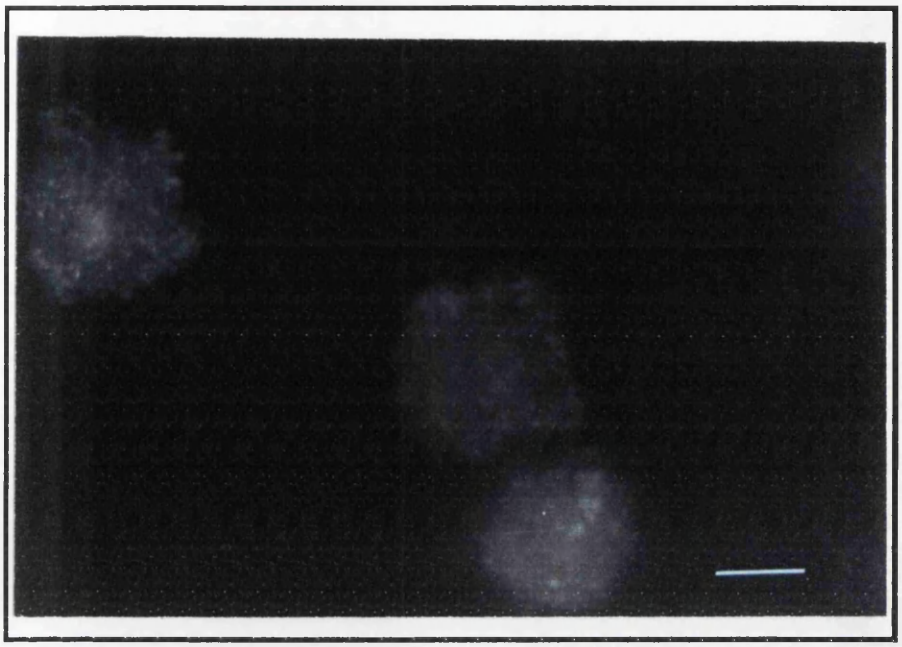

Figure 10. Distribution of phosphorylated tyrosine residues in P388D1 macrophage-like cells on a flat quartz substrate. Cells were stained with PY20 monoclonal antibody and Texas Red sheep anti-mouse secondary antibody. Scale bar represents 10µm.

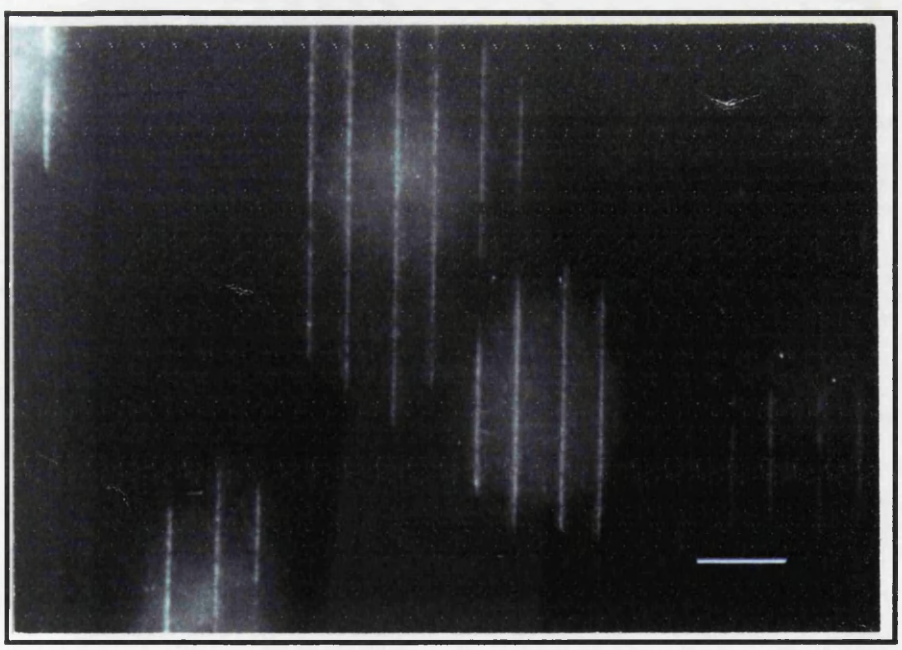

Figure 11. Distribution of phosphorylated tyrosine residues in P388D1 macrophage-like cells on a grooved quartz substrate. Cells were stained with PY20 monoclonal antibody and Texas Red sheep anti-mouse secondary antibody. Grooves are 1µm deep and 5µm wide. Scale bar represents 10µm.

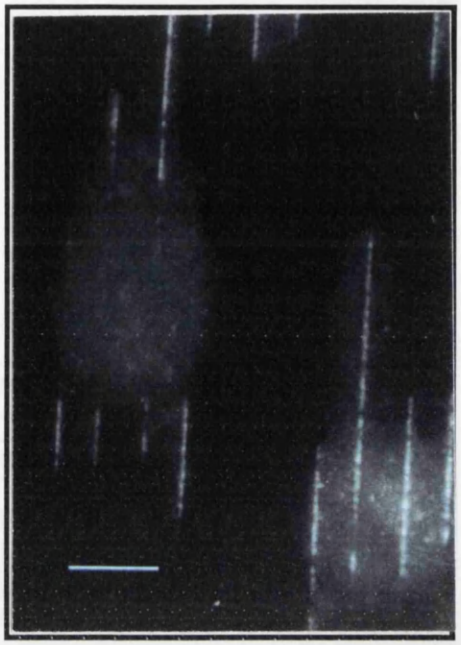

Figure 12. Distribution of phosphorylated tyrosine residues in P388D1 macrophage-like cells grown on a grooved quartz substrate. Cells were stained with PY20 monoclonal antibody and Texas Red sheep anti-mouse secondary antibody. Grooves are 1µm deep and 5µm wide. Scale bar represents 10µm.

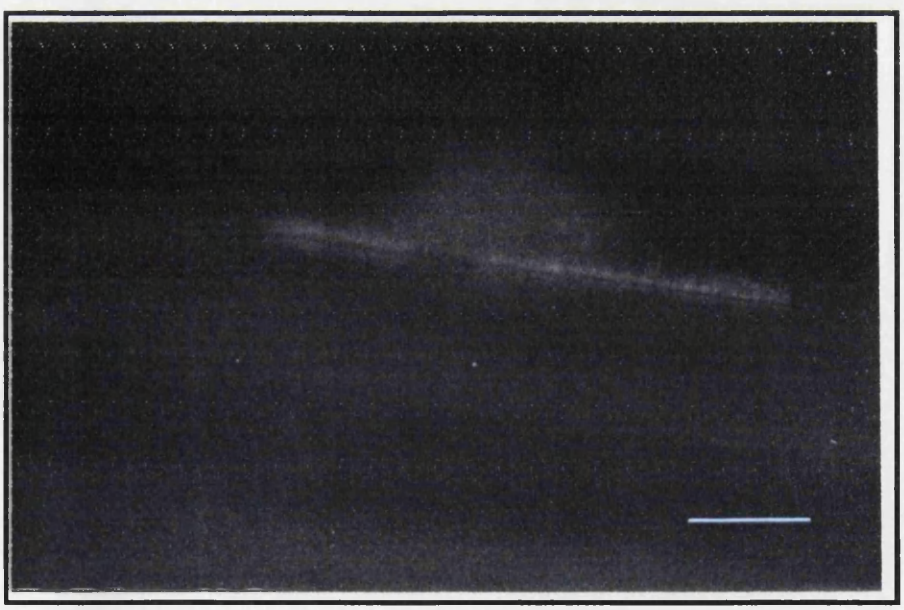

Figure 13. Distribution of phosphorylated tyrosine residues in P388D1 macrophage-like cells grown on a grooved polydioxanone (PDS) substrate. Cells were stained with PY20 monoclonal antibody and Texas Red sheep anti-mouse secondary antibody. Grooves are 6µm deep and 12.5µm wide. Scale bar represents 10µm.

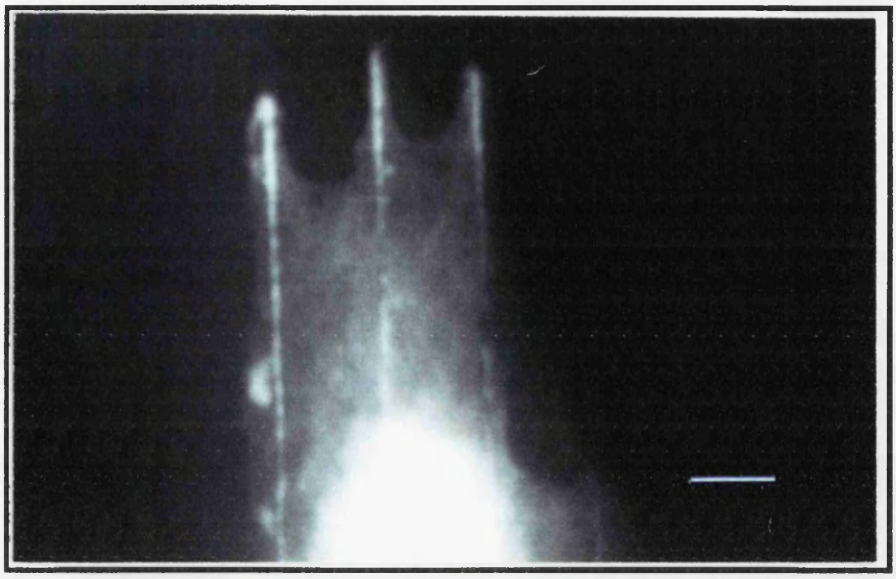

Figure 14. Distribution of F-actin in P388D1 macrophage-like cells grown on a grooved quartz substrate. Cells were stained with TRITC-phalloidin. Grooves are 70nm deep and 12.5µm wide. Scale bar represents 10µm.

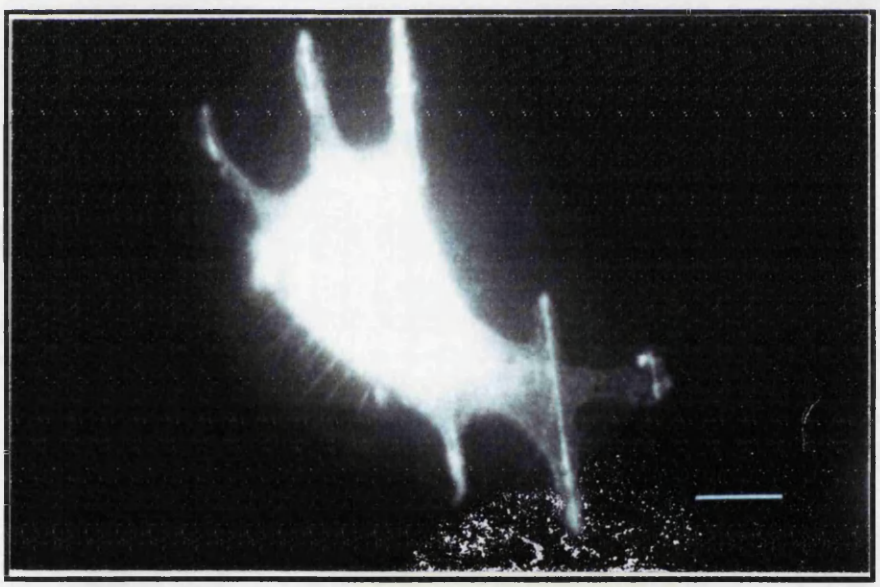

Figure 15. Distribution of F-actin in P388D1 macrophage-like cells grown on a grooved quartz substrate. Cells were stained with TRITC-phalloidin. Grooves are 70nm deep and 12.5µm wide. Scale bar represents 10µm.

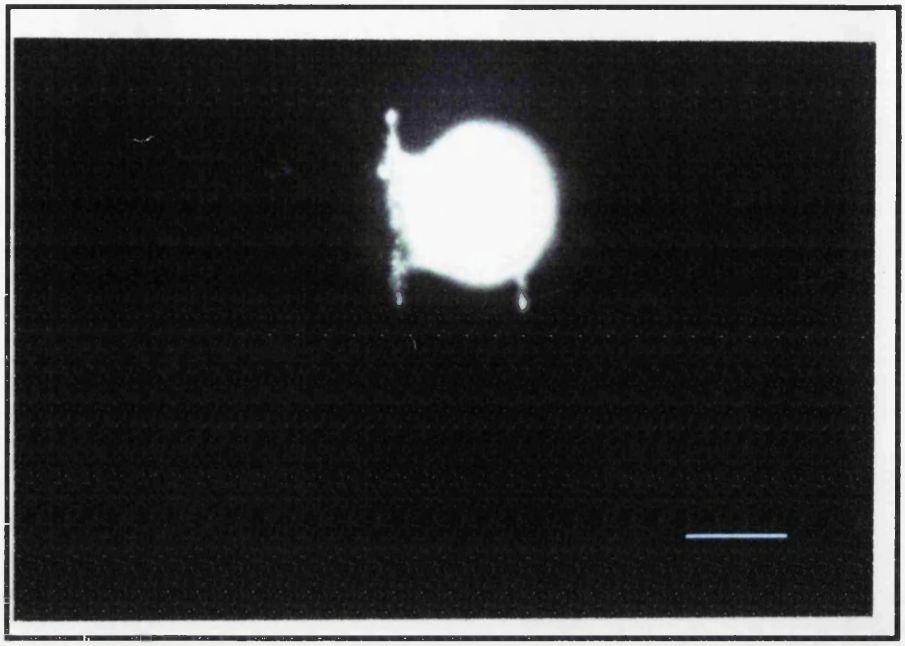

Figure 16. Distribution of phosphorylated tyrosine residues in P388D1 macrophage-like cells grown on a grooved quartz substrate. Cells were stained with PY20 monoclonal antibody and Texas Red sheep anti-mouse secondary antibody. Grooves are 88nm deep and 12.5µm wide. Scale bar represents 10µm.

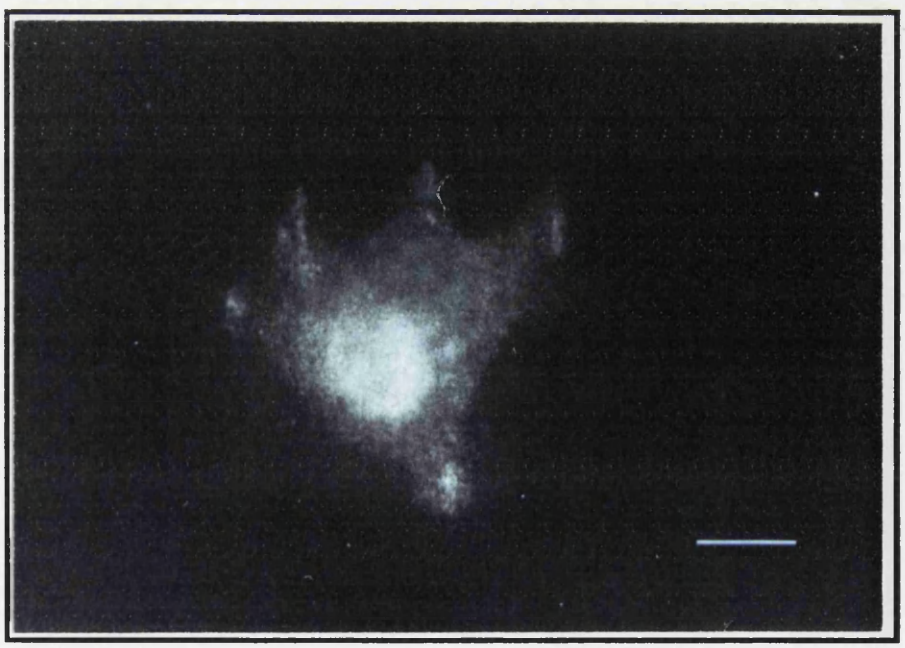

Figure 17. Distribution of phosphorylated tyrosine residues in P388D1 macrophage-like cells grown on a grooved quartz substrate. Cells were stained with PY20 monoclonal antibody and Texas Red sheep anti-mouse secondary antibody. Grooves are 70nm deep and 12.5µm wide. Scale bar represents 10µm.

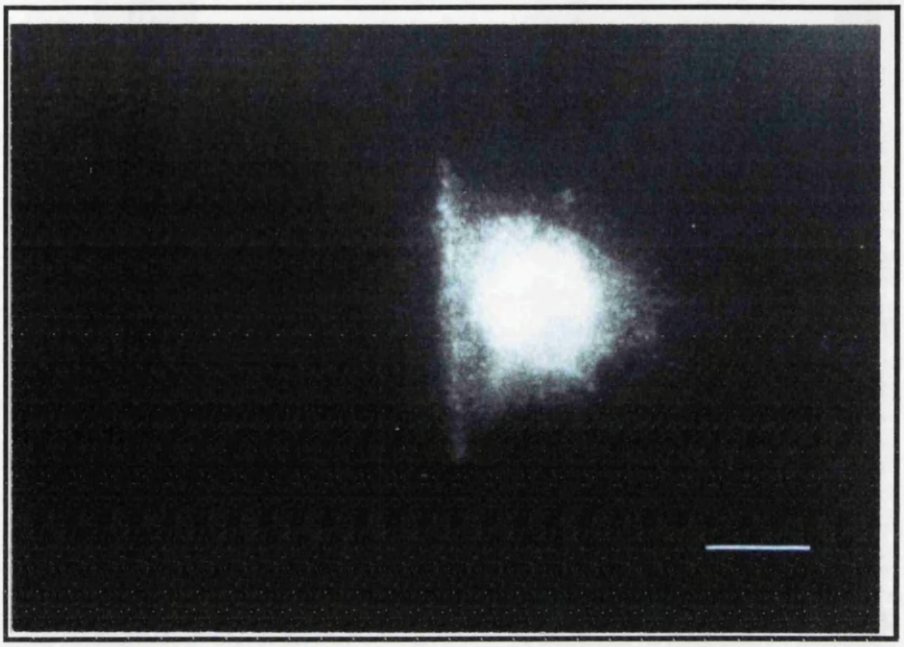

Figure 18. Distribution of phosphorylated tyrosine residues in P388D1 macrophage-like cells grown on a grooved quartz substrate. Cells were stained with PY20 monoclonal antibody and Texas Red sheep anti-mouse secondary antibody. Grooves are 44nm deep and 12.5µm wide. Scale bar represents 10µm.

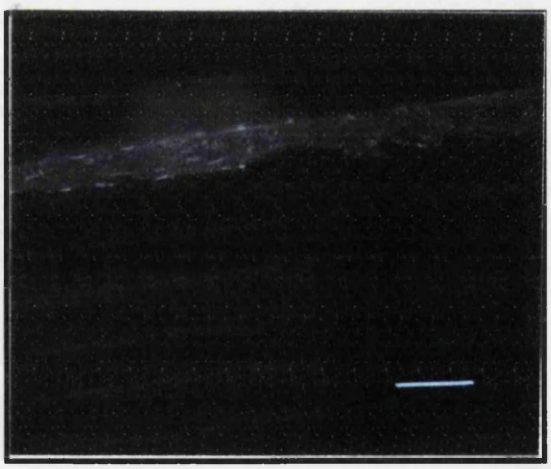

Figure 19. Distribution of phosphorylated tyrosine residues in BHK cells grown on a grooved quartz substrate. Cells were stained with PY20 monoclonal antibody and Texas Red sheep anti-mouse secondary antibody. Grooves are 6µm deep and 12.5µm wide. Scale bar represents 20µm.

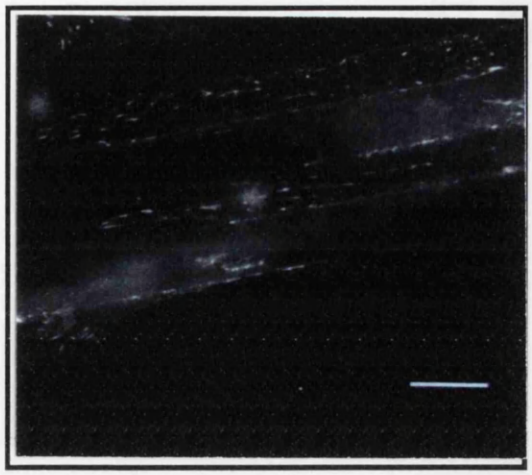

Figure 20. Distribution of phosphorylated tyrosine residues in BHK cells grown on a grooved quartz substrate. Cells were stained with PY20 monoclonal antibody and Texas Red sheep anti-mouse secondary antibody. Grooves are 6μm deep and 12.5μm wide. Scale bar represents 20μm.

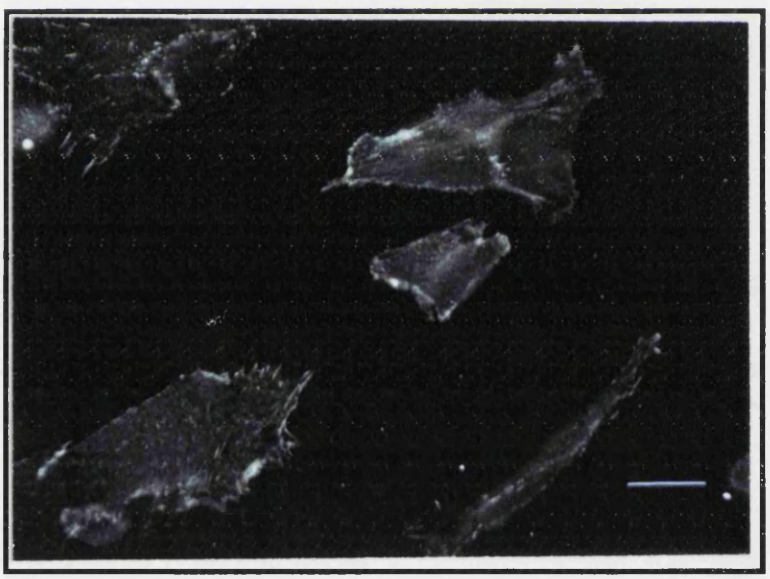

Figure 21. Distribution of phosphorylated tyrosine residues in BHK cells grown on a flat quartz substrate. Cells were stained with PY20 monoclonal antibody and Texas Red sheep anti-mouse secondary antibody. Scale bar represents 20μm.

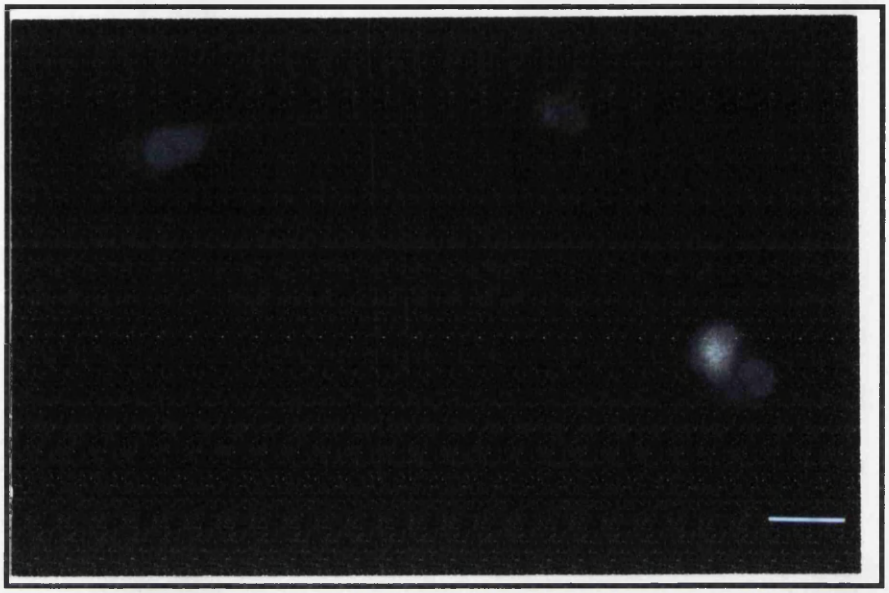

Figure 22. Negative control for staining of phosphorylated tyrosine residues. BHK cells are shown, on a flat quartz substrate, stained only with the secondary antibody (Texas Red). Scale bar represents 20µm.

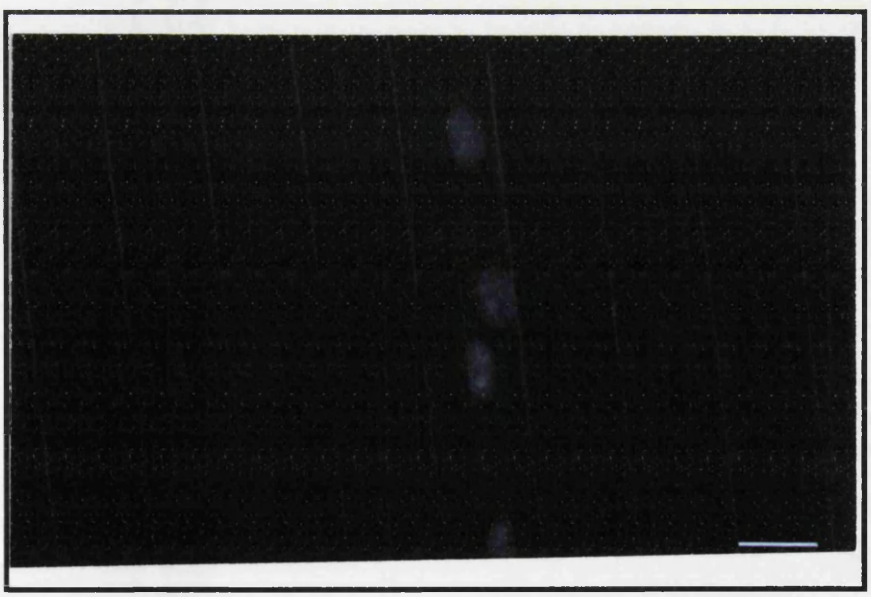

Figure 23. Negative control for staining of phosphorylated tyrosine residues. BHK cells are shown, on a grooved quartz substrate, stained only with the secondary antibody (Texas Red). Grooves are 6µm deep and 12.5µm wide. Scale bar represents 20µm.

staining in P388D1 cells cultured on grooved substrata mimics that of the staining for phosphorylated tyrosine residues.

When P388D1 cells were cultured on quartz structures of nanometric depth the same specific staining pattern of phosphorylated tyrosine residues was observed along groove/ridge boundaries. This was observed on structures with a depth of only 88 (Figure 16), 70 (Figure 17) and even 44 nanometres (Figure 18).

The same phenomenon was observed in fibroblasts and other cell types tested, which also showed specific staining of phosphorylated tyrosine residues localised along groove/ridge boundaries (Figures 19 and 20) and randomly dispersed points of fluorescent stain within cells grown on flat substrata (Figure 21). But, in the case of fibroblastic cells, the staining pattern was observed only on microgrooved, not nanogrooved, structures. Also, the staining pattern observed in BHK cells (Figures 19, 20 and 21) appeared more in the form of lines, similar to that which would be expected when staining for focal adhesions, as opposed to the dot-like staining pattern observed in the macrophage-like cells.

Figures 22 and 23 are negative controls, stained with only secondary antibody (sheep anti-mouse Texas Red) and show BHK cells on flat and microgrooved quartz structures, respectively. Although a feint outline of the cell nucleus could be seen in each case, no specific staining pattern was observed.

Tyrphostins as Inhibitors of Tyrosine Phosphorylation

Initially it was hoped that the experiment would determine whether tyrphostins would inhibit the alignment of BHK cells along microgrooved structures. But, it was observed that the tyrphostins actually inhibited the attachment and spreading of cells on the substrate, therefore no measure of cell alignment could be made. Instead, numbers of cells attached (per field of view) on flat coverslips were

counted, in order to determine the effect of tyrphostins on cell attachment. Figure 24 shows the number of BHK cells attached to a flat substrate after a 24 hour incubation with various tyrphostins (at 50μM concentration). As Tyrphostin 1 is a negative control for other Tyrphostins (Calbiochem product information leaflet), it can be seen that incubation for 24 hours in the presence of Tyrphostins 25, B44(-), B46, B50(+) and B56 all dramatically reduce cell attachment to a planar glass substrate. Attachment is reduced to at least half that observed in the negative control sample, and in the case of B50(+) and B56 only around a fifth of the number of cells in the control sample have attached.

It should be noted that as the cells failed to align on grooved subtrates following incubation with tyrphostins, immunofluorescence was not carried out to observe any possible staining of the cells. In future this should be carried out to confirm that any phosphorylation observed by immunofluorescence had been abolished by the tyrphostins. Although Tyrphostin 1 acts as a negative control, it would also have been useful to include a second control, of cells with no Tyrphostin added.

Western Blots

Using samples of protein from cells grown on flat and grooved quartz substrates no distinct bands (corresponding to phosphorylation of tyrosine residues) were observed on the autotoradiographs. It is probable that the reason for this was the small amount of protein in each sample run on the SDS gels.

DISCUSSION

Indirect Immunofluorescence

From the results it appears that phosphorylation of tyrosine residues may be related to contact guidance or, more generally, cell adhesion. The P388D1 macrophages in particular appear to be very sensitive to surface topography, and showed specific staining for phosphorylated tyrosine, located along groove ridge

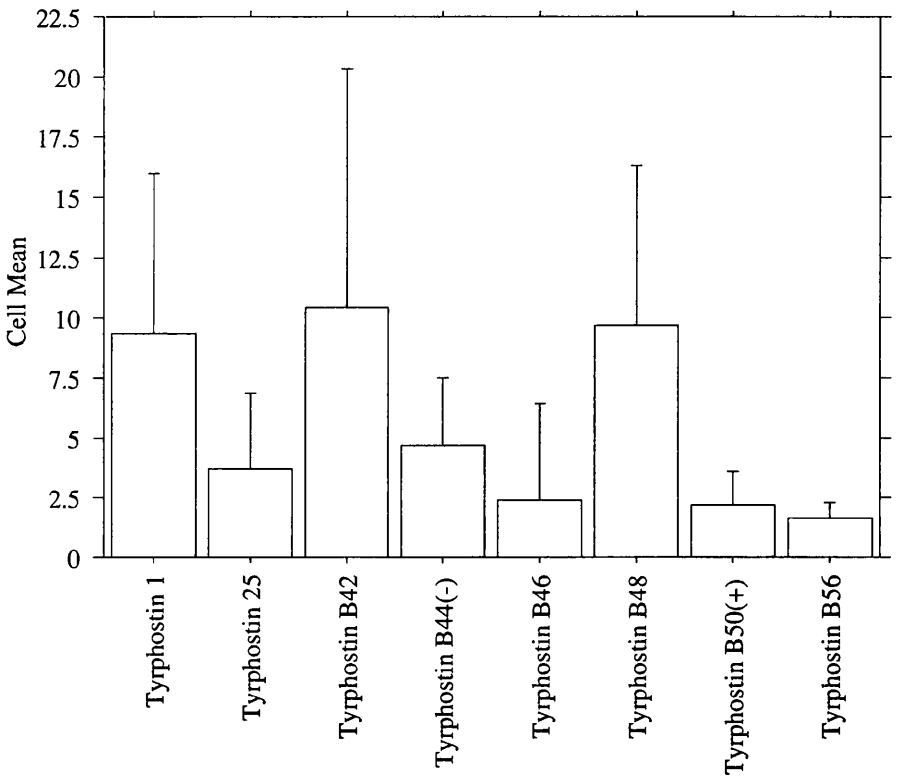

Figure 24. Effect of Tyrphostins (at 50μM concentration) on attachment of BHK cells to glass coverslips. Error bars represent +/-1 Standard Deviation. Results are means of 4 counts for each sample.

boundaries, on microgrooved fused silica structures as shallow as 44 nanometres. This depth corresponds to the size of a single collagen fibre, and therefore helps substantiate the theory of topographical cell guidance *in vivo.*

Although it is not clear from these results exactly what protein(s) are being phosphorylated, it is likely to be proteins involved in formation of focal contacts, or actin-binding proteins. This theory is supported by a study of Meyle *et al* (1994) who grew gingival fibroblasts on a microgrooved silicone biomaterial and found, using laser scanning microscopy, that the focal adhesion sites were oriented along the substratum microstructures. A comparison of fibroblast spreading and proliferation on hydrophilic and hydrophobic surfaces (Groth and Altankov, 1995) showed co-localisation of phosphotyrosine activity with formation of focal contacts and clustering of beta (1) integrins. Turner *et al* (1995) also found that treatment of cultured, serum-starved rat aortic smooth muscle cells with angiotensin II caused rapid tyrosine phosphorylation of the protein, paxillin, and the tyrosine kinase pp125 (FAK), both components of actin-associated focal adhesion sites.

These studies, carried out on planar substrata, demonstrate the presence of phosphorylated tyrosine residues in focal adesion sites, and suggest a direct role for tyrosine phosphorylation upon stimulation of cell membrane receptors. Therefore, the specific tyrosine phosphorylation I observed in cells grown on micro- and nano-grooved substrata may occur as a direct result of clustering of membrane receptors, and thereby stimulation of intracellular signalling, when the receptors come in contact with the grooves.

The fact that fibroblastic cells do not show staining of phosphorylated tyrosine residues on grooved structures of nanometric depth suggests that macrophage-like cells may be more sensitive to topography than other cell types. This would not be

unexpected as the role of macrophages *in vivo* requires them to be able to detect molecules of a very small size.

Tyrphostins as Inhibitors of Tyrosine Phosphorylation

The fact that the Tyrphostins were shown to inhibit cell attachment and spreading is consistent with the results reported by Romer (1995) who used Tyrphostins AG 213 and AG 808 to investigate the role of FAK (nonreceptor focal adhesion kinase) in cytoskeletal organisation and cell spreading. He found a dramatic decrease in FAK activity in FAK immunoprecipitates from Human Umbilical Vein Endothelial Cells (HUVECs) that had been plated on fibronectin, then treated with the Tyrphostins (at 100μM concentration). It was also shown that, in comparison with untreated controls, Tyrphostin-treated cells demonstrated a lack of focal adhesions and a sparse and disorganized stress fibre formation. Nobes *et al* (1995) also reported that Tyrphostin A25 (150μM) was able to block LPA (lysophosphatidic acid)-stimulated stress fibre formation in Swiss 3T3 cells. Furthermore, as the Tyrphostin did not inhibit the ability of microinjected rho protein to induce stress fibre formation, they concluded that LPA activation of rho is mediated by a tyrosine kinase.

Although the exact signalling pathway is no doubt very complex, these data suggest that tyrosine phosphorylation is an essential component of the events leading to cytoskeletal organisation following cell adhesion to extracelluar matrix.

Western Blots

It was not thought that the problem with the blots was due to any defect in the method of blotting used as the method and apparatus were checked using varying concentrations of serum samples and proved to be working well (Figure 25). The figure shows an autoradiograph of a blot from an SDS gel on which decreasing (1:50; 1:100; 1:200) concentrations of human serum, reading from left to right,

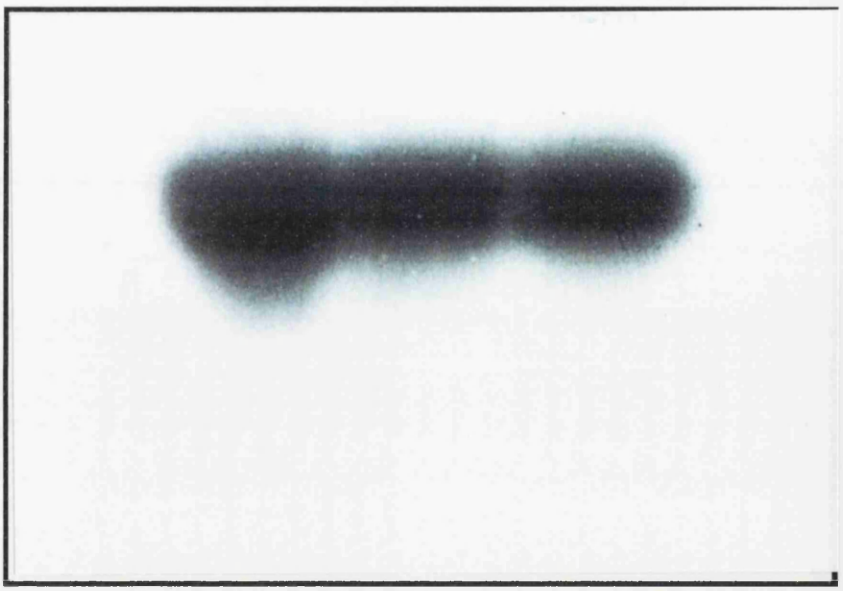

Figure 25. Western blot (control) showing serum samples (reading from left to right, 1:50; 1:100; 1:200 dilutions) probed with radiolabelled serum albumin antibody.

were run. The blot was then probed for serum albumin using a radiolabelled antibody.

The structures used for cell culture of the grooved/non-grooved samples for Western blotting were slides of dimension 76mm x 26mm. In an attempt to get a larger amount of protein to run on the gels, cells were pooled from duplicate structures, but again this did not result in any clear cut bands on an autoradiograph. In the time available it was not possible to cultivate larger samples of cells, but this should be carried out in the future.

CHAPTER 4

IMPLANTATION OF POLYDIOXANONE STRUCTURES

INTRODUCTION

The low level of immunogenicity and *in vivo* degradation rate of polydioxanone (PDS) sutures are well documented (Lerwick, 1983; Ray *et al*, 1981; Ethicon Ltd. data sheet, 1989). However, as it is important to examine the interaction between any implantable biomaterial, in all its fabricated forms, and the tissue with which it will come in contact, further studies were necessary in order to determine the *in vivo* cellular response to microfabricated PDS grooved structures. As a result of these experiments it was hoped to discover the cellular response to the PDS structures and also the rate of degradation of the structures. It was especially important to check whether fabrication of microgrooves in the PDS material substantially altered the rate of PDS degradation, as Wojciak-Stothard *et al* (1996) found that, *in vitro*, macrophages showed preferential attachment to grooved, compared with flat, substrates, and that macrophages appeared to be activated when they were grown on grooves. Therefore, if the microgrooved PDS implants were acting as a "macrophage trap", they may be expected to degrade more quickly than non-grooved PDS, due to the presence of these extra, "activated", macrophages in close proximity to the implant material.

Oxygen plasma-etching of the PDS structures, after fabrication, should result in uniform surface chemistry. But, as PDS is sensitive to exposure to the atmosphere (and is therefore normally stored in nitrogen), it was thought that any residual oxygen left behind on the surface may affect the degradation rate of the PDS. Therefore, comparisons were also made between oxygen plasma-etched and non-oxygen plasma-etched PDS structures.

PDS structures (cut to 10mm x 5mm) were implanted intramuscularly in male Sprague-Dawley rats for 7, 21, 35, 49, 70 and 91 days. The grooves (5μm deep; 12.5μm wide) were oriented along the long axis of the implants, which were placed in pouches in the lumbar muscle, one plate on either side of the midline. Grooves were thus oriented antero-posteriorly, parallel with the muscle fibres.

After the requisite periods in tissue, one of the implants was removed, along with surrounding muscle tissue, fixed in formalin and processed to thin sections by wax histology (two blocks per implant). Ethicon Trichrome stain (Haematoxylin, Saffron, Phloxine) was used to stain the sections, which were then examined under the light microscope for analysis of effects on the implant and also the local tissue reaction. The remaining implant, and surrounding tissue, was cut into two halves, one of which was processed as above (one block) and the other prepared for scanning electron microscope (SEM) examination, after glutaraldehyde fixation and critical-point drying.

RESULTS

HISTOLOGICAL ANALYSIS

Non-Oxygen Plasma-Etched PDS Structures

7 days post-implantation

The PDS structure is surrounded by organised tissue reaction, with fibrous exudate, mainly macrophages and fibroblasts, with some new collagen deposition. A few eosinophils can be seen, and neutrophils are notable in some sections. The grooves are still intact, with cells (probably macrophages), cell debris, or exudate seeming to occupy grooves. (See figures 26 A and B).

21 days post-implantation

The tissue reaction is more mature (more macrophagic; fewer polymorphonuclear cells; more collagen capsule). Fibroblasts and new collagen are dominant, with

some macrophages. Grooves are seen widely on the PDS structure and some grooves show evidence of cracks emerging from them into the implant. The impression of grooves can be observed in the immediate tissue, with cells, debris, and exudate present. (See figures 27 A and B).

35 days post-implantation

The tissue capsule is now mostly fibroblasts and collagen in layers with some, discontinuous, layers of macrophages. The edges of the grooves on the implant, where observed, show evidence of rounding. There is the impression of grooves observed in the immediate tissue, with cells, debris, and exudate present. This surface layer of grooved tissue has often split from the implant (probably due to processing). (See figures 28 A and B).

49 days post-implantation

The tissue reaction is as seen previously. The grooves of the implant are still well in evidence, but now rounded at the edges. The impression of grooves is observed in the immediate tissue, with cells, debris, and exudate present. Again, this surface layer of grooved tissue has often split from the implant. The layer of tissue lying adjacent to and within the grooves is often cellular, including macrophages. (See figures 29 A and B).

70 days post-implantation

The tissue reaction is well organised, with fibroblasts and collagen, but now with a greater population of macrophages, probably associated with the beginning of absorption of the PDS. This is clearly seen at the implant edges. The grooves of the implant are much less evident now, possibly due to substantial break up of the implant due to sectioning, this latter accelerating as absorption increases. The surface of the grooved PDS can occasionally be seen, having split from the rest of

the implant, and showing evidence of cells and tissue, in a tooth-like pattern. (See figure 30).

91 days post-implantation

The tissue reaction is again well organised, with fibroblasts and collagen, and with a greater population of macrophages, probably associated with the ongoing absorption of the PDS implants. The grooves of the implant, whilst not abundant, can still be observed in some areas, and single cells can be seen within the grooves. The surface of the grooved PDS can occasionally be seen, having split from the rest of the implant, and again showing evidence of cells and tissue, in a tooth-like pattern. (See figures 31 A and B).

Oxygen Plasma-Etched PDS Structures

7 days post-implantation

The PDS implants are surrounded by an organised tissue reaction, with fibrous exudate (marked in some sections), mainly macrophages and fibroblasts, and some new collagen deposition. A few eosinophils and neutrophils can be observed in some sections. The grooves of the implant are still intact, with cells (probably macrophages), cell debris, or exudate seeming to occupy grooves. (See figures 32 A and B).

21 days post-implantation

The tissue reaction is now more mature (more macrophagic, fewer polymorphonuclear cells, more collagen capsule), though fairly thin. Fibroblasts, macrophages and new collagen are dominant. Grooves are still present on the implant, and the impression of grooves can be observed, in places, in the immediate tissue, with cells, debris, and exudate present. (See figures 33 A and B).

35 days post-implantation

The tissue capsule is now mostly fibroblasts and collagen in layers, with some, discontinuous, layers of macrophages. The grooves of the PDS structures are not prominent, and the edges of the grooves, where observed, show evidence of much rounding. The impression of the grooves can be observed in the immediate tissue, with cells, debris and exudate present. (See figures 34 A and B).

49 days post-implantation

The tissue reaction is as seen at 35 days. The grooves of the implant are still in evidence, but again much rounded at the edges. The layer of tissue lying adjacent to, and within, the grooves is often cellular, including macrophages. (See figure 35).

70 days post-implantation

The tissue reaction is well organised, with fibroblasts and collagen, but now with a greater population of macrophages, probably associated with the limited beginning of absorption of the PDS. This is clearly seen at the implant edges. The grooves of the implant cannot be observed now, possibly due to substantial break-up of the implant due to sectioning, this latter accelerating as absorption increases. The impression of grooves in tissue is not seen. However, there is evidence of a "castellated" pattern to the reaction edge, implying the former presence of grooves. (See figures 36 A and B).

91 days post-implantation

The tissue reaction is again well organised, with fibroblasts and collagen, and with a greater population of macrophages, probably associated with the greater absorption of the PDS implants. The grooves of the implant are not abundant. The surface of the formerly-grooved PDS can occasionally be seen, having split from the rest of the implant, and showing evidence of cells and tissue, in a tooth-like pattern. Again

there is evidence of a "castellated" pattern to the reaction edge, implying the former presence of grooves. (See figures 37 A and B).

In many of the sections (from all timepoints) there is some shattering of the PDS structures, in both oxygen plasma-etched and non-oxygen plasma-etched samples. This is almost certainly due to the sectioning process, with the plane of cracking aligned at about 45° to the implant surface. Also, the PDS implants are not present in all sections, due to processing.

SCANNING ELECTRON MICROSCOPY (SEM) ANALYSIS

SEM analysis was carried out on non-oxygen plasma-etched samples, explanted at 21, 35 and 49 days. The grooves were clearly observed on all explanted PDS structures up to 49 days *in vivo*. Tissue is present in many grooves, but there is no particular evidence of cellular orientation along the groove direction (figure 38). This is probably due to damage during processing of the samples, and to general masking by the adherent tissue matrix. The tissue capsules have also been moulded into a reverse impression of the grooved surfaces, at all timepoints investigated (figure 39).

DISCUSSION

HISTOLOGICAL ANALYSIS

The PDS structures, with both types of etched surface, formed an apparently biocompatible surface, based on local effects after *in vivo* implantation, similar to historical data on untreated PDS material and PDS suture (Ethicon Ltd.). Both oxygen plasma-etched and non-oxygen plasma-etched grooves became filled by cellular and non-cellular material and debris as soon as 7 days post-implantation, and evidence of single cells (macrophages and fibroblasts) within grooves exists from 7 days to 91 days *in vivo*. However, from the sections taken in this study, it was not possible to say whether cells are oriented by the grooves. It is interesting to

A

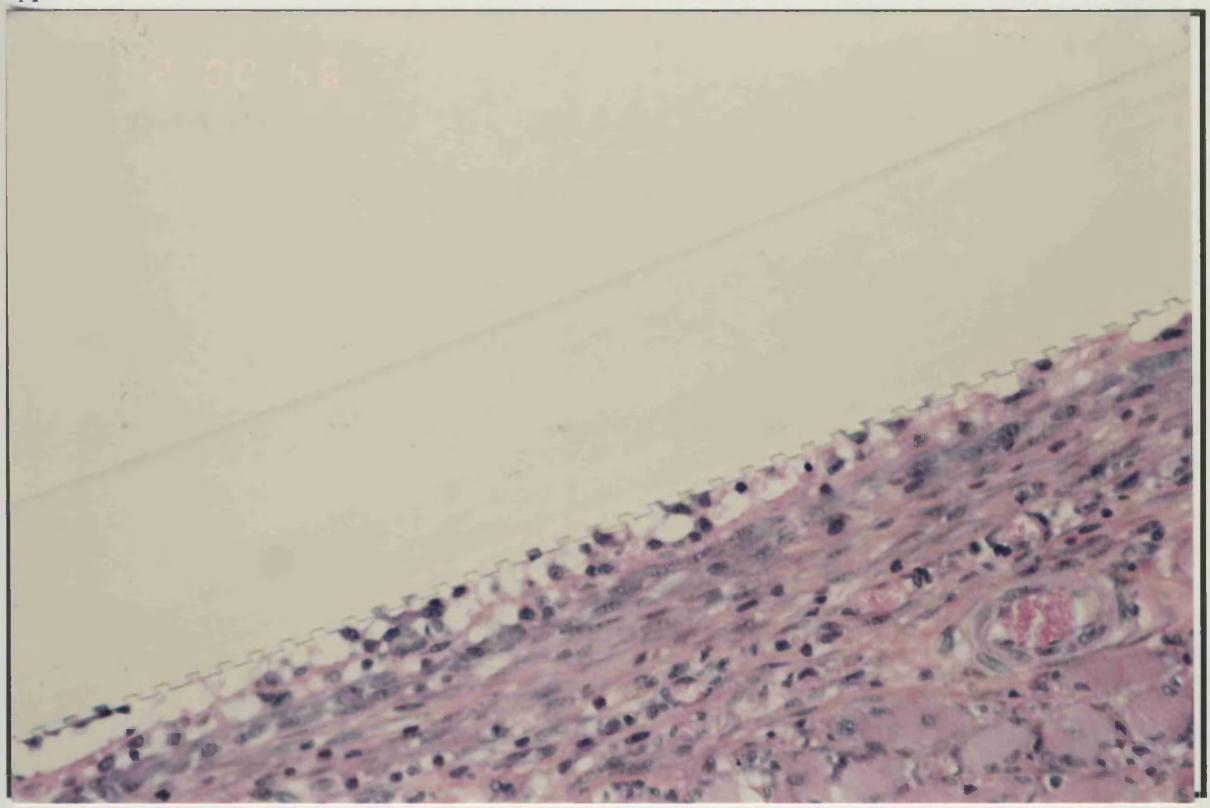

B

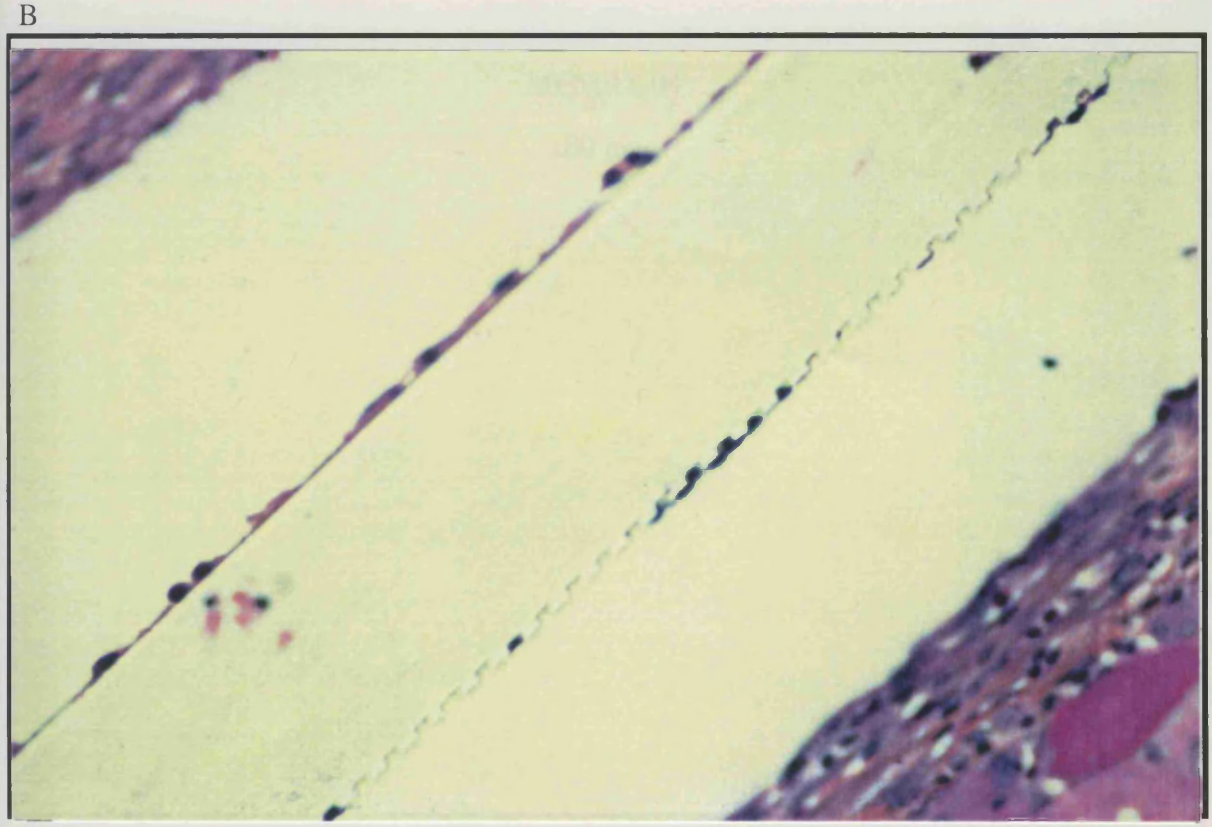

Figure 26. Photomicrographs showing transverse sections of non-oxygen plasma-etched PDS structures in rat lumbar muscle, 7 days post-implantation. Grooves are still intact, with cells and tissue seeming to occupy some of the grooves. A) Mag. x62.5. B) Mag. x80.

A

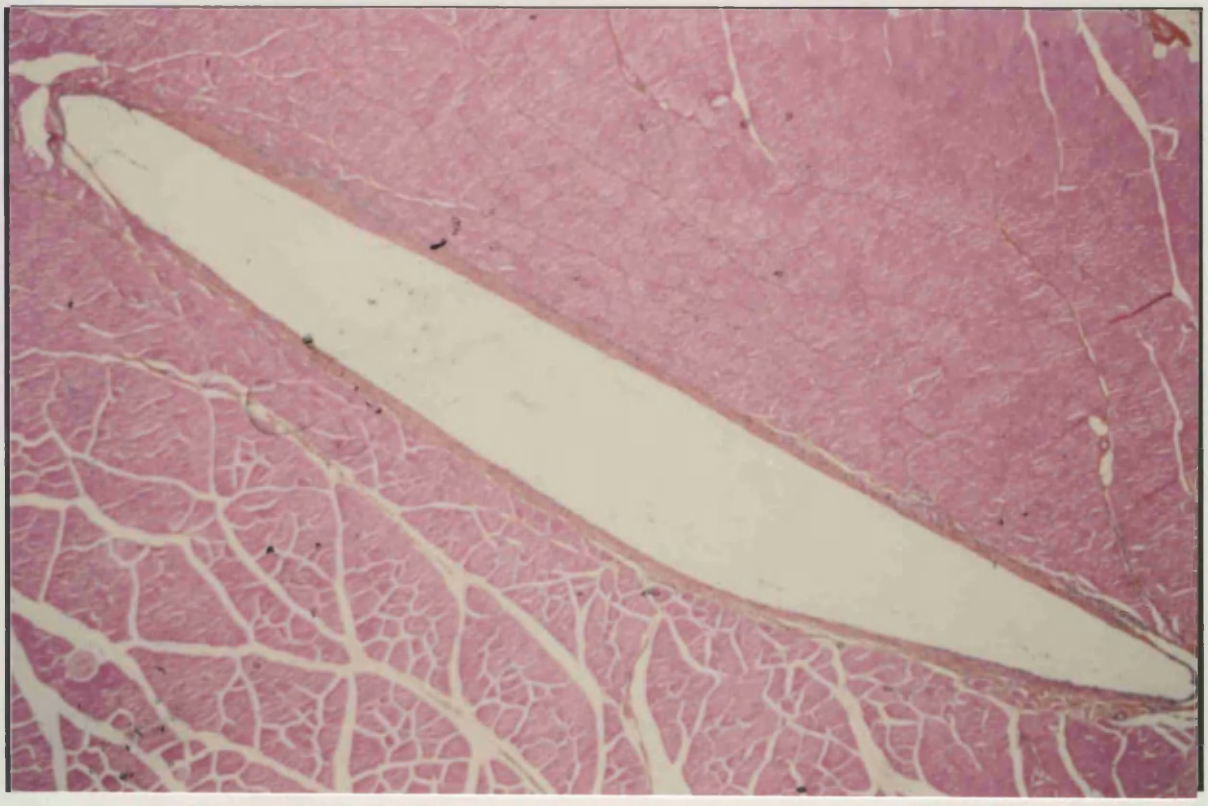

B

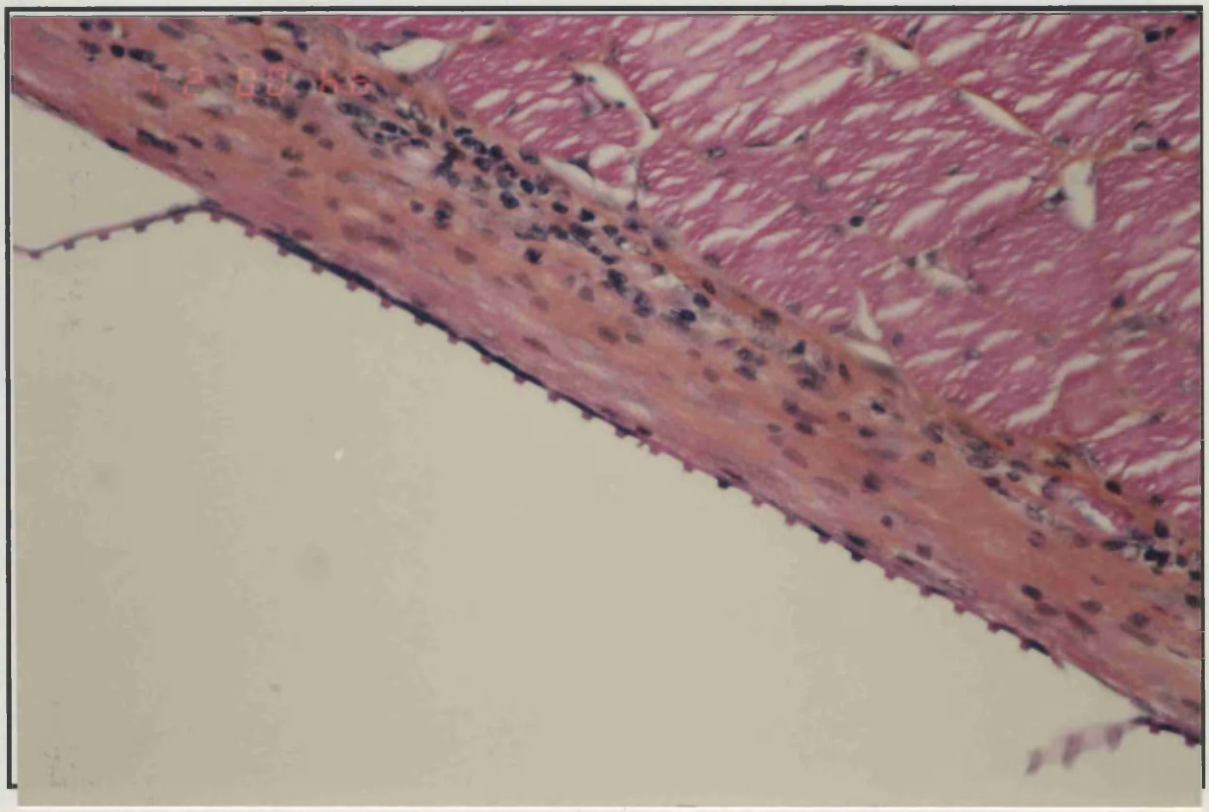

Figure 27. Photomicrographs showing transverse sections of non-oxygen plasma-etched PDS structures in rat lumbar muscle, 21 days post-implantation. A) Overall view of the implant site, which shows signs of becoming surrounded by a collagen capsule (Mag. x6.25). B) The impression of grooves left on tissue adjacent to the implant site (Mag. x80).

A

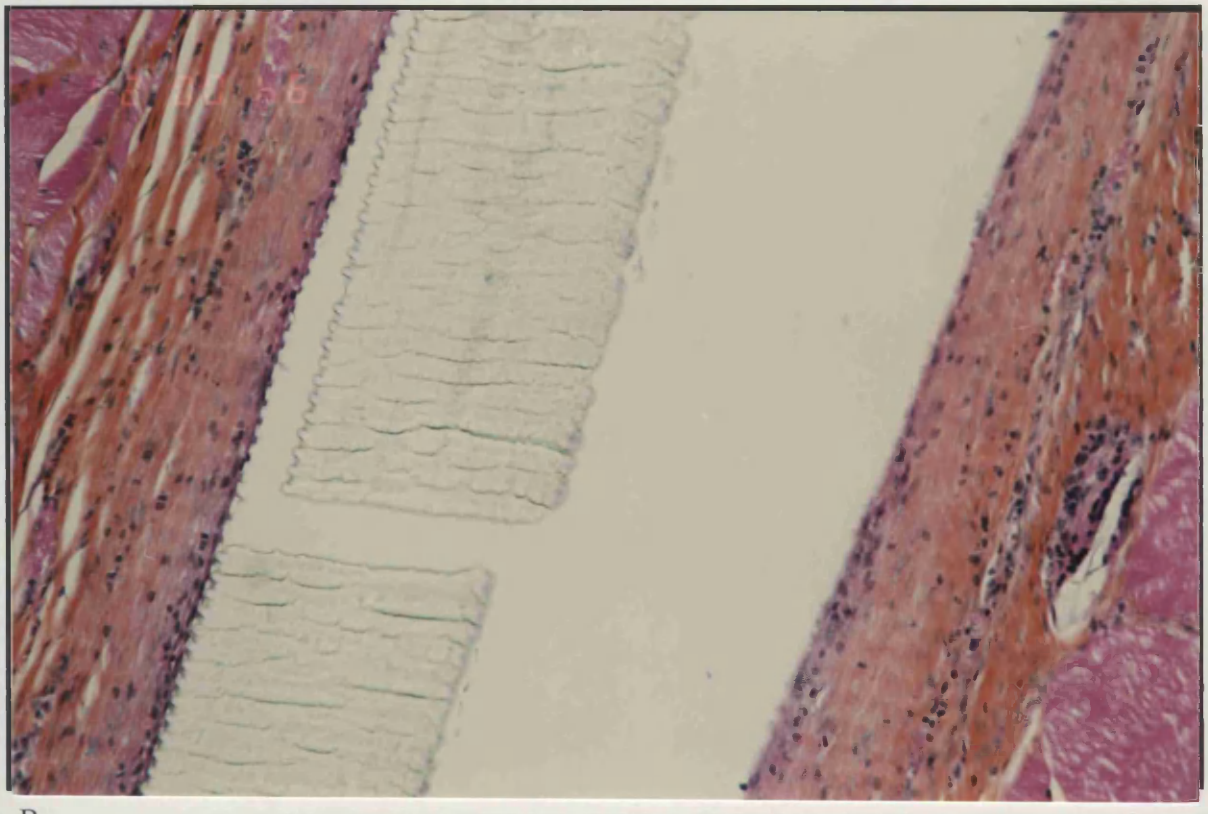

B

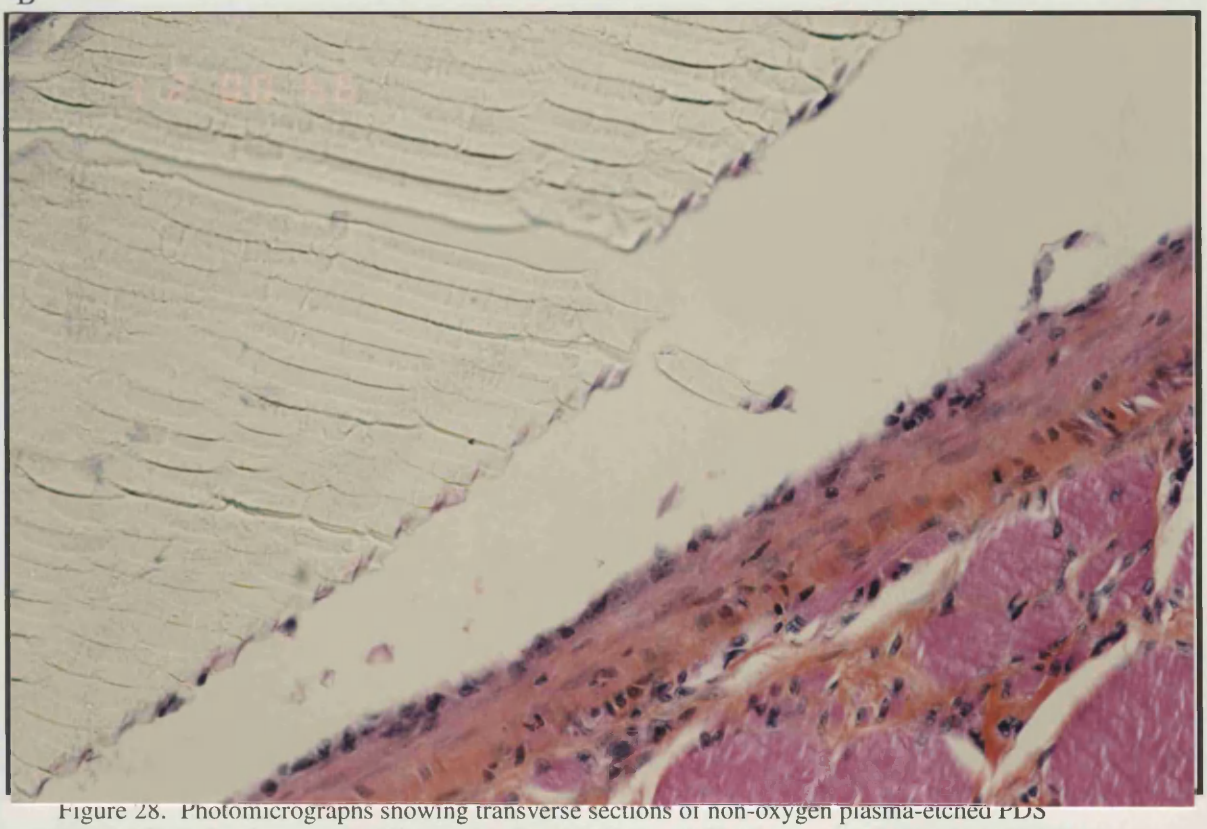

Figure 28. Photomicrographs showing transverse sections of non-oxygen plasma-etched PDS structures in rat lumbar muscle, 35 days post-implantation. A) The tissue capsule now consists of cells and collagen in layers. The grooves on the PDS implant, and imprinted in tissue, can still be observed and the PDS shows cracks emerging from the grooves into the implant (Mag. x40). B) Non-grooved edge of implant, showing obvious cracks in the PDS (Mag. x62.5).

A

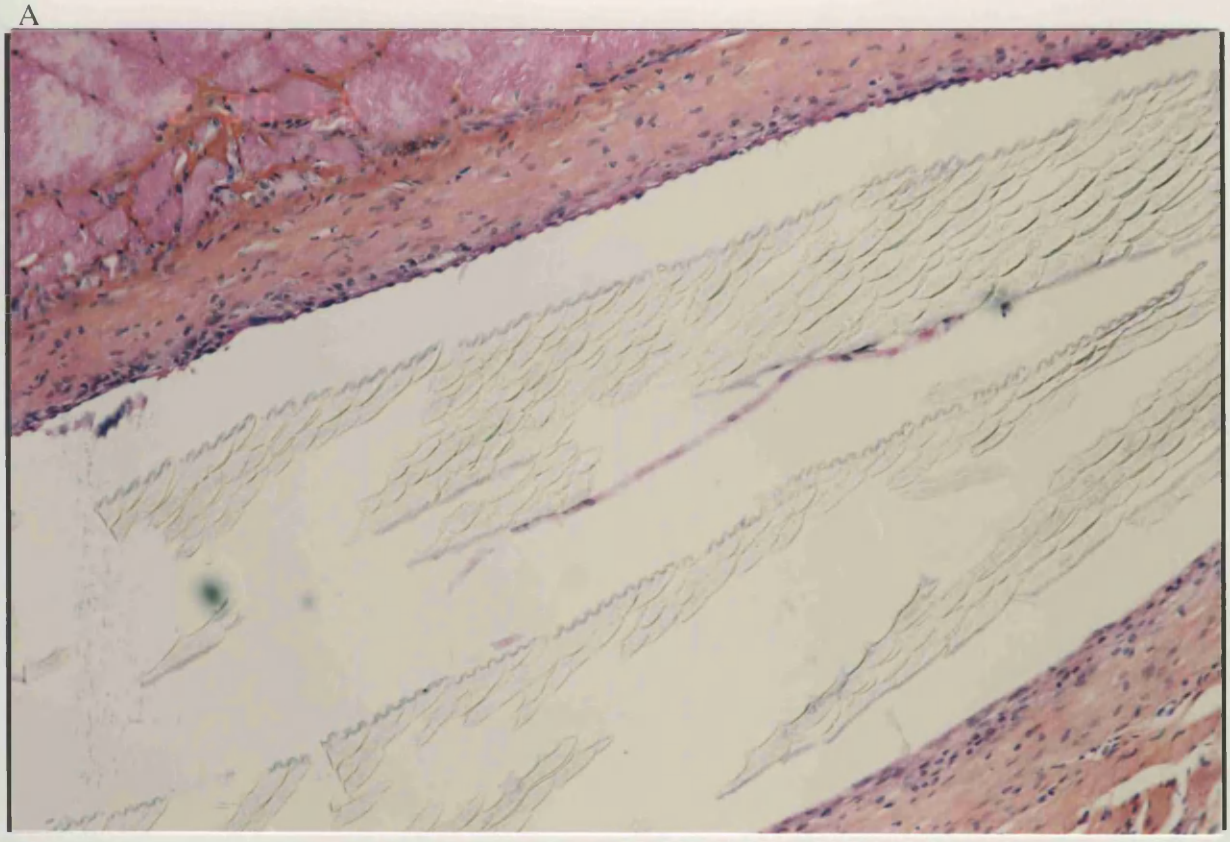

B

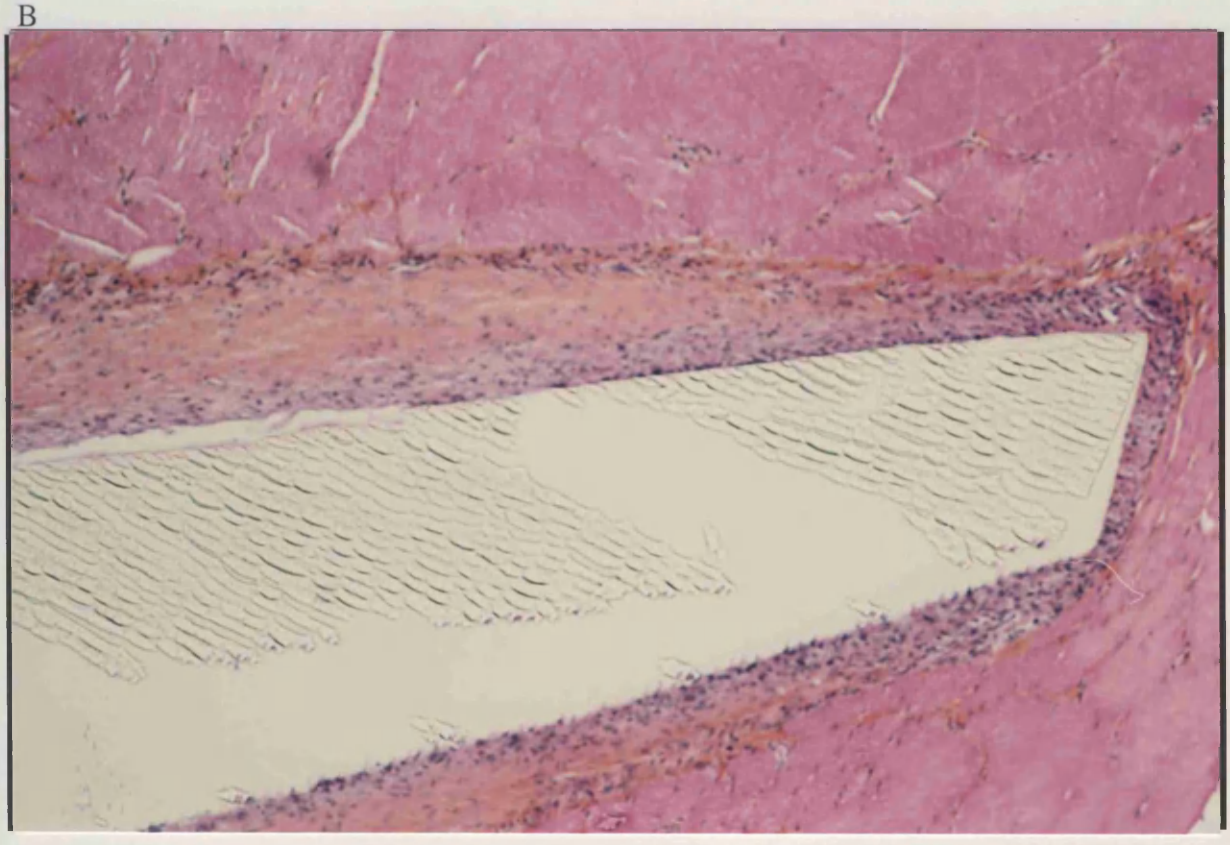

Figure 29. Photomicrographs showing transverse sections of non-oxygen plasma-etched PDS structures in rat lumbar muscle, 49 days post-implantation. A) Grooves of the implant are still well in evidence, but rounded at the edges. Two grooved edges can be seen as the implant has folded over on itself. (Mag. x31.25). B) The layer of tissue lying adjacent to and within the grooves is mainly cellular, with some collagen (Mag. x25).

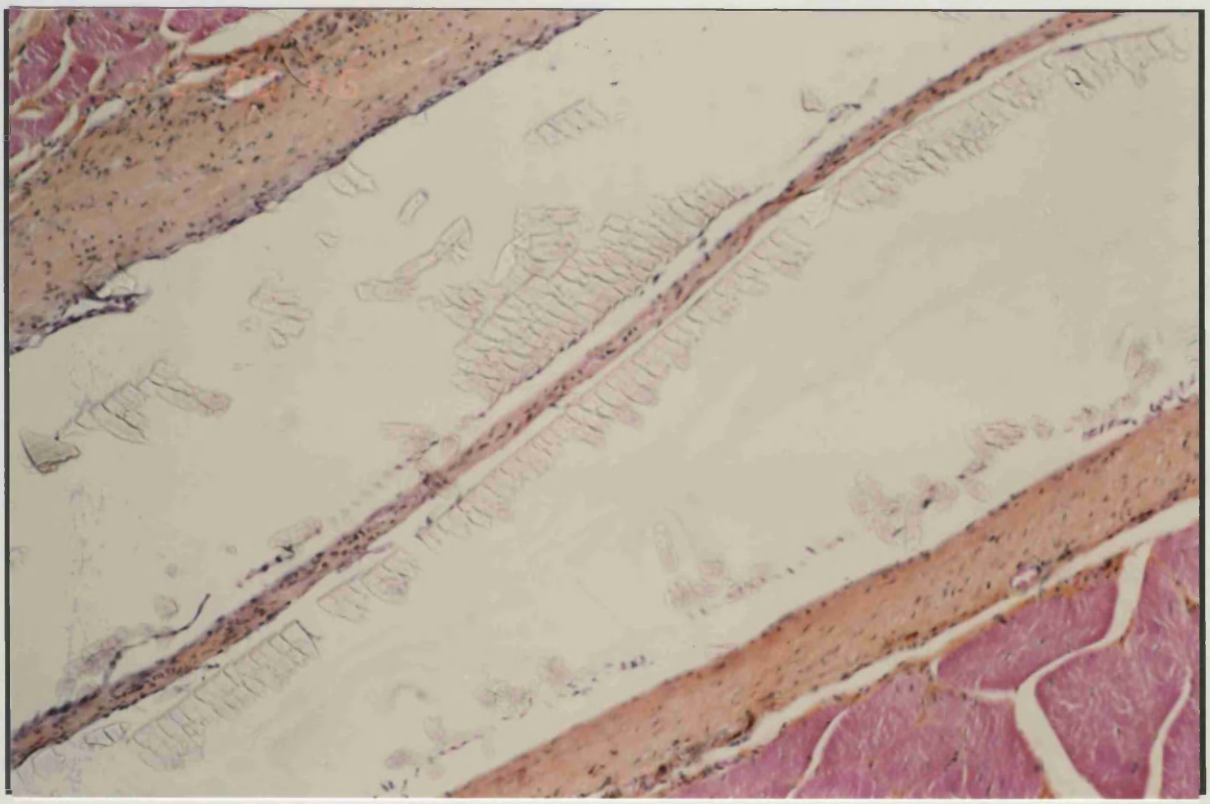

Figure 30. Photomicrograph showing transverse section of non-oxygen plasma-etched PDS structure in rat lumbar muscle, 70 days post-implantation. The grooves of the implant are much less evident, probably due to break up of the implant due to sectioning, enhanced by increased absorption of the PDS. The surface of the grooved PDS can be seen in areas, split from the rest of the implant, showing evidence of cells and tissue in a groove-like pattern (Mag. x25).

A

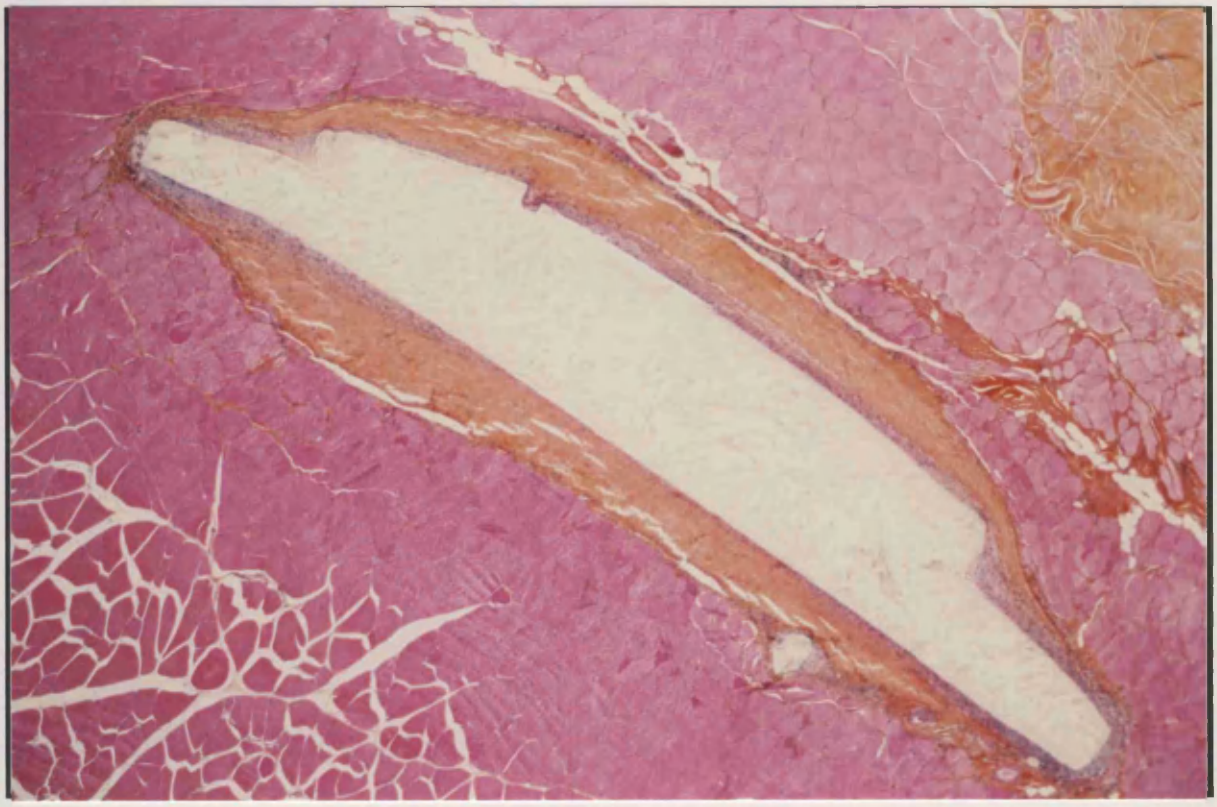

B

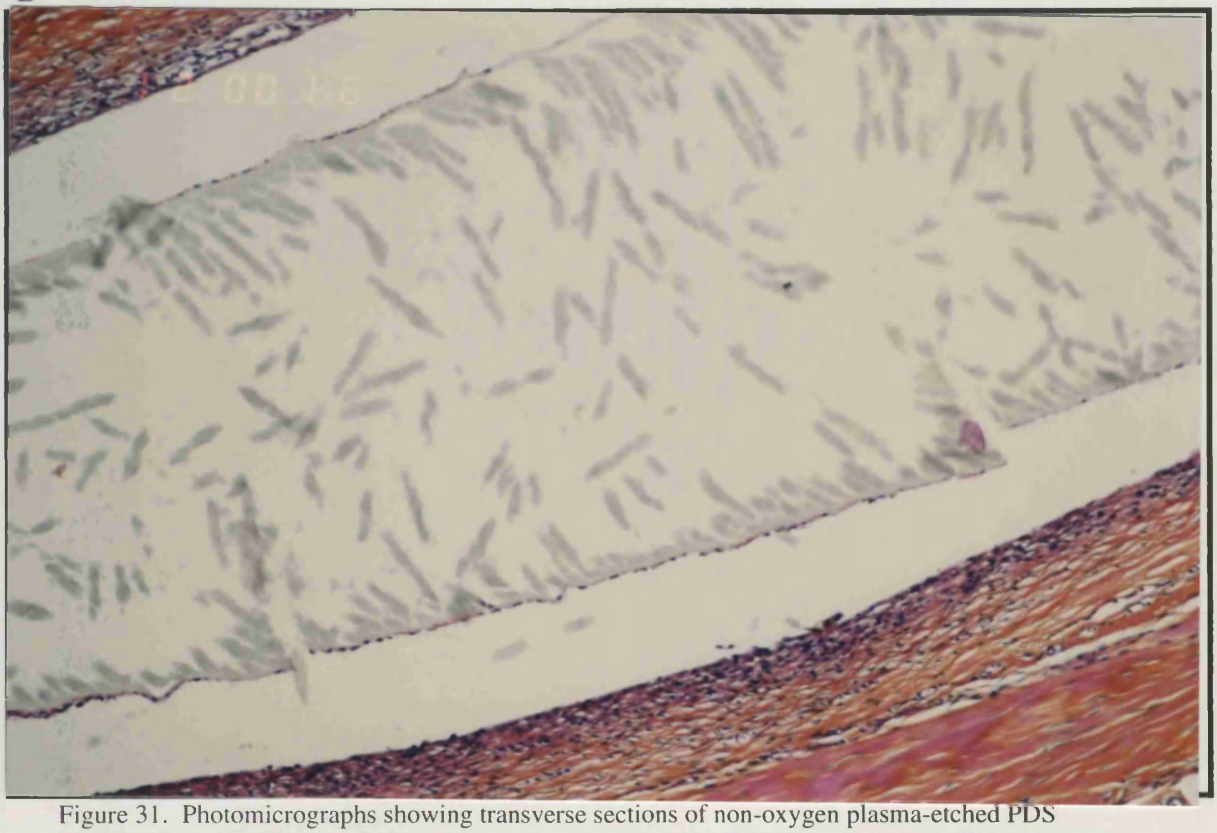

Figure 31. Photomicrographs showing transverse sections of non-oxygen plasma-etched PDS structures in rat lumbar muscle, 91 days post-implantation. A) The implant has broken into two pieces and is immediately surrounded by a cellular layer, then a capsule of collagen (Mag. x6.25). B) The tissue reaction is well organised, and rounded grooves can still be observed on some areas of the implant. The PDS is much degraded, marked by increased shattering of the plate during processing (Mag. x25).

A

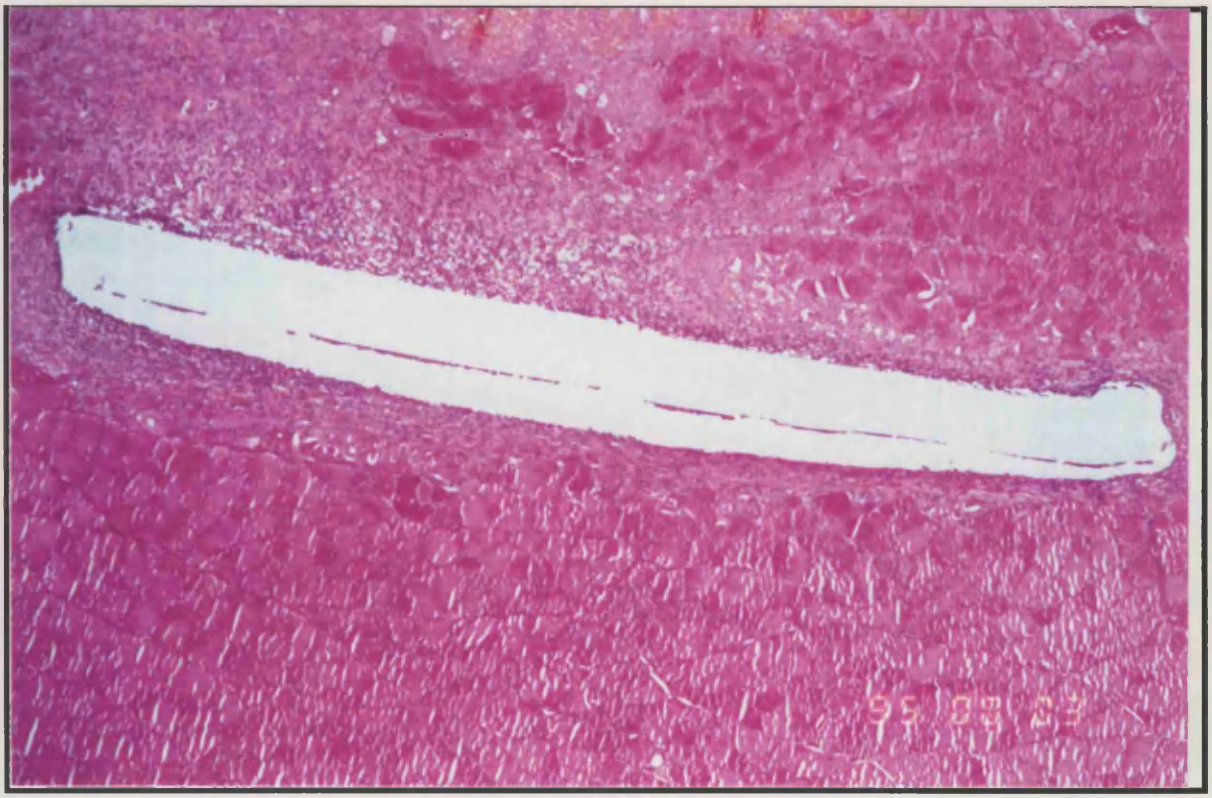

B

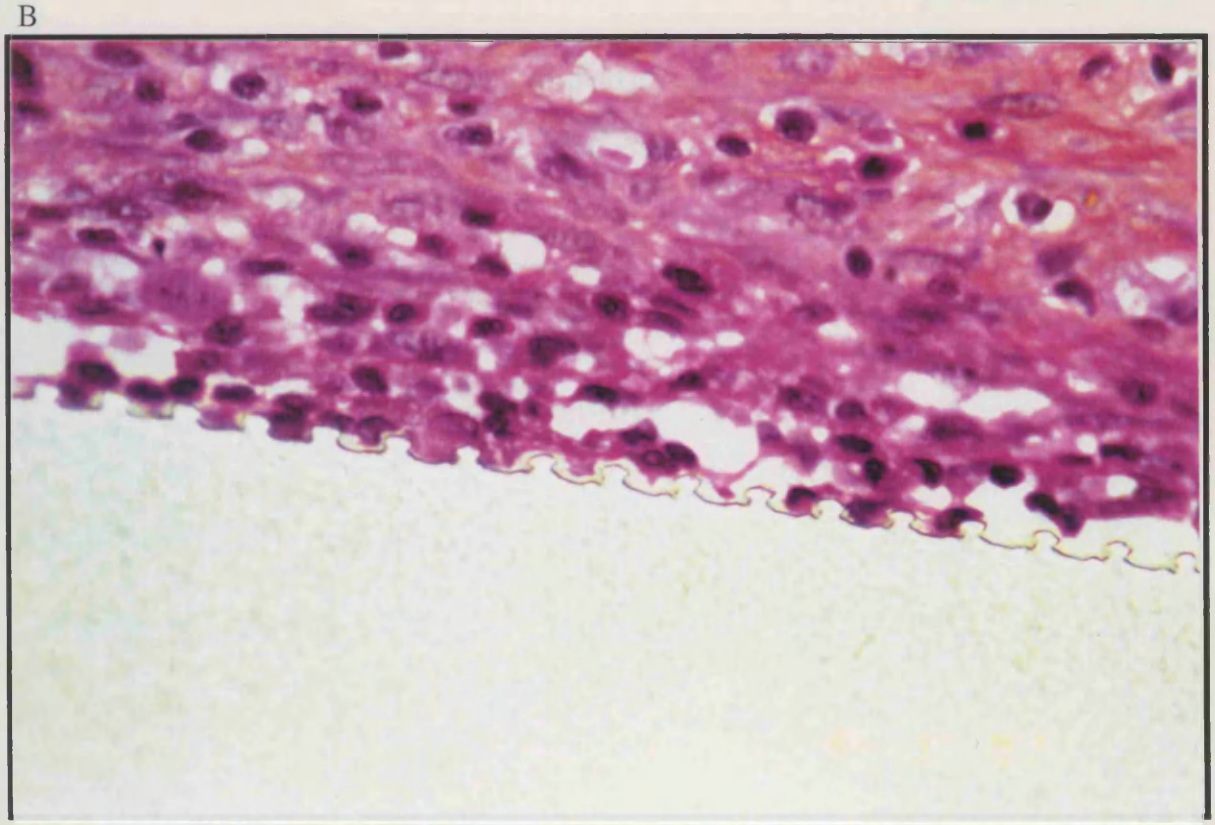

Figure 32. Photomicrographs showing transverse sections of oxygen plasma-etched PDS structures in rat lumbar muscle, 7 days post-implantation. A) The implant is surrounded by organised tissue reaction, mainly cells with some new collagen deposition (Mag. x10.8). B) Cells can be observed seeming to occupy individual grooves of the implant (Mag. x160).

A

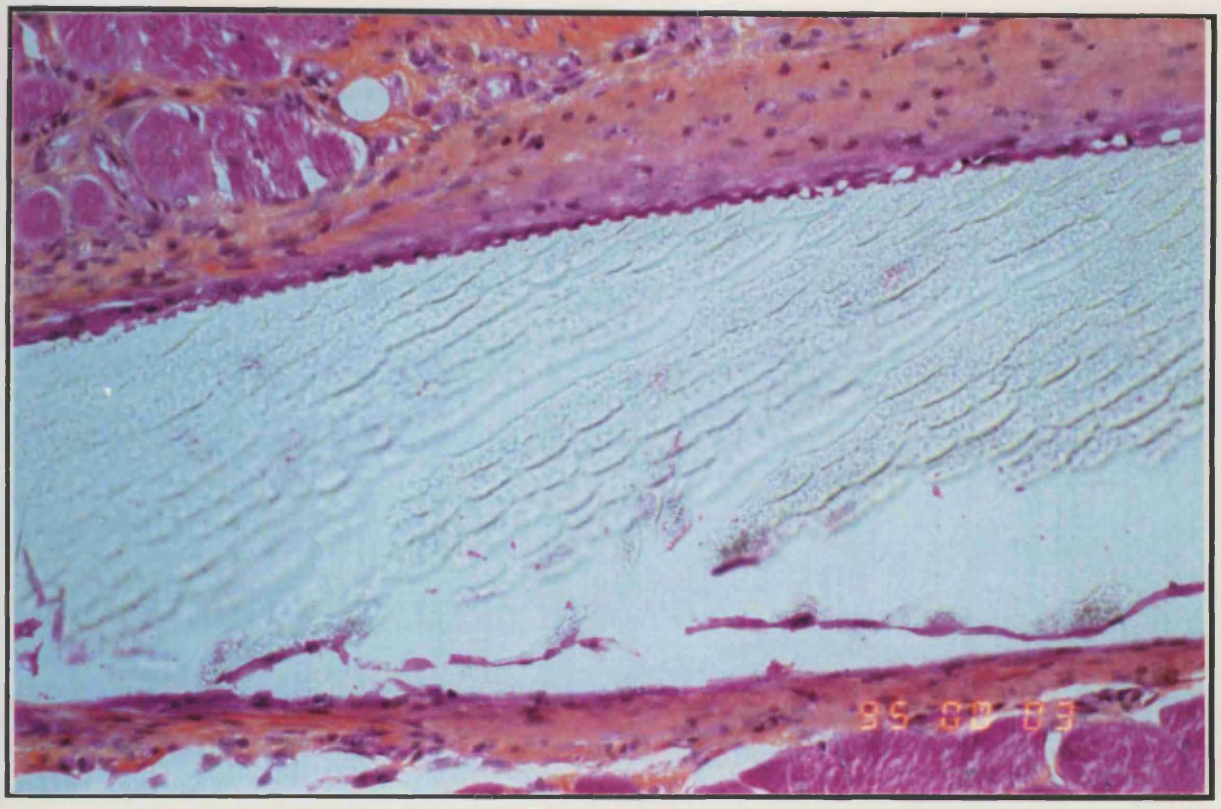

B

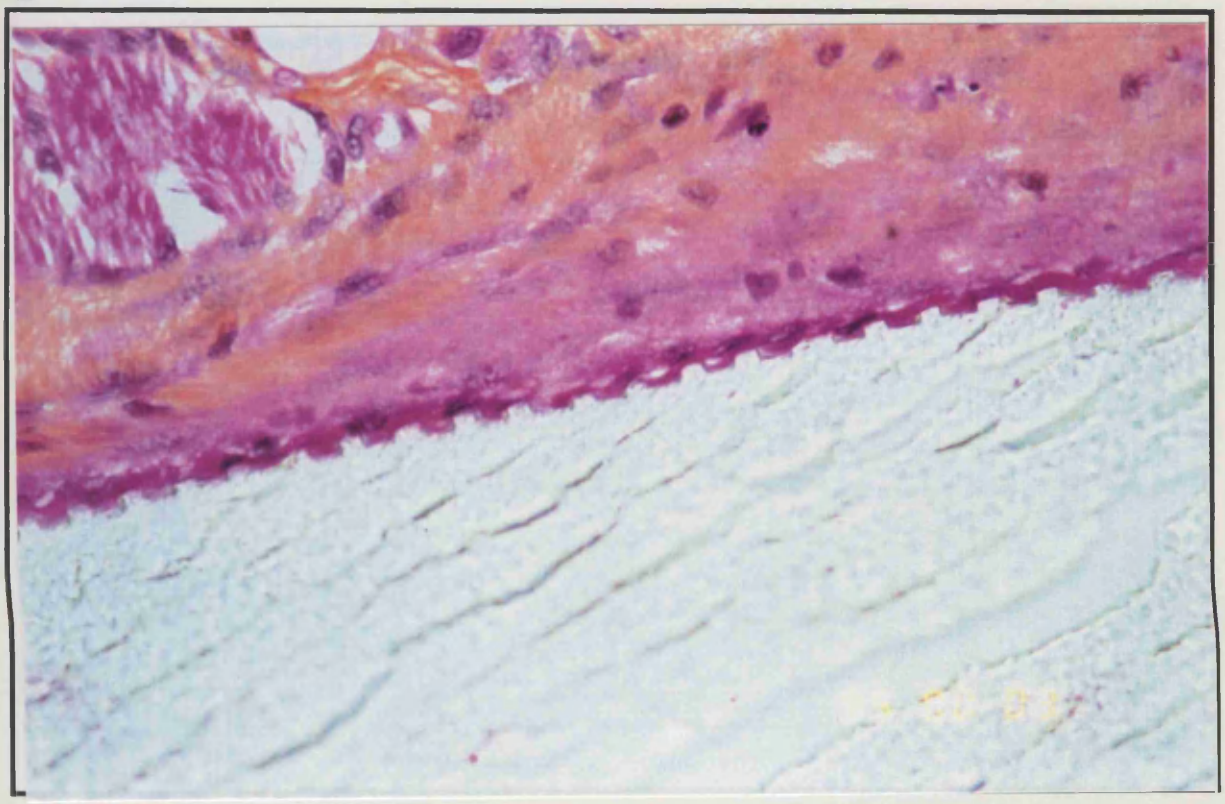

Figure 33. Photomicrographs showing transverse sections of oxygen plasma-etched PDS structures in rat lumbar muscle, 21 days post-implantation. The tissue reaction is more mature. Grooves are still present on the implant, which now shows evidence of cracking, and the impression of grooves can be observed in the surrounding tissue. A) Mag. x50. B) Mag. x125.

A

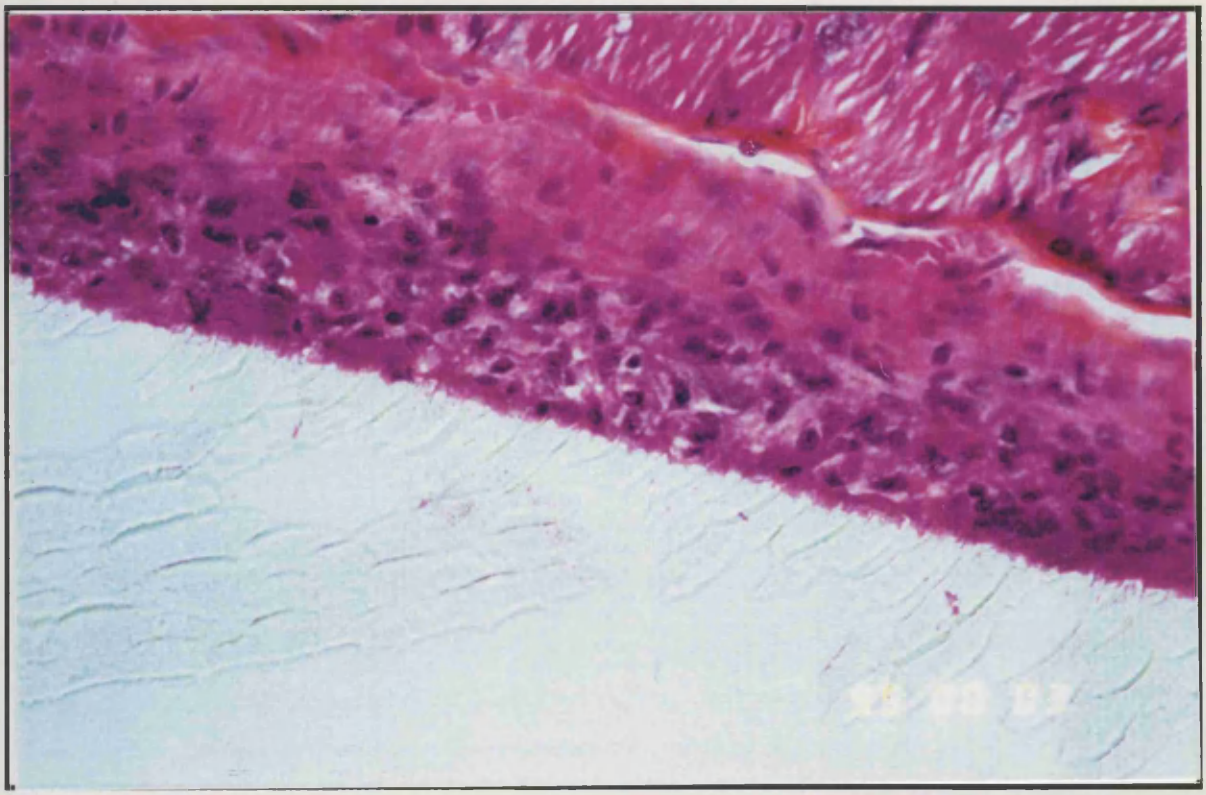

B

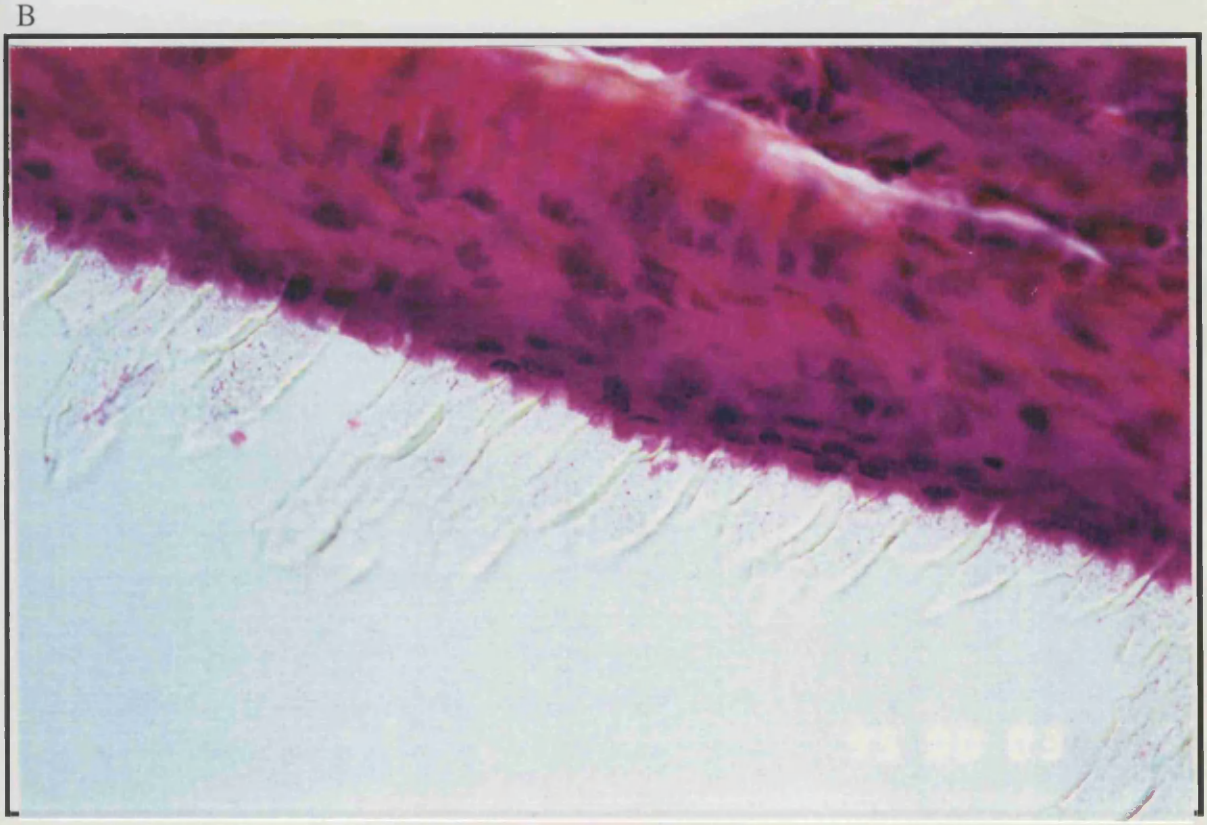

Figure 34. Photomicrographs showing transverse sections of oxygen plasma-etched PDS structures in rat lumbar muscle, 35 days post-implantation. The tissue capsule surrounding the implant now consists of cells and collagen in layers. The grooves of the PDS structure are not prominent, and where observed they show evidence of much rounding. A) Mag. x80. B) Mag. x125.

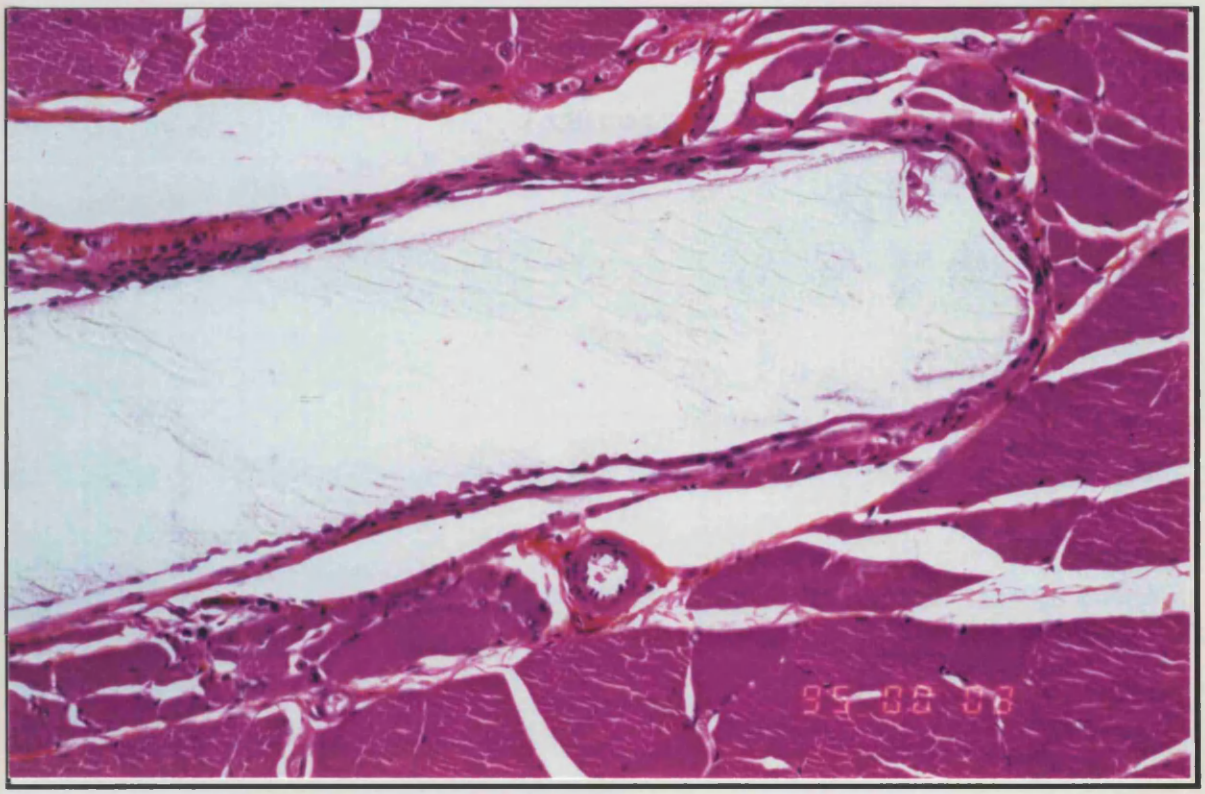

Figure 35. Photomicrograph showing transverse section of oxygen plasma-etched PDS structure in rat lumbar muscle, 49 days post-implantation. The tissue reaction is as seen at 35 days. The layer of tissue adjacent to the implant is often cellular, and the grooves of the implant are still in evidence but much rounded at the edges (Mag. x50).

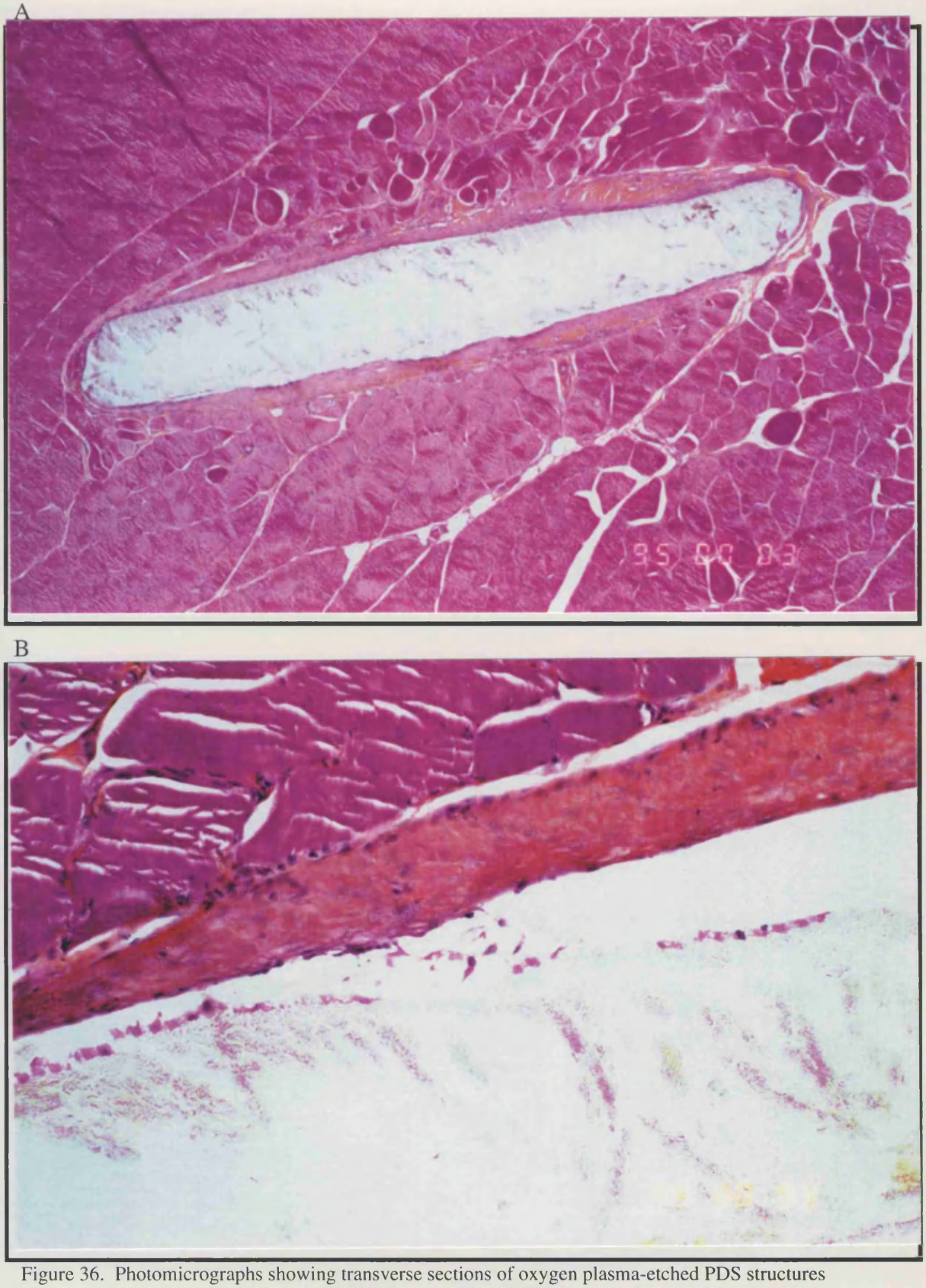

Figure 36. Photomicrographs showing transverse sections of oxygen plasma-etched PDS structures in rat lumbar muscle, 70 days post-implantation. A) The implant is immediately surrounded by a layer of cells (probably macrophages associated with increased absorption of the PDS), then a collagen capsule. There is much shattering of the PDS plate, probably due to increased PDS absorption (Mag. x10.8). B) Parts of the implant that have split from the surrounding tissue show evidence of tissue/PDS in a groove-like pattern (Mag. x.50).

A

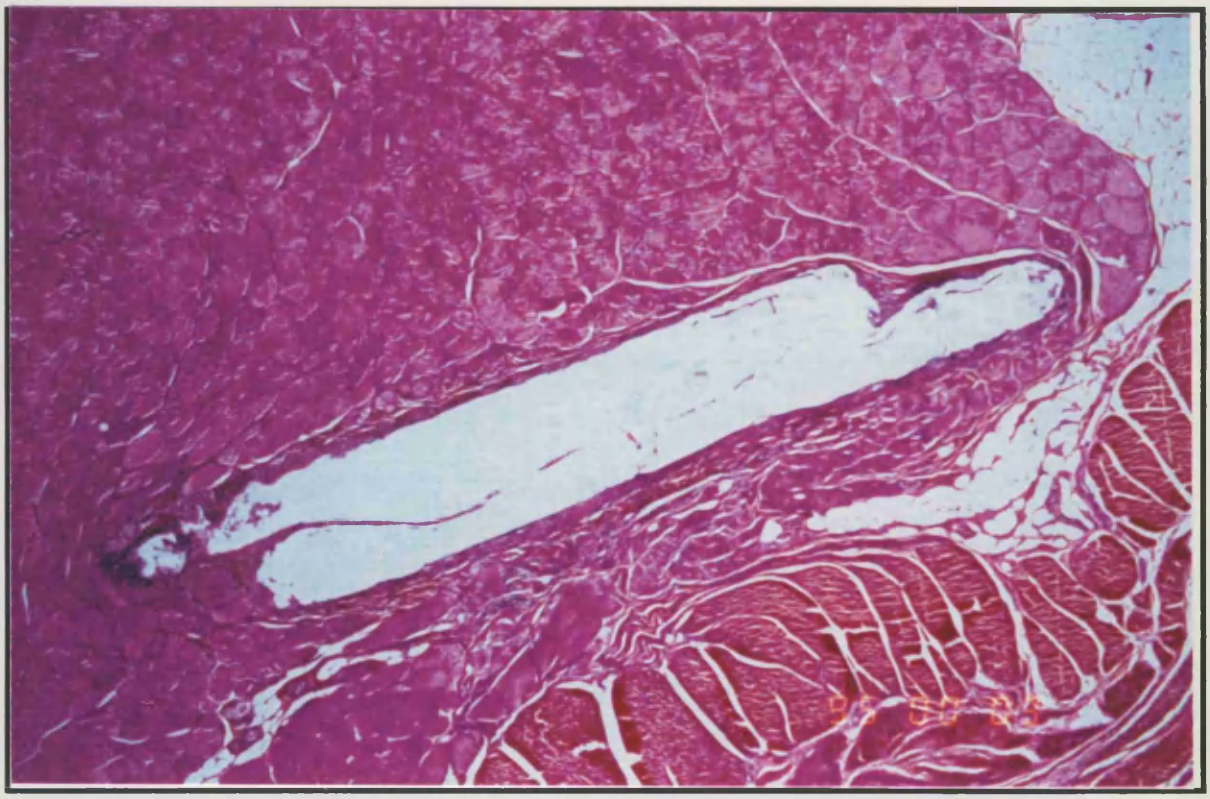

B

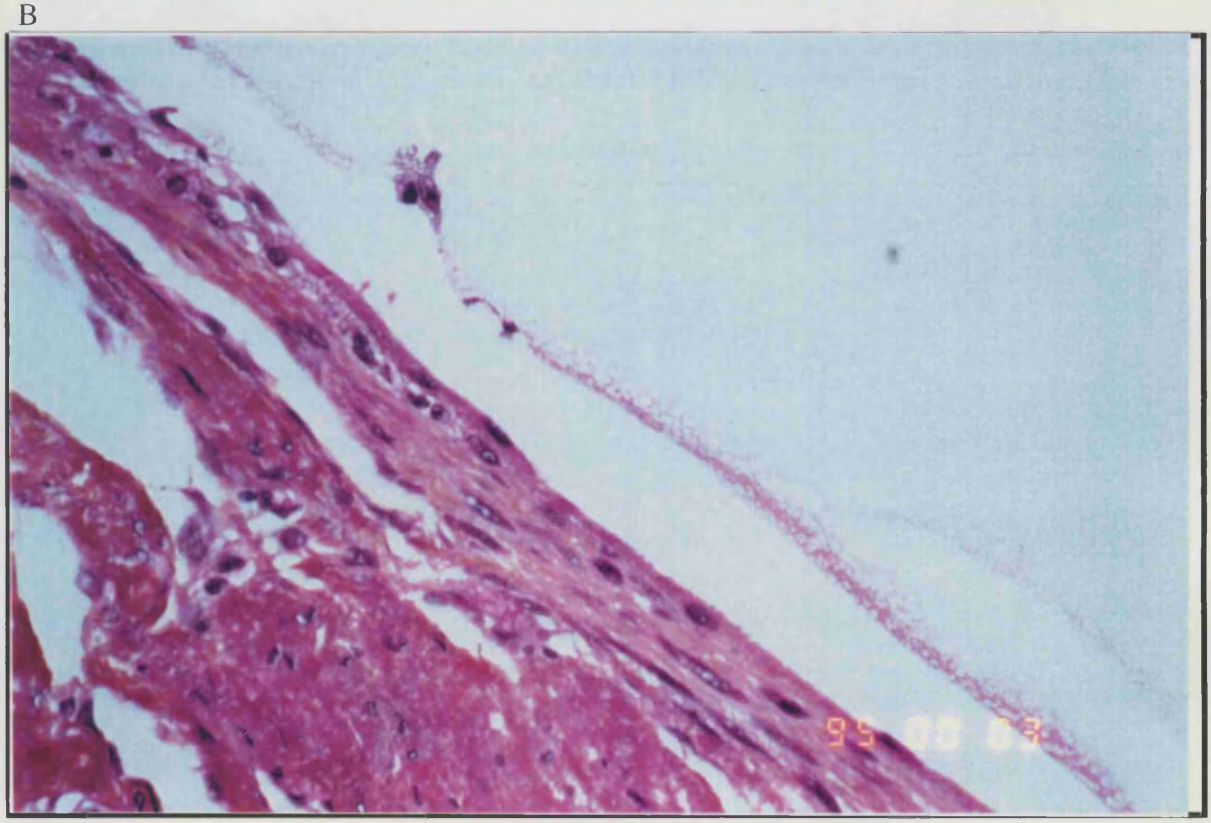

Figure 37. Photomicrographs showing transverse sections of oxygen plasma-etched PDS structures in rat lumbar muscle, 91 days post-implantation. A) The tissue reaction surrounding the implant is well organised (Mag. x8.4). B) The grooves of the implant are not abundant and the PDS material is showing clear signs of degradation (Mag. x100).

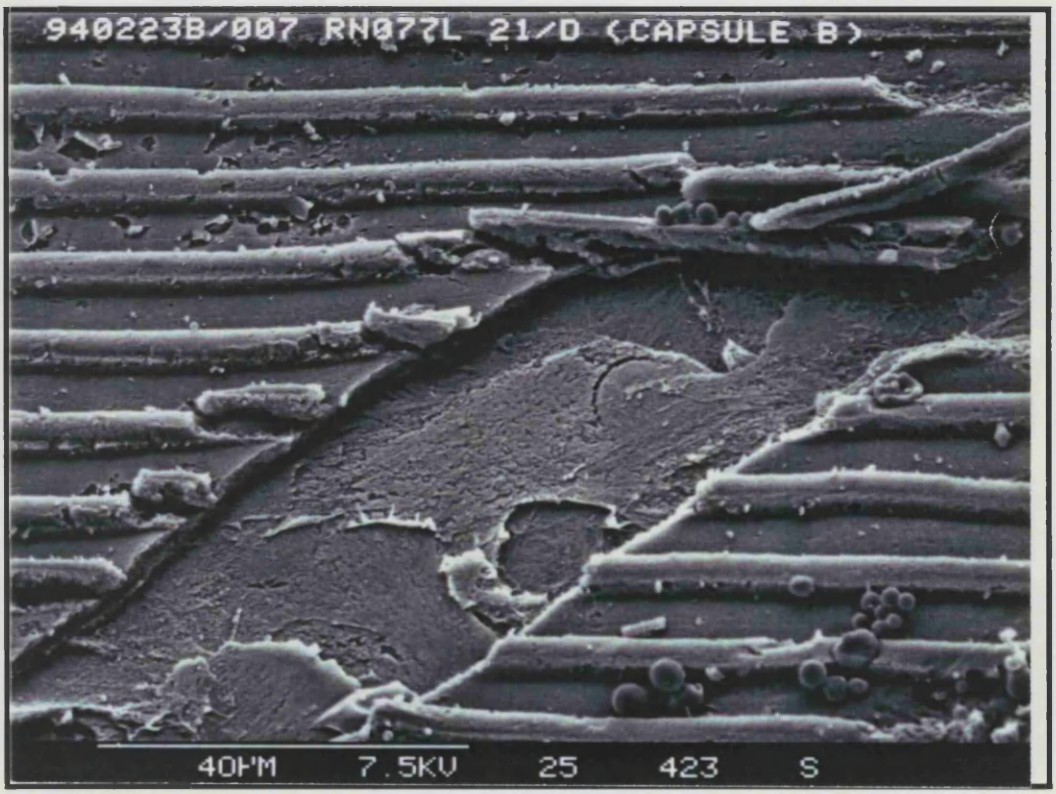

Figure 38. SEM micrograph showing impression of grooves in tissue of rat lumbar muscle, 21 days post-implantation. A layer of flattened cells can be seen beneath, where the uppermost tissue has been removed.

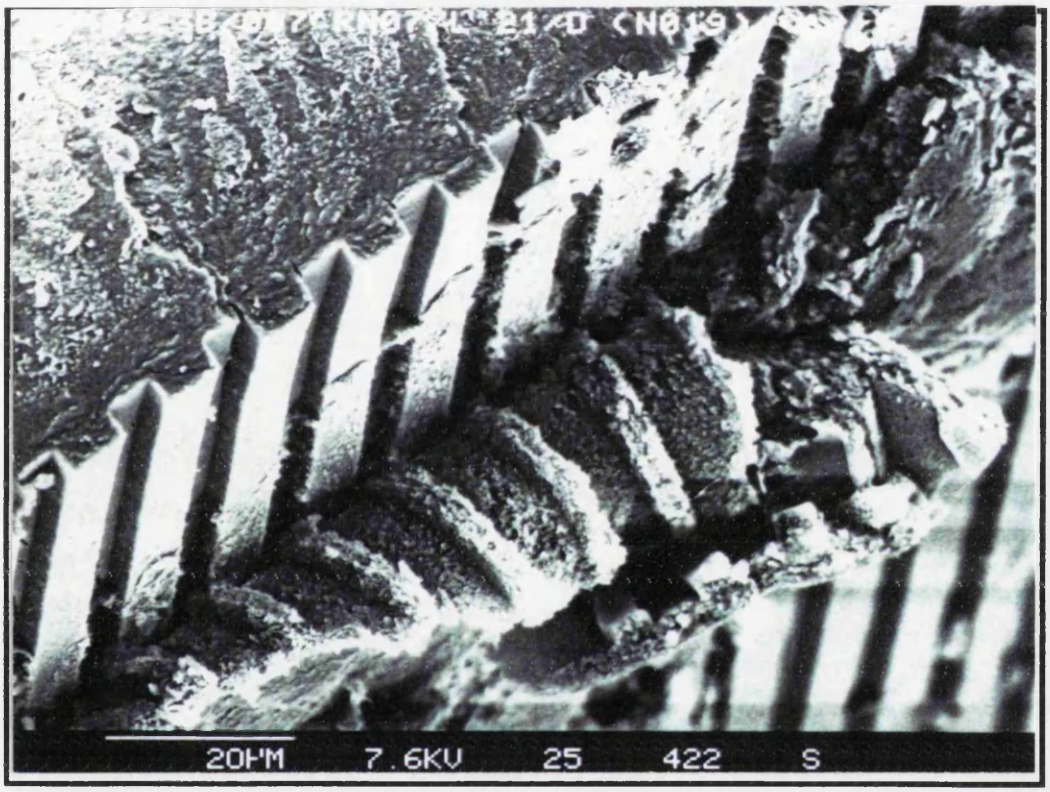

Figure 39. SEM micrograph showing a transverse section of rat lumbar muscle peeled back from a non-oxygen plasma-etched PDS structure, 21 days post-implantation. The tissue capsule has been moulded into a reverse impression of the grooves, but it is not clear whether cells were aligned by the grooves *in vivo*.

note that the non-plasma-etched grooves seemed to survive longer (up to 91 days) *in vivo*, with little change in structure, than the oxygen plasma-etched grooves.

It should also be noted that identification of cell types present at the implant site was carried out in consultation with experts from Ethicon Ltd. However, ideally, immunohistochemical staining would have been carried out in order to confirm the identities of the various cell types present.

SEM ANALYSIS

The SEM micrographs support the findings of the light micrographs in showing substantial adherent tissue on the explanted implants at all periods. As with the histological analysis, it was not possible to say whether the cells were oriented by the grooves *in vivo*, and the implants examined (non-oxygen plasma-etched) did not seem adversely degraded during the periods of implantation. SEM analysis was not carried out on oxygen-plasma etched PDS implants, but if this had been possible, these samples may have been expected to show more obvious signs of degradation (at the later timepoints) than the non-oxygen plasma-etched samples, in accordance with the results obtained from the histological study.

As mentioned previously, work by Wojciak-Stothard *et al* (1996) described preferential attachment and increased phagocytic activity of macrophages when the cells were grown, *in vitro*, on a grooved substrate. If activated macrophages (presumably producing reactive oxygen species) were attached to the grooved implant surface in large numbers, then it may be expected that the patterned PDS would be more rapidly degraded than previously studied PDS implants. It was therefore important to determine whether fabrication of microgrooves in the PDS material would have an adverse effect on the rate of degradation, or alter the biocompatibility, of the material (either through the fabrication process itself, or accumulation of macrophages at the implant site).

In conclusion, absorption of the microgrooved PDS structures *in vivo* does not seem adversely affected by the presence of grooves, with respect to historical data on the absorption of untreated PDS plates (Ethicon Ltd.). It would also appear that the PDS structures represent a relatively biocompatible substrate, and the results of this study certainly seem to indicate that the non-oxygen plasma-etched PDS grooves will remain intact *in vivo* long enough to be of use to encourage tissue repair.

CHAPTER 5

MOLECULAR STUDIES

INTRODUCTION

As a consequence of my discovery (Wojciak-Stothard *et al*, 1996) that tyrosine phosphorylation may play a role in the signalling mechanism involved in cell shape changes on topographical substrates, it was decided to carry out additional studies to try to find out more about the specific proteins and molecules involved in contact guidance.

Messenger RNA fingerprinting is a technique that allows identification of genes that are expressed in one RNA population but missing in another. The Delta RNA fingerprinting kit used in this study is based on improvements to the methods described by McClelland *et al*, 1993. Using this method, sequences of cDNA are amplified (during PCR fingerprinting reactions) based on chance homology to arbitrary primers. The sequences of the PCR primers used in this RNA fingerprinting study are shown in Figure 40, below.

P4: 5'-ATTAACCCTCACTAAATGCTGGTAG-3'

P5: 5'-ATTAACCCTCACTAAAGATCTGACTG-3'

P6: 5'-ATTAACCCTCACTAAATGCTGGGTG-3'

T3: 5'-CATTATGCTGAGTGATATCTTTTTTTTTAG-3'

T4: 5'-CATTATGCTGAGTGATATCTTTTTTTTTCA-3'

T6: 5'-CATTATGCTGAGTGATATCTTTTTTTTTCG-3'

T7: 5'-CATTATGCTGAGTGATATCTTTTTTTTTGA-3'

Figure 40. Sequences of the arbitrary PCR primers used for RNA fingerprinting.

The "P" primers are designed such that the nine bases at the 3'-end (the positions most significant for priming events) favour common sequence motifs found in the coding region of eukaryotic messenger RNA's. The "T" primers have the general structure: 5'-anchor-$(dT)_9N_{-1}N_{-1}$, where N_{-1} = A, G, or C, and the 5' anchor provides the extra length needed for the high-stringency PCR cycles.

Three initial PCR cycles are performed at low annealing temperature (i.e. low stringency) to allow the (P) primers to anneal and initiate DNA synthesis. Due to the low stringency of these cycles, each P primer will bind sites on many cDNAs with imperfect and/or incomplete matches. The products of these early cycles are then amplified (using the P primer and downstream T primer) during 22-25 high stringency PCR cycles. These PCR reactions produce characteristic "fingerprints" of the starting RNA, when examined by polyacrylamide electrophoresis and autoradiography.

The technique was used, in this instance, to compare RNA from cell populations grown on flat surfaces with that from cell populations grown on micro- and nano-grooved fused silica (quartz) structures, in order to try to discover whether topographical cues promote differential gene expression.

Differentially expressed bands were excised from the gels, then cloned into a TA-type cloning vector . This system exploits the activity of thermostable polymerases which preferentially add a single adenosine nucleotide to the 3' end of double stranded DNA. These PCR products can then be inserted into a suitable thymidine tailed vector. Once cloned, the inserts were excised from the vector (using appropriate restriction enzymes with restriction sites on either side of the insert), then sequenced using a chain-termination sequencing method.

RESULTS

MESSENGER RNA FINGERPRINTING

MG-63 Osteosarcoma Cells

This experiment was a comparison of the messenger RNA fingerprints of MG-63 osteosarcoma cells which had been cultured for 24 hours on flat quartz or grooved quartz structures (6μm deep; 12.5μm wide). The first four lanes in figure 41 show the fingerprints of the flat (control) and grooved mRNA samples in the presence of primers P4 and T7. Lanes five to eight show the fingerprints of the mRNA samples in the presence of primers P4 and T6.

For each cDNA sample (in this case one flat [control] sample and one grooved sample), "A" (1 in 10 dilution of original cDNA sample) and "B" (1 in 40 dilution of original cDNA sample) dilutions were made. Both dilutions were fingerprinted for each sample as in some cases a band will show up in one dilution, but will be absent from the other dilution; however, real differentially expressed bands will always appear in both dilutions. Thus, fingerprinting both dilutions provides a positive control for true differentially expressed bands.

Reading from left to right, lane 1 shows control (flat surface) sample "A" dilution; lane 2 shows grooved sample "A" dilution; lane 3 shows control sample "B" dilution; and lane 4 shows grooved sample "B" dilution (all amplified in the presence of primers P4 and T7). Lanes 5 to 8 show the samples in the same order, but this time amplified in the presence of primers P4 and T6.

P388D1 cells

P388D1 macrophage-like cells were cultured on flat (control) or grooved (70nm deep; 12.5μm wide) quartz substrates for twenty four hours. Then, control "A" and groove "A" dilution (where "A" dilution is 1:10 dilution of each original cDNA) samples of P388D1 macrophage messenger RNA (mRNA) were run on

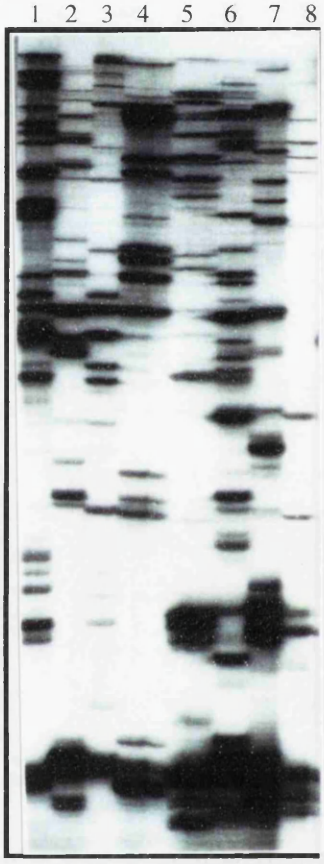

Figure 41. Autoradiograph showing messenger RNA fingerprints of MG-63 osteosarcoma cells which had been cultured for 24 hours on non-grooved or grooved (6µm deep; 12.5µm wide) quartz structures. Lane 1: non-grooved (control) "A" dilution; lane 2: grooved "A" dilution; lane 3: non-grooved "B" dilution; lane 4: grooved "B" dilution (all samples amplified in the presence of primers P4 and T7). Lanes 5-8 show the samples run in the same order, but this time amplified in the presence of primers P4 and T6.

a denaturing 5% polyacrylamide/8M urea gel, in 0.5x TBE buffer. The control and groove samples were each run in the presence of the following (random) primer pair combinations: P4 and T3; P4 and T4; P5 and T3; P5 and T4; P6 and T3; P6 and T4. Control and groove samples for each set of primer pairs were run adjacent to each other on the gel.

When the control and groove lanes are compared (Figure 42) a different band pattern, representing varying sized mRNA fragments, can be observed in each lane. The varying band pattern between control (cells grown on a flat surface) and groove samples corresponds to fragments of mRNA that are differentially expressed in the two samples. The mRNA sequences have been amplified based on chance homology to the arbitrary primers, producing characteristic fingerprints of the starting cDNA. Differentially expressed bands can be observed with each of the six sets of primer pairs tested.

Figure 43 shows a comparison between Retinal Pigmented Epithelial (RPE) cell mRNA, that in lanes 1 and 2 is untreated, and in lanes 3 and 4 the cells have been treated with hydrogen peroxide. All four samples had the same set of primer pairs (Figure and data courtesy of Dr Gordon Reid). These samples are shown as a further control, to support the data from the grooved/flat mRNA fingerprinting. The identical fingerprint of the adjacent lanes indicates that there is no differential gene expression between the two RPE cell RNA populations. Thus, confirming that the results observed with the flat/grooved P388D1 and MG-63 cell samples are true differences and not just a defect in the method, that would be observed with any samples used.

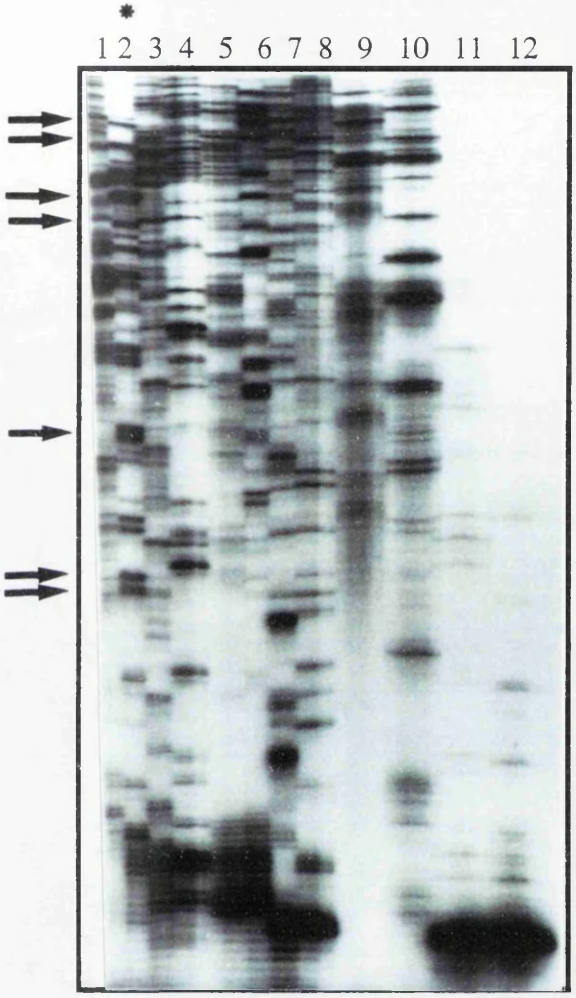

Figure 42. Autoradiograph showing messenger RNA fingerprints of P388D1 macrophage-like cells which had been cultured for 24 hours on non-grooved or grooved (70nm deep; 12.5µm wide) quartz structures. Odd numbered lanes are non-grooved (control) "A" dilutions; even numbered lanes are grooved "A" dilutions. Samples were amplified in the presence of the following primer pair combinations: lanes 1 and 2 - P4 and T3; lanes 3 and 4 - P4 and T4; lanes 5 and 6 - P5 and T3; lanes 7 and 8 - P5 and T4; lanes 9 and 10 - P6 and T3; lanes 11 and 12 - P6 and T4. Arrows indicate bands (1, 2, 3, 4, 5/6, 7 and 8, reading from top to bottom) that were excised from the gel (lane 2), then cloned and sequenced.

Figure 43. Autoradiograph showing messenger RNA fingerprints of Retinal Pigmented Epithelial (RPE) cells that in lanes 1 and 2 are untreated, and in lanes 3 and 4 have been treated with hydrogen peroxide. All four samples had the same set of primer pairs.

REAMPLIFICATION OF DIFFERENTIALLY EXPRESSED mRNA FINGERPRINTING BANDS

Seven bands were cut from the denaturing 5% polyacrylamide/8M urea gel in figure 42, as shown. The DNA obtained from the bands cut out of the fingerprinting gel was reamplified, then run on an agarose gel containing ethidium bromide (figure 44). The figure shows the reamplification products of bands 1, 2, 3, 4, 5/6, 7, and 8, from the 70nm deep groove fingerprinting experiment (figure 42), reading from left to right of the gel. Only the brightest bands (uppermost band, in lane 3) were excised and purified (through Spin-X columns) for cloning. The feint, smaller bands observed in lanes 1, 2, 3, and 5 were assumed to be primer-dimer bands. A 1Kb ladder is shown in lane 8 of the gel.

CLONING

Plasmids were minipreped from recombinant colonies (as described in materials and methods chapter), then the reamplified DNA inserts (corresponding to reamplified bands from the mRNA fingerprinting gels) were excised from the plasmid using restriction enzymes. The restriction digests were run on an agarose gel, containing ethidium bromide, to check that the insert had been excised from the plasmid. Figure 45 shows restriction digests of, from left to right, human Heme Oxygenase (control), band 2 and band 8. The smaller bands (those that have run further on the gel) in lanes 2, 3 and 4 correspond to the cloned DNA of Heme Oxygenase, band 2 and band 8, respectively. The larger bands (nearer the top of the gel) are the remains of the plasmid, minus the insert. As lane 1 represents a 1Kb ladder, it can be estimated that the sizes of the inserts are 500bp, 600bp and 150bp, for Heme Oxygenase, band 2 and band 8, respectively.

Figure 44 . Agarose gel showing reamplification products of differentially expressed mRNA fingerprinting bands. Reading from left to right, lanes 1-7 show the reamplification products of bands 1, 2, 3, 4, 5/6, 7, and 8 cut from the P388D1/70nm deep groove mRNA fingerprinting gel. A 1Kb ladder is shown in lane 8 of the gel.

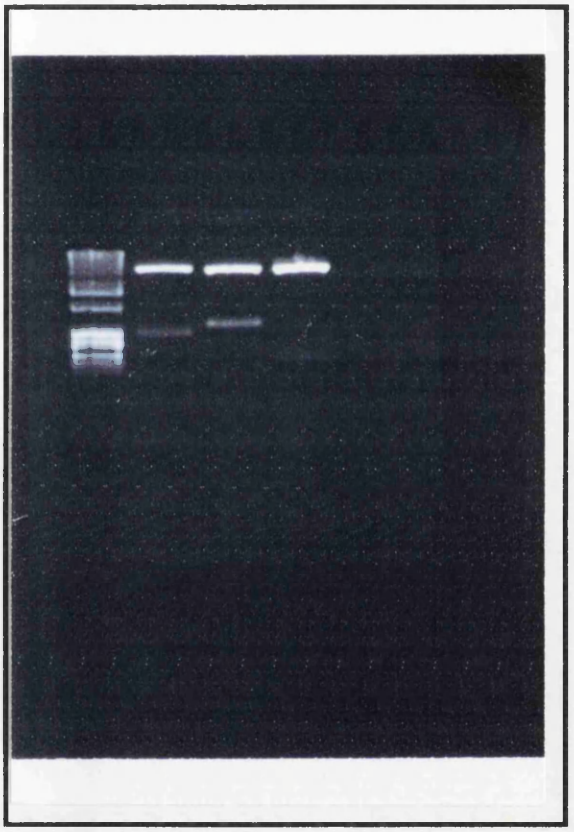

Figure 45 . Agarose gel showing restriction digests of Heme Oxygenase (control), band 2 , and band 8. The smaller bands (i.e. those that have run further on the gel) in lanes 2, 3, and 4 correspond to the cloned DNA of Heme Oxygenase, band 2, and band 8, respectively. The larger bands (nearer the top of the gel) are the remains of the plasmid, minus the insert. Lane 1 shows a 1Kb ladder.

SEQUENCING

All sequences were read manually, then entered into the basic local alignment search tool (BLAST) "BLASTN" program, using "BCM Search Launcher" on Netscape. This sequence comparison tool compares a nucleotide query sequence against a nucleotide sequence database (Altschul *et al*, 1990). A known sequence for human mRNA Heme Oxygenase was initially entered, to ensure that the programme was suitable and able to correctly match DNA sequences.

Where a band has more than one possible sequence this is due to the fact that the sequencing annealing reaction was carried out with different primers (i.e. either of the two fingerprinting primers, or the T7 primer present in the plasmid) at different times in order to try to get as much sequence information as possible. Any overlapping sequences were then matched, and those that didn't match were entered into the database as separate sequences.

Band 1

GTA TAA CAA TTC ACA CAG AAA CAG CTA TGA CCA TGA TTA CGC CAA CTC TAA TAC GAC TCA CTA TAG GGA AAG CTT GCA TGC CTG CAG GTC GAC TCT AGA GGA TCT ACT AGT CAT ATG GAT CGG ATC CCC GGG TAC CGA GCT CGA ATT CAC TGG CCG TCG TTT TAC AAC GTC GTG ACT GGG AAA ACC CTG GCG TTA CCC AAC TTA ATC GCC TTG CAG CAC ATC CCC CTT GAT AGA CCA GCT GGC TAA TAG CGA AGA GGC CGA CGC AGT C

This is part of the cloning vector (i.e. pMOSBlue) sequence - there is no insert.

Band 2

Has 4 possible sequences:

1)

CTC TAG TAT ATG GAT TAT TAC CCT CAC TAA ATT GCT GGT AGT GGG TGG TTC TCA GGG CGC ACG CAT TCT TAA CCA GAC AAT GCC GCA GTT GCT GCG AAA CTG GGT GAT TCA GTC ACT ATC TGG CAT CAG AGC GGC AAA GGT TCG CAA CAA TCC GTT GAA CAG GCG TCT GCG AAG C

The closest match found for this sequence is with *E.coli* cell-envelope murG gene. Regions of homology are shown below, with the unknown sequence presented in bold type.

```
47  GTTGCTGCGAAACTGGGTGATTCAGTCACTATCTGGCATCAG 88
    ||||||||||||||||||||||||||||||||||||||||||
691 GTTGCTGCGAAACTGGGTGATTCAGTCACTATCTGGCATCAG 732

89  AGCGGCAAAGGTTCGCAACAATCCGTTGAACAGGCGTCTGC 129
    |||||||||||||||||||||||||||||||||||| |||
733 AGCGGCAAAGGTTCGCAACAATCCGTTGAACAGGCGTATGC 773


1   TGGGTGGTTCTCAGGGCGCACGCATTCTTAACCAGACAATGC 42
    ||||||||||||||||||||||||||||||||||||||||||
644 TGGGTGGTTCTCAGGGCGCACGCATTCTTAACCAGACAATGC 685

43  CGCAGTT 49
    ||||| |
686 CGCAGGT 692
```

2)

CTC ACT AAA TCT CTG GTA GCG TTA TCG CAG GCT TCG CTG ATC CAC ATT AAA GGC GAG TAT GAC GAA GAG GCC TTT AAC GAA GCC TTT GTG ATG CAT ACC ACC ACC TCG CCA GTT ATC CAT TGT TGC TTC

The closest match found for this sequence is with *E.coli* dnaE gene for DnaE. Regions of homology are shown below, with the unknown sequence presented in bold type.

```
1     CTCACTAAATCTCTGGTAGCGTTATCGCAGGCTTCGCTGATC 42
                          |||||||||||||||||||||||
2257                      CGTTATCGCAGGCTTCGCTGATC 2279

43    CACATTAAAGGCGAGTATGACGAAGAGGCCTTTAACGAAGCC 84
      ||||||||||||||||||||||||||||||||||||||||||
2280  CACATTAAAGGCGAGTATGACGAAGAGGCCTTTAACGAAGCC 2321

85    TTTGTGATGCATACCACCACCTCGCCAGTTATCCATTGTTGCTTC 129
      |||  ||||||||||||||||||||||
2322  TTTATGATGCATACCACCACCTCGCC 2347
```

3)

TGC ACG CGA AGT ATG GCT TGT CGT AAC ACG ATG GCG CTG TAT TAT TCA GAG TCG CAC ATA CTC ATC GCG ACA CTC AGC ACG CCA GGT CTA ATA CGC GCT ATC TGC TAT ACG CAT ATC CGG TTG AGA CCA GGC GGT CTG GCC GGA TAC GTG C

The closest match found for this sequence is with Herpes simplex virus type I (HSVI) short unique sequence. Regions of homology are shown below, with the unknown sequence presented in bold type.

```
88    GACCTGGCGTGCTGAGTGTCGCGATGAGTATGTGCG 53
      |||  ||||||  |||  ||||||||||  |  ||  |||
5104  GACTTGGCGTTCTGTGTGTCGCGATGTCTCTGCGCG 5139
```

4)

CTA CTT AAA GGA CGG AAC GAT AAT TCG GCA CGG CAA GGT ATG GCT TGT CGT AAC ACG ATG GCG CTG TAT TAT TCA AGT CGC ACA TAC TCA TCG CGA CAC TCA GCG ACG CAG GTC TAA TAG AGA TAT CTG CTA TAG CCA TAT CGC GTT GAG ACG CGT CTG CGA T

This sequence had "no known matches" on the database and is therefore a unique sequence.

Band 3

Sequence is the same as that for Band 1 (i.e. cloning vector sequence).

Band 4

(Only have very short sequence due to the direction that the primers were bound).

GAC AAT TTT GTT GAG ATG GTC GTA AAT CAC TC

The closest match found for this sequence is with Sus scrofa apolipoprotein B (allele Lpb-5). Regions of homology are shown below, with the unknown sequence presented in bold type.

```
31    TGTTAAAACAACTCTACCAGCATTTAGTG 3
      |||||||||||||||||    || ||||||
1140  TGTTAAAACAACTCTATTTTCAGTTAGTG 1168
```

Band 5/6

Has 3 possible sequences:

1)

CGA ATA AAG TCT GCA GGA TGG TCG TAA ATC ACT CGC GCA TTC TGG TGT CGT ATC ACT CC

This sequence had "no known matches" on the database and is therefore a unique sequence.

2)

GCT TAT TTC AGG TCC TAC CAG CAT TTA GTG AGG GTT AAC CCT ACC AGC ATT TAG TGA GGG TTA ATA ATC GGA TCC CGG TAC CGA

GCT CGA ATT CAC TGG CCG TCG TTA CAC GTC GTG ACT GGA ACC TGC TAC CAC T

The closest match found for this sequence is with an oligonucleotide from the polycloning region of pUC19. Regions of homology are shown below, with the unknown sequence presented in bold type.

```
74 CCCGGTACCGAGCTCGAATTCACTGGCCGTCGTTACACGTCGT 116
   || |||||||||||||||||||||||||||||||  ||  |||
13 CCGGGTACCGAGCTCGAATTCACTGGCCGTCGTTTTACAACGT 55
```

3)

GGG GAT CAC TCC GTC TCC TTT GTG CTT GGT ATG GAT CTC CTC TCT ATA GAG AGG TCT GCG ACC CTG TGC ACA GGG CTA CAT GTC GAC AAG GCT CTT CTC CTC ATA TAT AGG TGT AGA GGT CTG CG

This sequence had "no known matches" on the database and is therefore a unique sequence.

Band 7

ATT ATT AAC CCT CAC TAA ATG CTG GTA GAT TAA CC

The closest match found for this sequence is with sequence 7 from patent US 5427932. Regions of homology are shown below, with the unknown sequence presented in bold type.

```
4 ATTAACCCTCACTAAATG 21
  |||||||||||||||| |
7 ATTAACCCTCACTAAAGG 24
```

Band 8

Has 2 possible sequences:

1)

TAT TAA CCC TCA CTA AAT GCT GGT AGA TTA ACC CTA AAA AAA AAG ATA TAC TCA GCA TAA TG

The closest match found for this sequence is with sequence 7 from patent US 5427932. Regions of homology are shown below, with the unknown sequence presented in bold type.

```
2 ATTAACCCTCACTAAATG 19
  |||||||||||||||| |
7 ATTAACCCTCACTAAAGG 24
```

2)

AGG GTT AAT AAT CCA TAT GAC TAG TAG ATC CTC TAG AGT CGA CCT GCA GGC ATG CAA GCT TTC CCT ATA GTG AGT CGT ATT AGA GCT TGG CGT AAT CAT GGT CAT AGC TGT TTC CTG TGT GAA ATT GTT ATC CGC TCA CAA TTC CAC ACA ACA TAC GAG CCG GAA GCA TAA AGT GTA AAG CCT

The closest match found for this sequence is with pT7T3A19 cloning vector. Regions of homology are shown below, with the unknown sequence presented in bold type.

```
27  GATCCTCTAGAGTCGACCTGCAGGCATGCAAGCTTTCCCTATAGTGA 73
    ||||||||||||||||||||||||||||||||||||||||||||||
206 GATCCTCTAGAGTCGACCTGCAGGCATGCAAGCTTTCCCTATAGTGA 252

74  GTCGTATTAGAGCTTGGCGTAATCATGGTCATAGCTGTTTCCTGTGT 120
    ||||||||||||||||||||||||||||||||||||||||||||||
253 GTCGTATTAGAGCTTGGCGTAATCATGGTCATAGCTGTTTCCTGTGT 299
```

```
121 GAAATTGTTATCCGCTCACAATTCCACACAACATACGAGCCGGAAGC 167
    |||||||||||||||||||||||||||||||||||||||||||||||
300 GAAATTGTTATCCGCTCACAATTCCACACAACATACGAGCCGGAAGC 346

168 ATAAAGTGTAAAGCCT 183
    ||||||||||||||||
347 ATAAAGTGTAAAGCCT 362
```

DISCUSSION

With the messenger RNA fingerprinting kit used here there are 90 possible combinations of upstream and downstream primers (i.e. 10 arbitrary "P" primers and 9 oligo (dT) or "T" primers). Each P primer can also be used alone or in pairwise combination with other P primers, and the same applies to T primers. Therefore, there are many fingerprinting possibilities/possible primer combinations and in this study only a very few were tried. It should also be noted that in this study all mRNA samples were extracted from cells that had been allowed to attach to substrata for twenty four hours. It would be interesting to try earlier timepoints to try to identify early signals involved in contact guidance. Similarly, a study of later timepoints would also be of interest.

From the fingerprinting gels, only bands that were present in grooved samples and not in flat samples were selected and excised for sequencing. This was due to the fact that I was investigating the possibility of grooved structures inducing a change in the expression of certain genes. However, it should be noted that bands present in samples from cells grown on flat substrates, but not in samples from cells grown on grooved substrates, could also have been excised then cloned and sequenced, as they also demonstrate differential gene expression.

Due to the massive workload involved in cloning and sequencing only a very few bands, it was not possible to investigate fully the differential expression of all the various bands observed on the fingerprinting gels. Although unfortunate, it is

therefore not surprising, that through choosing only seven random bands from one fingerprinting gel, no major discoveries were made concerning differential gene expression induced by topographical stimuli. It is very probable that the sequences which have close homology with cloning vectors are, in fact, parts of the cloning vector used in the study and that the (band) insert was not properly excised from the vector, or not even present initially. The fact more than one sequence was found for certain bands may possibly be due to more than one band being excised from the fingerprinting gel and inserted into the vector. Alternatively, the sequences may represent small fragments of the same gene, as some of the sequences are relatively short.

It is possible, though, that some of the sequences that found "no known matches" on the database may be small novel peptides produced by the cells in response to the grooved substrate. This molecular study on the response of cells to topographical stimuli has since been continued in the laboratory and much progress has been made (see "Discussion", chapter 7).

Many of the bands chosen for sequencing could also have represented fragments of the same gene, therefore it would have been interesting to have been able to carry out Northern blots on the fingerprinting gels. A probe could have been made from the gene sequence of, for example, actin or fibronectin (or other proteins whose expression may be expected to be affected by the growth of cells on grooved structures), then this probe used to identify any matching sequences present on the fingerprinting gels.

A further possibility would have been to carry out subtractive hybridisation of the genes from cells grown on grooved and non-grooved substrates. This would have involved extracting the mRNA from both the grooved and non-grooved cell extracts, then synthesizing (^{32}P-labelled) single strand cDNA from the grooved

sample by reverse transcriptase. Sequences that were not specific to the grooved sample would be discarded by hybridisation with non-grooved sample mRNA's. Therefore, any remaining unhybridised single strand cDNA would represent a gene specific to cells that had been grown on the grooved substrate, and these cDNA's could then be cloned, sequenced and identified. Similarly, genes specific to cells grown on the non-grooved surface could be identified by synthesizing (^{32}P-labelled) single strand cDNA from the non-grooved cell extracts.

CHAPTER 6

DISCUSSION

TYROSINE PHOSPHORYLATION

In this project a role for tyrosine phosphorylation in the mechanism of cell contact guidance was discovered. Phosphorylation of tyrosine residues was found, in many cell types, co-localised along groove/ridge boundaries when cells were cultured on micro- and nano-grooved substrates. Previously, *in vitro* studies have shown changes in the distribution of cytoskeletal components when cells exhibit contact guidance on such structures (in fibroblasts, Oakley and Brunette, 1993; in normal and transformed fibroblasts and epithelial cells, Rovensky and Samoilov, 1994; in porcine epithelial cells, Oakley and Brunette, 1995; in astrocytes, Webb *et al*, 1995) and also that focal contacts are positioned on discontinuities in the substratum (Meyle *et al*, 1994). But, a role for tyrosine phosphorylation in direct response to such topographical cues had not previously been demonstrated.

It is well known that the small GTP-binding proteins, rho and rac, are involved in signal transduction pathways that link growth factor receptors to the activation of actin polymerisation. Although the exact mechanism involved in initiating actin polymerisation in response to extracellular factors is not known, a role for tyrosine phosphorylation somewhere in this signalling cascade would be consistent with the observation that several components of the focal adhesion multiprotein complex are phosphorylated on tyrosine residues (Turner and Burridge, 1991; Bockholt and Burridge, 1993; Ridley and Hall, 1994; Schaller and Parsons, 1993).

In 1994 Ridley and Hall identified a genistein-sensitive tyrosine kinase involved in the actin-polymerisation signalling pathway, downstream of rho. They found that, as well as inhibiting stress fibre formation induced by extracellular factors and micro-injected rho protein, the tyrosine kinase inhibitor genistein inhibited the clustering of phosphotyrosine-containing proteins at focal adhesions and also the increased tyrosine phosphorylation of several proteins, including $pp125^{FAK}$. They also suggested the possibility of further tyrosine kinases playing a role in the signal transduction pathway, one of which could act upstream of rho.

A definite role for tyrosine phosphorylation upstream in the rho signalling pathway was reported by Nobes *et al* in 1995. They reported that induction of actin stress fibres in Swiss 3T3 cells, by LPA, is blocked by prior incubation of the cells (for 30-60 minutes) with the tyrosine kinase inhibitor, Tyrphostin A25. This provides evidence of a role for a tyrosine kinase upstream of rho in the LPA/rho/stress fibre signalling pathway. The study by Nobes *et al* also suggested that a tyrosine kinase/phosphotyrosine phosphatase cycle is being maintained in cells, as phosphatase inhibition (by orthovanadate) leads to kinase activation even in quiescent cells. This theory would also explain their observation that inhibition of rho in quiescent cells, by C3 transferase (that ADP-ribosylates and inactivates rho), causes cells to round up and detach from the substrate. They propose that activation of the rho GTPase switch is not an all or nothing event, but that fluctuations in the rho equilibrium in the cell can have specific cellular effects.

From these studies it can be seen that much work has been done in attempting to elucidate the signalling mechanism involved in the formation of cellular stress fibres and focal adhesions, cellular structures which play a major part in cell contact guidance. But, most of this work has involved the addition of exogenous growth factors in order to stimulate the intracellular signalling machinery. The

fact that many cell types have been shown to grow/move in response to various topographical cues *in vitro* (and *in vivo*) suggests that topography alone is enough to stimulate the cell cytoskeleton in a very specific manner. Therefore, in this study micro- and nano-grooved structures were used to investigate the signals a cell receives from a topographical cue that cause it to align to such structures. It would be expected that any specific intracellular signals induced via external stimulation by topographical cues would be directly related to the intracellular signalling observed in response to stimulation by exogenous growth factors.

The range of protein tyrosine kinase inhibitors known as Tyrphostins have been shown to interfere with adhesion-associated tyrosine phosphorylation of $pp125^{FAK}$ in endothelial cells, in addition to reducing focal adhesion and stress fibre formation (Romer *et al*, 1994). In this project, phosphorylation of tyrosine residues, localised along groove ridge boundaries, has been demonstrated within cells when the cells were cultured on micro- and nano-grooved substrata. This phosphorylation pattern was consistently observed, particularly in cellular processes that extended along the substrate, parallel to the grooves. Tyrphostins were utilised as phosphorylation inhibitors to find out what effect, if any, they would have on the alignment of cells on these grooved substrata. It was found that the Tyrphostins tested not only prevented cell alignment on grooved structures, but also prevented cell attachment to the substrate (data not shown). When the effects of the various Tyrphostins on cell adhesion to planar substrates were studied it was found that five of the Tyrphostins tested had a marked inhibitory effect on attachment of cells to the substrate. These were, in decreasing order of inhibition of cell attachment: Tyrphostin B56, Tyrphostin B50, Tyrphostin B46, Tyrphostin 25 and Tyrphostin B44(-).

This effect on cell attachment is not surprising when it is considered that Tyrphostin B56 is an inhibitor of epidermal growth factor (EGF) receptor autophosphorylation (Calbiochem product information leaflet). It was shown by Lyall *et al* (1989) that Tyrphostins of this type prevented stimulation of DNA synthesis and cellular proliferation in living cells, processes normally catalyzed by activation of the cell surface receptor by EGF. Tyrphostins have also been shown to interfere with phosphorylation of other molecules that play a crucial role in cell attachment and spreading. Nobes *et al* (1995) have reported that the Tyrphostin A25 inhibits a tyrosine kinase responsible for stress fibre formation in Swiss 3T3 cells. Whilst, as mentioned previously, a study by Romer *et al* (1994) reported that Tyrphostins could interfere with adhesion-associated tyrosine phosphorylation of focal adhesion kinase ($pp125^{FAK}$) and also reduce focal adhesion and stress fibre formation in endothelial cells.

POSSIBLE ROLE FOR FYN AND LYN

During the course of this project it was not possible to identify the protein(s) shown to be phosphorylated in the immunofluorescence experiments. This work has recently been continued in the laboratory to try to elucidate which of the family of protein tyrosine kinases was involved in the observed phosphorylation. The non-specific tyrosine kinase inhibitor, staurosporine, inhibited the reaction of cells to topography, suggesting that the effect of kinases was on route to the reaction rather than a cause of the reaction. Genistein did not affect either cell reaction to topography or cellular phosphorylation, suggesting that rho-related reactions are not involved. Herbimycin was found to inhibit reaction of cells to topography and also cellular tyrosine phosphorylation, thus suggesting that the Src family of kinases are those involved in the topographically-induced phosphorylation (Adam Curtis, personal communication). Immunofluorescent

studies have been carried out using antibodies against a range of tyrosine kinases and it was found that only those against fyn and lyn (members of the src family of non-receptor protein tyrosine kinases) showed the same localisation of tyrosine phosphorylation as that described previously in this project.

The lyn protein tyrosine kinase ($p53/56^{lyn}$ - two proteins produced by alternative splicing of lyn mRNA's) associates with the immunoglobulin complex on B cell surfaces (Yamanashi *et al*, 1991; Lin *et al*, 1992) and is believed to participate in activating phosphatidylinositol-3-kinase (Yamanashi *et al*, 1992). The fyn protein tyrosine kinase ($p59^{fyn}$) also has two isoforms. Fyn T associates with components of the T cell antigen receptor complex and has been shown to be involved in T cell receptor signalling (Perlmutter *et al*, 1993). The second isoform of the protein, fyn B, is one of a group of kinases implicated in the processes of long term potentiation and spatial learning (Grant *et al*, 1992). As in other src family members, both fyn and lyn consist of four domains: an N-terminal domain where myristylation occurs, allowing for association with cell membranes; SH3 and SH2 domains which bind to proline-rich and phosphotyrosine-containing sequences, respectively, and facilitate interactions with other proteins; a catalytic kinase domain containing a tyrosine autophosphorylation site; and a negative regulatory tyrosine residue at the C-terminus (Superti-Furga and Courtneidge, 1995).

If *fyn* and *lyn* do indeed play a role in the signalling mechanism responsible for the phosphorylation pattern observed when cells respond to topography, it was reasoned that antisense mRNA against the expression of these genes should affect cellular topographic reactions. The antisense messages were shown to have effects on both cell morphology and cell migration. Antisense *fyn* and *lyn* reduced the rate of migration of epitenon cells on grooves of 88 nanometre depth,

and decreased the length of the same cells on grooved structures, following 24 and 48 hours culture (Tong-Tong Li, personal communication).

TOPOGRAPHY

Any protocol utilizing photolithography to produce microtextured substrata must address the issue of surface homogeneity. Photolithography of substrates followed by plasma etching may result in chemical heterogeneity between the etched and unetched regions of the substrate, as plasma etching has been shown to alter surface properties. Clark *et al* (1987) found an adhesive difference between etched and unetched perspex substrates, but overcame the problem by re-exposing the entire surface to oxygen plasma (blanket etching) at the end of the fabrication process.

It is likely that selective adsorption of proteins to specific areas of the substrate will alter the surface chemistry/energy and thereby become partly responsible for any observed effects of the substrate on cell behaviour. This problem is very difficult to overcome, but Brunette *et al* (Brunette, Exp. Cell Res., volumes 164 and 167, 1986; Brunette *et al*, 1983) appear to have avoided the problems of surface homogeneity by preparing grooved silicon surfaces using photolithography and plasma etching, then using these structures as templates to prepare epoxy replicas. The replicas were then coated with a thin layer of titanium, resulting in completely homogeneous grooved titanium surfaces.

In the case of the PDS used in this study it was not suitable to use oxygen plasma etching to produce a uniform surface, as the material is oxygen sensitive. But, as the PDS replica structures were produced from grooved silica templates the

structures could be presumed to have completely homogeneous PDS surfaces in the same way as the titanium structures used by Brunette.

It has also been suggested that the differential attachment of cells on grooved compared with non-grooved substrata could be caused by the cells showing a preference for grooved surfaces due to the increased surface area available for attachment. As the groove depth of the structures used in our study (Wojciak-Stothard *et al*, 1996) was of the nanometric scale, the difference in surface area between the grooved and non-grooved surfaces would be so negligble as to make it highly unlikely that the observed cell reactions were due to an increase in surface area on the grooved substrate. Furthermore, a study by Brunette (1988) investigating cell attachment on titanium grooved substrata (of micrometre dimensions), found that the increase in epithelial cell attachment observed on grooved substrata, compared with a smooth surface, was not due to the increased surface area of the grooved substrate. Therefore, the results of the *in vitro* cell attachment to microgrooved PDS structures reported in this project could be reasonably assumed to represent "real" differences in cell attachment.

Generally, the cell types tested tended to show preferential attachment to the grooved compared with the non-grooved PDS substrate. Therefore, it would seem reasonable to suggest that, *in vivo*, the grooved surface of PDS structures may encourage attachment and spreading of cells and therefore may be able to play a role in guiding cell regrowth and encouraging wound healing. The results from the *in vivo* study also support the use of microfabricated PDS as a future prosthetic device, as the implanted structures were found to be biocompatible and to have a suitable rate of degradation.

One of the main discoveries in this project is the fact that cells were found to respond to topographies of nanometric scale. These topographies correspond to

topographical cues that would realistically be encountered by cells *in vivo*, for example, in the region of the size of a single collagen fibre. It was shown that P388D1 (macrophage-like) cells can react to, and become activated by contact with, these ultrafine topographic features. Previously published data showed that contact of the cells with the patterned surface activated cell spreading, cell adhesion, and increased the number of protrusions of the cell membrane. Also, formation of focal contacts along discontinuities in the substratum was accompanied by the phosphorylation of tyrosine residues co-localized with F-actin (in increased quantity) and vinculin. Rat peritoneal macrophages have been shown to react in a similar way (Wojciak-Stothard *et al*, 1996). Other cell types tested in this project only demonstrated a similar pattern of tyrosine phosphorylation in response to larger topographical features, of the micrometric scale. This could probably be explained in terms of the role macrophages play *in vivo*: as their fuction is detection and removal of any foreign particles in the body, they would be expected to be extra sensitive (compared with other cell types) to any external topographical stimuli.

It would also appear that the surface chemistry of biomaterials can have an effect on cellular signalling via integrins. Groth and Altankov (1995) discovered that spreading and proliferation of fibroblasts on hydrophilic and hydrophobic surfaces is related to tyrosine phosphorylation in focal contacts. In order to learn more about the underlying mechanism of the biocompatibility of materials, they investigated the organisation of the β1 integrin (one subunit of the fibronectin receptor complex) and the phosphorylation of tyrosine residues in focal contacts. In the study, fibroblasts were allowed to adhere on hydrophilic glass and hydrophobic octadecyl glass (ODS) surfaces, in the presence and absence of preadsorbed fibronectin. It was found that adhesion and spreading of fibroblasts on ODS glass was diminished in comparison to clean glass, indicated by a diffuse actin stain and the absence of focal contacts and phosphotyrosine activity.

The preadsorbtion of fibronectin improved the interaction of fibroblasts with both surfaces, demonstrated by the formation of stress fibres and clustering of β1 integrins in the focal contacts, co-localised with an increased phosphotyrosine activity. Fibroblast proliferation (measured after 72 hours) was also found to be inhibited on ODS in comparison to glass but, again, preadsorption of fibronectin resulted in enhanced proliferation on both surfaces. Groth and Altankov suggest that adsorption of fibronectin to the materials may provide an environment more similar to natural extracellular matrix and therefore supply better conditions for cell signalling. They conclude that signalling via integrins, and any alterations in the signalling pathway that occur (in this case due to altered surface chemistry), may play an important role during cell-biomaterial interactions.

MECHANISMS OF TOPOGRAPHIC GUIDANCE

Hypotheses proposed for the mechanism of cellular topographic guidance have mainly related to cytoskeletal organisation. Originally Weiss (1945) formulated the hypothesis that cells responded to the molecular orientation of their environment. He cultured Schwann cells and nerve fibres in liquid or clotted media, with or without fibres of various sizes and materials. From his study, he explained the orientation of cells along glass fibres by saying that explanted tissues give off a colloidal exudate which spreads in an oriented fashion along the surface of the cell culture material, thereby causing the cells migrating from the explant to be oriented themselves. Strong evidence against this theory came from findings by both Curtis and Varde (1964) and Dunn and Heath (1976) who suggested that cells actually react to the shape of the underlying substratum, as changes in cell behaviour occur on substrates whose morphology is unlikely to alter the capillary spread of a microexudate.

Dunn and Heath (1976) attempted to discover the mechanism by which cells detect shape. They studied the reaction of chick heart fibroblasts on cylindrical substrata of varying radii of curvature, and prism edges of differing angle to the plane. As a result of these studies, they proposed a hypothesis for contact guidance which stated that intracellular bundles of microfilaments, involved in cell adhesion and locomotion, cannot assemble or operate in a bent condition and are therefore mechanically restricted by any discontinuity in the substratum, resulting in a cell being forced to move in a specific direction. A hypothesis for the mechanism of contact guidance in response to multiple topographical cues came from Ohara and Buck in 1979. They reported bridging of cells across multiple parallel (polystyrene) grooves, and suggested that cell-substratum contact occured only on groove ridge surfaces. They proposed that this would result in orientation of focal contacts which would, in turn, orient the cytoskeleton and ultimately the cell itself.

The discovery that cells are, in fact, influenced by very small topographical features was made initially by Clark *et al* (1991). Although they did not use structures as small as those used in this study, they did observe effects of ultrafine topography, of dimensions 100nm to 400nm deep and 130nm wide, on BHK cells, MDCK cells, and the outgrowth of neurites. They found that degree of BHK cell alignment and MDCK cell elongation were dependent on the depth of the structures, whereas the outgrowth of neurites from chick embryo neurones was mainly unaffected by the substrate topography. These findings are consistent with earlier findings (Clark *et al*, 1990, using structures with larger grooves (periods ranging from 4μm to 24μm [i.e. grooves from 2μm to 12μm wide separated by ridges from 2μm to 12μm wide] and 0.2μm to 1.9μm deep)), that decreasing grating period and increasing depth increased cell alignment, the latter effect being dominant.

Dunn and Heath's (1976) theory for the mechanism of topographic guidance (that cells exhibit contact guidance because they tend to avoid discontinuities in the substratum) does not seem a reasonable explanation for the contact guidance of cells by nanometric scale topography as structures of this size would not realistically impose severe restrictions on the cell cytoskeleton. Similarly, Ohara and Buck's (1979) hypothesis (that focal contacts can only form on the ridges of grooved substrata, thus influencing the direction of cell movement) can be contradicted by the studies of Clark *et al* (1991) who reported that degree of cell alignment on ultrafine topographical gratings was dependent mainly on groove depth. If the cells were simply bridging the grooves, as suggested by Ohara and Buck (1979), then depth of grooves would not be expected to have a marked effect on cell alignment. Further doubt is cast on Ohara and Buck's (1979) theory by a study of Meyle *et al* (1991) who, using parallel grooved substrata, showed that fibroblasts conformed to the contours of the underlying topography, demonstrating that cells can and do make contact with the bottom surface of the grooves, and not just the ridges, when they respond to substrates of grooved morphology.

These studies have concentrated on cell behaviour *in vitro*, but close contact of cells with any implanted device is important for mechanical interlocking of the prosthesis and successful wound healing. Further evidence against the contact guidance theory of Ohara and Buck (1979) is provided, in this project, in the investigation into the reaction of PDS grooved structures *in vivo*. Histological analysis of the grooved PDS plates, implanted in rat lumbar muscle, reveals that in some instances cells can clearly be seen within grooves, and in contact with the base of the grooves. Although it was impossible to tell from this study whether or not the cells were in fact aligned whilst they were sitting in the grooves, it would seem reasonable to assume, from results of many *in vitro* studies, that this was the case.

Further to my discovery that phosphorylated tyrosine residues are found localised along groove ridge boundaries in cells cultured on parallel grooved silica structures (even on substrata of nanometric scale depth) we (Wojciak-Stothard *et al*, 1996) proposed that the reaction of cells to topographical features may be initiated by the selective clustering of specific membrane receptors, followed by the phosphorylation of tyrosine. This phosphorylation could then initiate an intracellular signalling cascade, similar to that observed in the response of cells to growth factor molecules. Epidermal Growth Factor (EGF), Platelet-Derived Growth Factor (PDGF), and Hepatocyte Growth Factor/Scatter Factor (HGF/SF) all initiate a signal transduction cascade via the activation of the receptor tyrosine phosphorylation (Cantley *et al*, 1991).

Jewell *et al* (1995) reported the tyrosine phosphorylation of distinct proteins in response to antibody-mediated ligation and clustering of α_3 and α_6 integrins. Using anti-α_3 antibodies, they found stimulation of tyrosine phosphorylation of a 55 kDa protein, in prostate carcinoma cells (PC-3) and human umbilical vein endothelial cells (HUVEC). In contrast, anti-α_6 antibodies resulted in stimulation of tyrosine phosphorylation of a 90 kDa and 52 kDa protein, in the same cells. In PC-3 cells, clustering with anti-β1 antibodies triggered tyrosine phosphorylation of all of these proteins, whereas anti-β4 antibody resulted in tyrosine phosphorylation of a distict 62 kDa protein. As the PC-3 cells express both $\alpha 6\beta 1$ and $\alpha 6\beta 4$ integrins, Jewell *et al* suggest that these two receptors can transduce distinct signals. They also found no evidence of stimulation of tyrosine phosphorylation of pp125 focal adhesion kinase, following antibody-mediated ligation and clustering of integrins, although stimulation of phosphorylation was observed when cells attached and spread on fibronectin, laminin and anti-α3 monoclonal antibody.

Wojciak-Stothard *et al* (1996) reported an accumulation of αV integrins, co-localised with vinculin, F-actin, and phosphotyrosine staining, along groove ridge boundaries in P388D1 macrophages grown on nanogrooved substrata. Work in this project also demonstrated the same pattern of phosphorylation in various cell types, on both nano- and micro-machined grooved substrata. The work of Jewell *et al* supports the theory proposed here for the stimulation of tyrosine phosphorylation by topographical features: clustering of specific cell membrane receptors (integrins) on topographical features triggers phosphorylation of tyrosine residues on one or more proteins, this in turn, leading to an intracellular signalling cascade which can, among other things, regulate cellular contact guidance. The observation by Jewell *et al* (that crosslinking of different integrin heterodimers stimulates tyrosine phosphorylation of proteins different from those phosphorylated when cells are allowed to spread on a matrix) demonstrates that specific messages can be relayed to the cell in an integrin-specific manner, and also lends support to the idea of specific external topographical features inducing specific cellular events via stimulation of certain cell surface molecules.

It was thought that the tyrosine phosphorylation localised along groove/ridge boundaries, when cells were grown on grooved substrata in this study, may have been the result of phosphorylation of the pp125 focal adhesion kinase, as it is probable that the cells would be in close contact with the substrata at this point and therefore be forming focal adhesions. However, work in our laboratory has shown that antibodies to focal adhesion kinase do not show localisation along groove/ridge boundaries (Graham Tobasnick, personal communication). Despite this it is still likely that the phosphorylated residues observed are those present on one of the many proteins that comprise the focal adhesion complex, particularly as the staining pattern observed closely resembles that seen when staining for focal adhesions (as seen in Turner *et al*, 1995).

NATURE OF A POSSIBLE TOPOGRAPHY RECEPTOR

As discussed above, the links that have been demonstrated between external cell stimuli and intracellular molecular changes all act via cell membrane integrins. The fact that exogenous growth factors have been shown to stimulate intracellular signalling machinery, leading to specific changes in the cell cytoskeleton, raises the possibility that stimulation of a receptor by topographical features could induce a similar signalling cascade. In this way, signals from any substrate the cell comes in contact with could be relayed to the cell nucleus, ultimately leading to changes in gene expression, cell shape, cell behaviour, etc. Clustering of integrins on topographical features (as reported by Wojciak-Stothard *et al*, 1996) may result in tyrosine phosphorylation of one or more proteins, this in turn, leading to an intracellular signalling cascade, possibly involving fyn, lyn, and actin-binding proteins. These signals and phosphorylation/dephosphorylation of certain proteins (for example, actin-binding proteins) could lead to changes in the structure/distribution of the cell cytoskeleton and hence allow the cell to react appropriately to topographical stimuli. Although only speculative, due to the important role played by topographic guidance *in vivo* it would not be surprising if at least certain groups of cells possessed a membrane receptor of this type.

CHANGES IN GENE EXPRESSION

Although the mechanism of cell contact guidance is not known, it would be reasonable to assume that changes in gene expression will occur concomitantly with the changes in cell shape/movement observed when a cell is guided by its substrate. In order to investigate the interesting possiblility that changes in gene expression can occur as a result of a cell making contact with topographical features, I grew cells on smooth and grooved substrata, extracted their messenger

RNA (mRNA) and carried out mRNA fingerprinting. Any mRNA sample run on a fingerprinting gel displays unique bands (or "fingerprints"), therefore the mRNA from the two different samples (smooth and grooved) could be easily compared for any differences when run together on a gel. It was shown that there were distinct differences in gene expression between cells grown on smooth and those grown on grooved substrates.

The messenger RNA fingerprinting experiments have been continued in our laboratory and further bands, differentially expressed in cells grown on flat and cells grown on grooved surfaces, have been isolated, cloned and sequenced. These include fragments of the following genes: Mouse 28S rRNA (170bp); human alpha N-acetylgalactosaminidase (424bp); thymidine kinase (365bp); mouse 45S pre rRNA (135bp); and elastin (139bp) (Tong-Tong Li, personal communication).

In recent years a number of laboratories have started to investigate the molecular mechanisms that are involved in cellular contact guidance. As exposure to topographical stimuli causes changes in cell shape, it would seem probable that the signal for these cell shape changes would come from gene expression signals different from those received by cells grown on a smooth surface. Many studies have reported that the extent of cell spreading or cell shape can have effects on gene expression, therefore it would seem reasonable to suggest that the response of cells to topographical stimuli would have resultant effects on gene expression.

In 1977 Brunner proposed that cell differentiation occurred in response to signals received by the cell from its environment. He called the transfer of information from the cell membrane receptor to the genome "membrane impression" and suggested that this was responsible for the conversion of cells to new phenotypes. Evidence that variations in cell contact and cell shape can influence the gene

expression of cytoskeletal proteins was provided by Farmer *et al* (1983) who showed that regulation of the level and translation of actin mRNA could be affected by changes in cell configuration. Ungar *et al* (1986) also demonstrated that regulation of vinculin synthesis in cultured fibroblasts was dependent on cell contact and cell shape. This led Ireland *et al* (1987) to suggest that the cytoskeleton could act as a modulator between the cell surface and the nucleus. More recently, Chou *et al* (1995) reported changes in fibronectin gene expression in direct response to a topographical stimulus. They found that as well as altering cell shape, substratum topography could regulate fibronectin synthesis at the transcriptional and post-transcriptional level. They cultured human gingival fibroblasts on titanium-coated smooth or grooved substrata and found: increased fibronectin mRNA levels (by Northern Blot anlysis); increased secretion of fibronectin; increased stability of fibronectin mRNA; and an increase in the amount of fibronectin assembled into the extracellular matrix, in the cells grown on the grooved substrate.

Hong and Brunette (1987) showed that using physical means to alter epithelial cell shape, such as mechanical stretching or growth on less adhesive substrata, resulted in changes in cell proteinase secretion. They also found that proteinase secretion was related more to cell shape than to cell proliferation. This relates to work by Werb *et al* (1986) who used cytochalasin B to alter the morphology of rabbit synovial fibroblasts and reported that changes in cell shape induced synthesis of the extracellular matrix-degrading metalloproteinases, collagenase and stromelysin. They further reported (Werb *et al*,1989) that monoclonal antibodies to the fibronectin receptor, or peptides containing the RGD cell recognition sequence of fibronectin, also induced the expression of these genes, in the same cell type, without any changes in cell shape. As this induced gene expression was not observed when cells were grown on native fibronectin, these data lend further support to the hypotheses that specific external signals can lead

to specific changes in gene expression, even via the same cell membrane receptor (in this case the fibronectin receptor).

Work by Watt *et al* (1988) described how changes in "cell shape" controlled terminal differentiation of human epidermal keratinocytes. Although this may appear to contradict the results of Werb *et al* (1989), described above, in which no changes in cell shape were necessary for induction of gene expression by external stimuli, it should be noted that varying the area of a cell in contact with the substratum has an automatic effect on cell shape (as mentioned by Watt *et al*, 1988). Therefore, all of these studies actually reinforce the idea of a signalling mechanism, transmitted via cell surface receptors, that can result in cell shape changes via differential gene expression. Different external (including topographical) stimuli would result in differential occupation of the receptor molecules and thereby different signals would be relayed to the cell.

Many studies have shown that changes in cell shape that follow alterations in cell-cell and/or cell-extracellular matrix (ECM) contacts are associated with changes in the differentiation state of the cells. For example, chondrocytes turn into fibroblast-like cells when cultured on fibronectin, where the cells have a well spread phenotype and express type I collagen. However, in suspension culture, the cells have a spherical morphology and express chondrocyte type II collagen (Benya and Schaffer, 1982) . The importance of cell-cell and cell-matrix contacts in allowing tissue specific gene expression was also demonstrated in primary cultures of liver hepatocytes. These cells rapidly lose the transcription of liver-specific genes when grown in monolayer culture, unless cell-cell contact is maintained (Clayton, 1985).

Adhesion of cells to a substrate has long been recognised as a prerequisite for normal cell growth in culture (Stoker *et al*, 1968; Folkman and Moscona, 1978),

suggesting that appropriate adhesion of the cell to components of the ECM is necessary for the transmission of the mitogenic signal to the cells nucleus. Therefore, given that the process of cell transformation is characterised by alterations in phenotype that include cell adhesion, cell shape, and the organisation of cytoskeletal proteins, it is not surprising to find that among the first tumour supressor genes identified are genes coding for both adhesion-like and extracellular proteins (Reviewed in Mikkelsen and Cavenee, 1990).

In recent years it was discovered that a variety of regulatory molecules involved in signal transduction and gene regulation were localised at the cytoplasmic domains of microfilament-membrane associations at cell adhesion sites (Reviewed in Burridge and Fath, 1989). The discovery of a linkage between actin-binding proteins and the phosphoinositide signalling pathway (Goldschmidt-Clermont *et al*, 1990) led to the suggestion that the cytoskeleton could regulate gene expression, either by association with the second messenger system, and/or by controlling the localization of regulatory molecules.

FUTURE WORK

This study has described preliminary experiments in an attempt to further elucidate the mechanisms of cell contact guidance, with a view to exploit the process for use in tissue repair. A role for tyrosine phosphorylation in the contact guidance signalling pathway has been suggested, but future work should involve the identity of the protein(s) involved.

It has also been shown here that cells exhibit differential gene expression when grown on grooved and non-grooved surfaces. Work has been continued in the laboratory and has identified some of the proteins involved. This may help in

identifying further proteins involved in the topographical signalling cascade (assuming there is one), but it is also important to be sure that topographical cues on any implant do not have any adverse effects on gene expression and thereby cellular function.

As a consequence of some of the work reported in this thesis the development of a biodegradable implant to aid wound repair is now a more realistic possibility. Implantation of microgrooved PDS structures has established that: the microfabricated structures are biocompatible (comparable with PDS suture) and do not result in any adverse tissue reaction; the grooves on the (non-oxygen plasma-etched) PDS structures remain intact for up to 91 days *in vivo*; oxygen-plasma etching of the structures accelerates the rate of PDS degradation *in vivo*.

These results suggest that a microgrooved prosthetic device fabricated in PDS could be of use as a biodegradable implant to aid wound healing. The next step, therefore, will be to perfect design of a grooved PDS implant and examine its effectiveness in wound healing in a suitable animal model. Ultimately, a possible use for such a device would be to help guide the regrowth of healing tendons, thereby preventing adhesion formation and associated immobility.

Hopefully, with advances in cell engineering, in the future it should be possible to engineer implants such that they have a positive effect on wound healing in the tissue where they are situated.

CHAPTER 7

REFERENCES

Abbas, A.K., Lichtman, A.H. and Pober, J.S. (1991) *Cytokines*. In: "Cellular and Molecular Immunology", edited by M.J. Wonsiewicz; W.B. Saunders Company, Philadelphia 225-243.

Abercrombie, M. and Dunn, G.A. (1975) *Adhesions of Fibroblasts to Substratum During Contact Inhibition Observed By Interference Reflection Microscopy*, Exp. Cell Res. **92** 57-62.

Altschul, S.F., Gish, W., Miller, W., Myers, E.W. and Lipman, D.J. (1990) *Basic Local Alignment Search Tool*, J. Mol. Biol. **215** 403-410.

Artandi, C. (1980) *A Revolution in Sutures.*, Surg. Gynecol. Obstet. **150** 235-236.

Aspenberg, P., Goodman, S., Toksvig-Larsen, S., Ryd, L. and Albrektsson, T. (1992) *Intermittent Micromotion Inhibits Bone Ingrowth/Titanium Implants in Rabbits*, Acta. Orthop. Scand. **63(2)** 141-145.

Benya, P.D. and Schaffer, J.D. (1982) *Dedifferentiated Chondrocytes Reexpress the Differentiated Collagen Phenotype When Cultured in Agarose Gels*, Cell **30** 215-224.

Ben-Ze'ev, A. (1987) *The Role of Changes in Cell Shape and Contacts in the Regulation of Cytoskeleton Expression During Differentiation*, J. Cell Sci. Suppl. **8** 293-312.

Ben-Ze'ev, A. (1991) *Animal Cell Shape Changes and Gene Expression*, BioEssays **13** 207-212.

Bockholt, S.M. and Burridge, K. (1993) *Cell Spreading on Extracellular Matrix Proteins Induces Tyrosine Phosphorylation of Tensin*, J. Biol. Chem. **268** 14565-14567.

Bowers, K.T., Keller, J.C., Randolph, B.A., Wick, D.C. and Michaels, C.M. (1992) *Optimization of Surface Micromorphology For Enhanced Osteoblast Responses In Vitro*, The International Journal of Oral and Maxillofacial Implants **7** 302-310.

Bray, D. (1992) *Cell Behaviour.* In: "Cell Movements"; Garland Publishing Inc., New York 31-44.

Britland, S., Perridge, C., Denyer, M., Morgan, H., Curtis, A. and Wilkinson, C. (1996) *Morphogenetic Guidance Cues Can Interact Synergistically and Hierarchically in Steering Nerve Cell Growth*, Experimental Biology Online (electronic journal) **1:2**.

Brunette, D.M. (1986) *Fibroblasts on Micromachined Substrata Orient Hierarchically to Grooves of Different Dimensions*, Exp. Cell Res. **164** 11-26.

Brunette, D.M. (1986) *Spreading and Orientation of Epithelial Cells on Grooved Substrata*, Exp. Cell Res. **167** 203-217.

Brunette, D.M. (1988) *The Effect of Surface Topography on Cell Migration and Adhesion.* In: "Surface Characterization of Biomaterials", edited by B.D. Ratner; Elsevier Science Publishers B.V., Amsterdam 203-218.

Brunette, D.M., Kenner, G.S., Gould, T.R.L. (1983) *Grooved Titanium Surfaces Orient Growth and Migration of Cells From Human Gingival Explants*, J. Dent. Res. **62(10)** 1045-1048.

Brunette, D.M., Schindelhauer, N., Chehroudi, B. and Gould, T.R.L. (1988) *Effects of Grooved Titanium Substrata on Cell Shape In Vivo and In Vitro*, J. Dent. Res. **67** 347.

Brunner, G. (1977) *Membrane Impession and Gene Expression*, Differentiation **8** 123-132.

Burridge, K. and Fath, K. (1989) *Focal Contacts: Transmembrane Links Between the Extracellular Matrix and the Cytoskeleton*, BioEssays **10(4)** 104-108.

Burridge, K., Fath, K., Kelly, T., Nuckolls, G. and Turner, C. (1988) *Focal Adhesions: Transmembrane Junctions Between the Extracellular Matrix and the Cytoskeleton*, Ann. Rev. Cell Biol. **4** 487-525.

Burridge, K., Turner, C.E. and Romer, L.H. (1992) *Tyrosine Phosphorylation of Paxillin and pp125 FAK Accompanies Cell Adhesion to Extracellular Matrix: A Role in Cytoskeletal Assembly*, J. Cell Biol. **119** 893-903.

Camporese, D.S., Lester, T.P. and Pulfrey, D.L. (1981) *A Fine Line Silicon Shadow Mask for Inversion Layer Solar Cells*, IEEE Electron Device Letters **2(3)** 61-63.

Cantley, L.C., Auger, K.R., Carpenter, C., Duckworth, B., Graziani, A., Kapeller, R. and Soltoff, S. (1991) *Oncogenes and Signal Transduction*, Cell **64** 281-302.

Chehroudi, B. and Brunette, D.M. (1995) *Effects of Surface Topography on Cell Behaviour.* In: "Encyclopedic Handbook of Biomaterials and Bioengineering", Part A: Materials, Vol. 1, edited by D.L. Wise, D.J. Trantolo, D.E. Altobelli, M.J. Yaszemski, J.D. Gresser and E.R. Schwartz; Marcel Dekker, Inc. (New York; Basel; Hong Kong) 813-842.

Chehroudi, B., Gould, T.R.L. and Brunette, D.M. (1989) *Effects of a Grooved Titanium-Coated Implant Surface on Epithelial Cell Behaviour In Vitro and In Vivo*, J. Biomed. Mat. Res. **23** 1067-1085.

Chehroudi, B., Gould, T.R.L. and Brunette, D.M. (1990) *Titanium-Coated Micromachined Grooves of Different Dimensions Affect Epithelial and Connective-Tissue Cells Differently In Vivo*, J. Biomed. Mat. Res. **24** 1203-1219.

Chehroudi, B., Gould, T.R.L. and Brunette, D.M. (1992) *The Role of Connective Tissue in Inhibiting Epithelial Downgrowth on Titanium-Coated Percutaneous Implants*, J. Biomed. Mat. Res. **26** 493-515.

Chehroudi, B., Soorany, E., Black, N., Weston, L. and Brunette, D.M. (1995) *Computer Assisted Three-Dimensional Reconstruction of Epithelial Cells Attached to Percutaneous Implants*, J. Biomed. Mat. Res. **29** 371-379.

Chen, H.-C., Appeddu, P.A., Parsons, J.T., Hildebrand, J.D., Schaller, M.D. and Guan, J.L. (1995) *Interaction of Focal Adhesion Kinase with Cytoskeletal Protein Talin*, J. Biol. Chem. **270** 16995-16999.

Chen, H.-C. and Guan, J.L. (1994) *Association of Focal Adhesion Kinase With its Potential Substrate Phosphatidylinositol 3-Kinase*, Proc. Natl. Acad. Sci. USA **91** 10148-10152.

Chou, L., Firth, J.D., Uitto, V.-J. and Brunette, D.M. (1995) *Substatum Surface Topography Alters Cell Shape and Regulates Fibronectin mRNA Level, mRNA Stability, Secretion and Assembly in Human Fibroblasts*, J.Cell Sci. **108** 1563-1573.

Chu, C.-C. and Williams, D.F. (1984) *Effects of Physical Configuration and Chemical Structure of Suture Materials on Bacterial Adhesion*, Am. J. Surg. **147** 197-204.

Clark, P., Connolly, P., Curtis, A.S.G., Dow, J.A.T. and Wilkinson, C.D.W. (1987) *Topographical Control of Cell Behaviour: I. Simple step cues*, Development **99** 439-448.

Clark, P., Connolly, P., Curtis, A.S.G., Dow, J.A.T. and Wilkinson, C.D.W. (1990) *Topographical Control of Cell Behaviour: II. Multiple grooved substrata*, Development **108** 635-644.

Clark, P., Connolly, P., Curtis, A.S.G., Dow, J.A.T. and Wilkinson, C.D.W. (1991) *Cell Guidance By Ultrafine Topography <u>In</u> <u>Vitro</u>*, J. Cell Sci. **99** 73-77.

Clark, R.E., Boyd, J.C., Moran, J.F. (1974) *New Principles Governing the Tissue Reactivity of Prosthetic Materials*, J. Surg. Res. **16** 510-522.

Clayton, D.F., Harrelson, A.L. and Darnell, J.E., Jr. (1985) *Dependence of Liver-Specific Transcription on Tissue Organisation*, Mol. Cell. Biol. **5(10)** 2623-2632.

Conn, J.J., Oyasu, R., Welsh, M. and Beal, J.M. (1974) *Vicryl (Polyglactin 910) Synthetic Absorbable Sutures*, Am. J. Surg. **128** 19-23.

Curtis, A., Wilkinson, C. and Wojciak-Stothard, B. (1995) *Accelerating Cell Movement*, J. Cellular Engineering **1** 35-38.

Curtis, A.S.G. and Clark, P. (1990) *The Effects of Topographic and Mechanical Properties of Materials on Cell Behaviour*, Critical Reviews in Biocompatibility **5** 343-362.

Curtis, A.S.G. and Varde, M. (1964) *Control of Cell Behaviour: Topological Factors*, Journal of the National Cancer Institute **33** 15-26.

Dow, J.A.T., Clark, P., Connolly, P., Curtis, A.S.G. and Wilkinson, C.D.W. (1987) *Novel Methods for the Guidance and Monitoring of Single Cells and Simple Networks in Culture*, J. Cell Sci. Suppl. **8** 55-79.

Dunn, G.A. (1982) *Contact Guidance of Cultured Tissue Cells: A Survey of Potentially Relevant Properties of the Substratum.* In: "Cell Behaviour", edited by R. Bellairs, A.S.G. Curtis and G.A. Dunn; Cambridge University Press, Cambridge, U.K. 247-280.

Dunn, G.A. and Brown, A.F. (1986) *Alignment of Fibroblasts on Grooved Surfaces Described By a Simple Geometric Transformation*, J.Cell Sci. **83** 313-340.

Dunn, G.A. and Heath, J.P. (1976) *A New Hypothesis of Contact Guidance in Tissue Cells*, Exp. Cell Res.**101** 1-14.

Farmer, S.R., Wan, K.M., Ben-Ze'ev, A. and Penman, S. (1983) *Regulation of Actin mRNA Levels and Translation Responds to Changes in Cell Configuration*, Mol. Cell. Biol. **3(2)** 182-189.

Folkman, J. and Moscona, A. (1978) *Roll of Cell Shape in Growth Control*, Nature **273** 345-349.

Gausch, C.R., Hard, W.L. and Smith, T.F. (1966) *Characterisation of an Established Line of Canine Kidney Cells*, Proc. Soc. Exp. Biol. Med. **122** 931-939.

Gelberman, R.H., Vande Berg, J.S., Lundborg, G.N. and Akeson, W.H. (1983) *Flexor Tendon Healing and Restoration of the Gliding Surface*, J. Bone Joint Surg. **65-A** 70-79.

Gingell, D. (1993) *Contact Signalling and Cell Motility.* In: "Cell Behaviour: Adhesion and Motility", The Society of Experimental Biology Symposium No. 47, edited by G. Jones, C. Wigley and R. Warn; The Company of Biologists Limited, Cambridge, UK 1-33.

Goldschmidt-Clermont, P.J., Machesky, L.M., Baldassare, J.J. and Pollard, T.D. (1990) *The Actin-Binding Protein Profilin Binds to PIP_2 and Inhibits Its Hydrolysis by Phospholipase C*, Science **247** 1575-1578.

Grant, S.G.N., O'Dell, T.J., Karl, K.A., Stein, P.L., Soriano, P. and Kandel, E.R. (1992) *Impaired Long-Term Potentiation, Spatial Learning, and Hippocampal Development in fyn Mutant Mice*, Science **258** 1903-1910.

Groth, T. and Altankov, G. (1995) *Fibroblast Spreading and Proliferation on Hydrophilic and Hydrophobic Surfaces is Related to Tyrosine Phosphorylation in Focal Contacts*, Journal of Biomaterials Science - Polymer edition **7 (3)** 297-305.

Gumbiner, B.M. (1996) *Cell Adhesion: The Molecular Basis of Tissue Architecture and Morphogenesis*, Cell **84** 345-357.

Haddad, R.J., Jr., Cook, S.D. and Thomas, K.A. (1987) *Biological Fixation of Porous-Coated Implants*, J. Bone Joint Surg. **69-A** 1459-1466.

Hall, A. (1994) *Small GTP-Binding Proteins and the Regulation of the Actin Cytoskeleton*, Annu. Rev. Cell Biol. **10** 31-54.

Harrison, R.G. (1910) *The Outgrowth ofthe Nerve Fiber as a Mode of Protoplasmic Movement*, J. Exp. Zool. **9(4)** 787-848.

Harrison, R.G. (1914) *The Reaction of Embryonic Cells to Solid Structures*, J. Exp. Zool. **17** 521-544.

Heath, J.P. and Dunn, G.A. (1978) *Cell to Substratum Contacts of Chick Fibroblasts and Their Relation to the Microfilament System. A Correlated Interference-Reflexion and High-Voltage Electron-Microscope Study*, J. Cell Sci. **29** 197-212.

Hong, H.L. and Brunette, D.M. (1987) *Effect of Cell Shape on Proteinase Secretion By Epithelial Cells*, J. Cell Sci. **87** 259-267.

Horder, T.J. and Martin, K.A.C. (1978) *Morphogenetics as an Alternative to Chemospecificity in the Formation of Nerve Connections*, Symp. Soc. Exp. Biol. **32** 275-358.

Ireland, G.W., Dopping-Hepenstal, P., Jordan, P. and O'Neill, C. (1987) *Effect of Patterned Surfaces of Adhesive Islands on the Shape, Cytoskeleton, Adhesion and Behaviour of Swiss Mouse 3T3 Fibroblasts*, J. Cell Sci. Suppl. **8** 19-33.

Jewell, K., Kapron-Bras, C., Jeevaratnam, P. and Dedhar, S. (1995) *Stimulation of Tyrosine Phosphorylation of Distinct Proteins in Response to Antibody-Mediated Ligation and Clustering of α3 and α6 integrins*, J. Cell Sci. **108** 1165-1174.

Könönen, M., Hormia, M., Kivilahti, J., Hautaniemi, J. and Thesleff (1992) *Effect of Surface Processing on the Attachment, Orientation, and Proliferation of Human Gingival Fibroblasts on Titanium*, J. Biomed. Mat. Res. **26** 1325-1341.

Koren,H.S., Handwerger, B.S. and Wunderlich, J.R. (1975) *Identification of Macrophage-Like Characteristics in A Cultured Murine Tumor Line*, J. Immunol. **114 (2)** 894-897.

Lerwick, E. (1983) *Studies on the Efficacy and Safety of Polydioxanone Monofilament Absorbable Suture*, Surg. Gynecol. Obstet. **156** 51-55.

Levitzki, A. (1990) *Tyrphostins - Potential Antiproliferative Agents and Novel Molecular Tools*, Biochem. Pharmacol. **40(5)** 913-918.

Lin, J. and Justement, B. (1992) *The MB-1/B29 Heterodimer Couples the B Cell Antigen Receptor to Multiple src Family Protein Tyrosine Kinases* J. Immunol. **149** 1548-1555.

Lo, S.H., Weisberg, E. and Chen, L.B. (1994) *Tensin: A Potential Link Between the Cytoskeleton and Signal Transduction*, BioEssays **16** 817-823.

Lyall, R.M., Zilberstein, A., Gazit, A., Gilon, C., Levitzki, A. and Schlessinger, J. (1989) *Tyrphostins Inhibit Epidermal Growth Factor (EGF)-Receptor Tyrosine Kinase Activity in Living Cells and EGF-stimulated Cell Proliferation*, J. Biol.Chem. **264** 14503-14509.

Maroudas, N.G. (1972) *Anchorage Dependence: Correlation Between Amount of Growth and Diameter of Bead, For Single Cells Grown on Individual Glass Beads*, Exp. Cell Res. **74** 337-342.

McCaig, C.D. (1986) *Electric Fields, Contact Guidance and the Direction of Nerve Growth*, J. Embryol. Exp. Morph. **94** 245-255.

McClelland, M., Chada, K., Welsh, J. and Ralph, D. (1993) *Arbitrary Primed PCR Fingerprinting of RNA Applied to Mapping Differentially Expressed Genes.* In: "DNA Fingerprinting: State of the Science", edited by S.D.J. Pena, R. Chakraborty, J.T. Epplen and A.J. Jeffreys; Birkhauser Verlag Basel/Switzerland 103-115.

Meyle, J., Gultig, K., Brich, M., Hammerle, H. and Nisch, W. (1994) *Contact Guidance of Fibroblasts on Biomaterial Surfaces*, Journal of Materials Science: Materials in Medicine **5 (6-7)**463-466.

Meyle, J., von Recum, A.F., Gibbesch, B., Hüttemann, W., Schlagenhauf, U. and Schulte, W. (1991) *Fibroblast Shape Conformation to Surface Micromorphology*, J. Appl. Biomat. **2** 273-276.

Mikkelsen, T. and Cavenee, W.K. (1990) *Suppressors of the Malignant Phenotype*, Cell Growth and Differentiation **1** 201-207.

Muguruma, M., Matsumura, S. and Fukazawa, T. (1990) *Direct Interactions Between Talin and Actin*, Biochemical and Biophysical Research Communications **171(3)** 1217-1223.

Nakatsuji, N., Gould, A.C. and Johnson, K.E. (1982) *Movement and Guidance of Migrating Mesodermal Cells in Ambystoma Maculatum Gastrulae*, J. Cell Sci. **56** 207-222.

Nobes, C.D., Hawkins, P., Stephens, L. and Hall, A. (1995) *Activation of the small GTP-binding proteins rho and rac by growth factor receptors*, J. Cell Sci. **108** 225-233.

Oakley, C. and Brunette, D.M. (1993) *The sequence of alignment of microtubules, focal contacts and actin filaments in fibroblasts spreading on smooth and grooved titanium substrata*, J. Cell Sci. **106** 343-354.

Oakley, C. and Brunette, D.M. (1995) *Respose of single, pairs, and clusters of epithelial cells to substratum topography*, Biochem. Cell Biol. **73** 473-489.

Ohara, P.T. and Buck, R.C. (1979) *Contact Guidance In Vitro. A light, transmission, and scanning electron microscopic study*, Exp. Cell Res. **121** 235-249.

Otey, C.A., Pavalko, F.M. and Burridge, K. (1990) *An Interaction Between α-Actinin and the β_1 Integrin Subunit In Vitro*, J. Cell Biol. **111** 721-729.

Owens, G. and Rubbra, J. (1946) *The Effect of Various Suture Materials in Wound Healing*, J. Kans. Med. Soc. **47** 300-303.

Parish, R.W., Schmidhauser, C., Schmidt, T. and Dudler, R.K. (1987) *Mechanisms of Tumour Cell Metastasis*, J. Cell Sci. Suppl. **8** 181-197.

Perlmutter, R.M., Levin, S.D., Appleby, M.W., Anderson, S.J. and Alberola-Ila, J. (1993) *Regulation of Lymphocyte Function by Protein Phosphorylation*, Ann. Rev. Immunol. **11** 451-499.

Pilliar, R.M., Lee, J.M. and Maniatopoulos, C. (1986) *Observations of the Effects of Movement on Bone Ingrowth into Porous-Surfaced Implants*, Clin. Orthop. **208** 108-113.

Postlethwait, R.W. (1970) *Polyglycolic Acid Surgical Suture*, Arch. Surg. **101** 489-494.

Poston, M.R., Fredieu, J., Carney, P.R. and Silver, J. (1988) *Roles of Glia and Neural Crest Cells in Creating Axon Pathways and Boundaries in the Vertebrate Central and Peripheral Nervous Systems.* In: "The Making of the Nervous System", edited by J.G. Parnavelas, C.D. Stern and R.V. Stirling; Oxford Science Publications 282-313.

Potenza, Major A.D. (1963) *Critical Evaluation of Flexor-Tendon Healing and Adhesion Formation Within Artificial Digital Sheaths*, J. Bone Joint Surg. **45-A** (**6**) 1217-1233.

Ray, J.A., Doddi, N., Regula, D., Williams, J.A. and Melveger, A. (1981) *Polydioxanone (PDS), A Novel Monofilament Synthetic Absorbable Suture*, Surg. Gynecol. Obstet. **153** 497-507.

Reiderer-Henderson, M.A., Gauger, A., Olson, L., Robertson, C. and Greenlee, T.K. Jr. (1983) *Attachment and Extracellular Matrix Differences Between Tendon and Synovial Fibroblastic Cells*, In Vitro **19 (2)** 127-133.

Rich, A. and Harris, A.K. (1981) *Anomalous Preferences of Cultured Macrophages for Hydrophobic and Roughened Substrata*, J. Cell Sci. **50** 1-7.

Ridley, A.J. and Hall, A. (1994) *Signal Transduction pathways regulating Rho-mediated stress fibre formation: requirement for a tyrosine kinase*, The EMBO Journal **13** 2600-2610.

Romer, L.H. (1995) *Integrin-Mediated Tyrosine Phosphorylation of Focal Adhesion Proteins and Organization of the Cytoskeleton.* In: "Topics in Molecular Medicine", vol. 1, edited by W. Siess, R. Lorenz, and P.C. Weber; Raven Press Ltd., New York 37-53.

Romer, L.H., McLean, N., Turner, C.E. and Burridge, K. (1994) *Tyrosine Kinase Activity, Cytoskeletal Organisation, and Motility in Human Vascular Endothelial Cells*, Mol. Biol. Cell **5** 349-361.

Rothkopf, D.M., Webb, S., Szabo, R.M., Gelberman, R.H. and May, J.W. (1991) *An Experimental Model For the Study of Canine Flexor Tendon Adhesions*, J. Hand Surg. **16A** 694-700.

Rovensky, Y.A. and Samoilov, V.I. (1994) *Morphogenetic Response of Cultured Normal and Transformed Fibroblasts, and Epitheliocytes, to a Cylindrical Substratum Surface. Possible role for the actin filament bundle pattern*, J. Cell Sci. **107** 1255-1263.

Rovensky, Y.A., Slavnaja, I.L. and Vasiliev, J.M. (1971) *Behaviour of Fibroblast-Like Cells on Grooved Surfaces*, Exp. Cell Res. **65** 193-201.

Schaller, M.D., Borgman, C.A., Cobb, B.S., Vines, R.R., Reynolds, A.B. and Parsons, J.T. (1992) *pp125^{FAK}, a Sructurally Distinctive Protein-Tyrosine Kinase Associated With Focal Adhesions*, Proc. Natl. Acad. Sci. USA **89** 5192-5196.

Schaller, M.D. and Parsons, J.T. (1993) *Focal Adhesion Kinase: An Integrin-Linked Protein Tyrosine Kinase*, Trends in Cell Biology **3** 258-262.

Schaller, M.D. and Parsons, J.T. (1994) *Focal Adhesion Kinase and Associated Proteins*, Curr. Opin. Cell Biol. **6** 705-710.

Schaller, M.D. and Parsons, J.T. (1995) *pp125^{FAK}-Dependent Tyrosine Phosphoprylation of Paxillin Creates A High-Affinity Binding Site For Crk*, Mol. Cell. Biol. **15(5)** 2635-2645.

Schliwa, M. and Honer, B. (1993) *Microtubules, Centrosomes and Intermediate Filaments in Directed Cell Movement*, Trends in Cell Biology **3** 377-380.

Singhvi, R. , Stephanopoulos, G.N. and Wang, D.I.C. (1992) *Effect of Substratum Morphology on Animal Cell Adhesion and Behaviour*, Mater. Res. Soc. Symp. Proc. **252** 237-245.

Singhvi, R., Stephanopoulos, G.N. and Wang, D.I.C. (1994) *Review: Effects of Substratum Morphology on Cell Physiology*, Biotechnology and Bioengineering **43** 764-771.

Stoker, M. and MacPherson, I. (1964) *The Syrian Hamster Fibroblastic Cell Line BHK21 and its Derivatives*, Nature **203** 1355-1357.

Stoker, M., O'Neill, C., Berryman, S. and Waxman, V. (1968) *Anchorage and Growth Regulation in Normal and Virus-Transformed Cells*, Int. J. Cancer **3** 683-693.

Superti-Furga, G. and Courtneidge, S.A. (1995) *Structure-Function Relationships in Src Family and Related Protein Tyrosine Kinases*, BioEssays **17(4)** 321-330.

Thomas, K.A. and Cook, S.D. (1985) *An Evaluation of Variables Influencing Implant Fixation by Direct Bone Apposition*, J. Biomed. Mat. Res. **19** 875-901.

Thomas, K.A., Kay, J.F., Cook, S.D. and Jarcho, M. (1987) *The Effect of Surface Macrotexture and Hydroxylapatite Coating on the Mechanical Strengths and Histologic Profiles of Titanium Implant Materials*, J. Biomed. Mat. Res. **21** 1395-1414.

Turner, C.E. (1994) *Paxillin: A Cytoskeletal Target For Tyrosine Kinases*, BioEssays **16(1)** 47-52.

Turner, C.E. and Burridge, K. (1991) *Transmembrane Molecular Assemblies in Cell-Extracellular Matrix Interactions*, Curr. Opin. Cell Biol. **3** 849-853.

Turner, C.E., Glenney, J.R., Jr. and Burridge, K. (1990) *Paxillin: A New Vinculin-Binding Protein Present in Focal Adhesions*, J. Cell Biol. **111** 1059-1068.

Turner, C.E., Pietras, K.M., Taylor, D.S. and Molloy, C.J. (1995) *Angiotensin II Stimulation of Rapid Paxillin Tyrosine Phosphorylation Correlates with the*

Formation of Focal Adhesions in Rat Aortic Smooth Muscle Cells, J. Cell Sci. **108** 333-342.

Ungar, F., Geiger, B. and Ben-Ze'ev, A. (1986) *Cell Contact- and Shape-Dependent Regulation of Vinculin Synthesis in Cultured Fibroblasts*, Nature **319** 787-791.

Walther, B.T., Öhman, R. and Roseman, S. (1973) *A Quantitative Assay for Intercellular Adhesion*, Proc. Natl. Acad. Sci. USA **70(5)** 1569-1573.

Watt, F.M., Jordan, P.W. and O'Neill, C.H. (1988) *Cell Shape Controls Terminal Differentiation of Human Epidermal Keratinocytes*, Proc. Natl. Acad. Sci. **85** 5576-5580.

Webb, A., Clark, P., Skepper, J., Compston, A. and Wood, A. (1995) *Guidance of Oligodendrocytes and Their Progenitors by Substratum Topography*, J. Cell Science **108** 2747-2760.

Weiss, P. (1945) *Experiments on Cell and Axon Orientation In Vitro: The Role of Colloidal Exudates in Tissue Organization*, J. Exp. Zool. **100** 353-386.

Weiss, P. (1959) *Interactions Between Cells*, Rev. Modern Physics **31(2)** 449-454.

Weiss, P. and Garber, B. (1952) *Shape and Movement of Mesenchyme Cells as Functions of the Physical Structure of the Medium. Contributions to a Quantitative Morphology*, Proc. Natl. Acad. Sci. **38** 264-280.

Weiss, P. and Taylor, A.C. (1956) *Fish Scales as Substratum for Uniform Orientation of Cells In Vitro*, Anat. Rec. **124** 381.

Werb, Z., Hembry, R.M., Murphy, G. and Aggeler, J. (1986) *Commitment to Expression of the Metalloendopeptidases, Collagenase and Stromelysin: Relationship of Inducing Events to Changes in Cytoskeletal Architecture*, J. Cell Biol. **102** 697-702.

Werb, Z., Tremble, P.M., Behrendtsen, O., Crowley, E. and Damsky, C.H. (1989) *Signal Transduction Through the Fibronectin Receptor Induces Collagenase and Stromelysin Gene Expression*, J. Cell Biol. **109** 877-889.

Wilkins, J.A. and Lin, S. (1982) *High-Affinity Interaction of Vinculin with Actin Filaments In Vitro*, Cell **28** 83-90.

Wilkinson, P.C. and Lackie, J.M. (1983) *The Influence of Contact Guidance on Chemotaxis of Human Neutrophil Leukocytes*, Exp. Cell Res. **145** 255-264.

Wojciak, B. and Crossan, J.F. (1993) *The Accumulation of Inflammatory Cells in Synovial Sheath and Epitenon During Adhesion Formation in Healing Rat Flexor Tendons*, Clin. Exp. Immunol. **93** 108-114.

Wojciak, B., Crossan, J., Curtis, A.S.G. and Wilkinson, C.D.W. (1995) *Grooved Substrata Facilitate In Vitro Healing of Completely Divided Flexor Tendons*, Journal of Materials Science: Materials in Medicine **6** 266-271.

Wojciak-Stothard, B., Curtis, A., Monaghan, W., Macdonald, K. and Wilkinson, C. (1996) *Guidance and Activation of Murine Macrophages by Nanometric Scale Topography*, Exp. Cell Res. **223** 426-435.

Wood, A. (1988) *Contact Guidance on Microfabricated Substrata: The Response of Teleost Fin Mesenchyme Cells to Repeating Topographical Patterns*, J. Cell Sci. **90** 667-681.

Wood, A. and Thorogood, P. (1984) *An Analysis of In Vivo Migration During Teleost Fin Morphogenesis*, J. Cell Sci. **66** 205-222.

Yamanashi, Y., Fukui, Y., Wongsasant, B., Kinoshita, Y., Ichimori, Y., Toyoshima, K. and Yamamoto, T. (1992) *Activation of Src-Like Protein-Tyrosine Kinase Lyn and its Association with Phosphatidylinositol 3-Kinase Upon B-Cell Antigen Receptor-Mediated Signaling*, Proc. Natl. Acad. Sci. USA **89** 1118-1122.

Yamanashi, Y., Kakiuchi, T., Mizuguchi, J., Yamamoto, T. and Toyoshima, K. (1991) *Association of B Cell Antigen Receptor with Protein Tyrosine Kinase Lyn*, Science **251** 192-194.

Zingg, W., Neumann, A.W., Strong, A.B., Hum, O.S. and Absolom, D.R. (1982) *Effect of Surface Roughness on Platelet Adhesion Under Static and Under Flow Conditions*, Can. J. Surg. **25(1)** 16-19.

PATENTS

Curtis, A.S.G. and Wilkinson, C.D.W. (1984) *Biomechanical Microstructures*, US Patent Office: Washington, Grant 220413 (5th December, 1988).

Curtis, A.S.G. and Wilkinson, C.D.W. (1985) *Biomechanical Structures*, European Patent, Patent Bulletin 1985/25, No. 843082306 (19th June, 1985).

Curtis, A.S.G. and Wilkinson, C.D.W. (1995) *Wound Healing Material*, Int. PCT, WO95/22305.